Antagonistic fluorescent pseudomonads cause evasion of the plant pathogen Verticillium by controlling hyphal growth and polarity

Dissertation
for the award of the degree
“Doctor rerum naturalium”
Division of Mathematics and Natural Sciences
of the Georg-August-Universität Göttingen
within the doctoral program “Microbiology and Biochemistry” of the
Georg-August University School of Science (GAUSS)

submitted by
Kai Nesemann
from Georgsmarienhütte

Göttingen 2020

Thesis Committee:

Referee: Prof. Dr. Gerhard H. Braus,
Department of Molecular Microbiology and Genetics,
Georg-August University of Göttingen

2nd referee: Prof. Dr. Rolf Daniel,
Department of Genomic and Applied Microbiology,
Georg-August University of Göttingen

3rd referee: Prof. Dr. Stefanie Pöggeler,
Department of Genetics of Eukaryotic Microorganisms,
Georg-August University of Göttingen

Members of the Examination Board:

Prof. Dr. Andrea Polle,
Department of Forest Botany and Tree Physiology, Büsgen Institute, Georg-August University of Göttingen

Prof. Dr. Ursula Kües,
Department of Forest Botany and Tree Physiology, Büsgen Institute, Georg-August University of Göttingen

Prof. Dr. Oliver Gailing,
Department of Forest Genetics and Tree Breeding, Büsgen Institute, Georg-August University of Göttingen

Date of the oral examination: 2021, January 12th

This work was accomplished in the group of Prof. Dr. Gerhard H. Braus, at the Department of Molecular Microbiology and Genetics, Institute of Microbiology and Genetics, Georg-August University of Göttingen.

Contents

Abstract

Soil borne phytopathogenic Verticillia constitute increasing yield losses. Due to a lack of resistant cultivars as well as appropriate fungicides, the usage of biocontrol agents like fluorescent pseudomonads might be a promising option to ecologically manage the pest. The impact of different mycotoxins against Verticillium is highly media dependent. *Pseudomonas fluorescens* DSM8569, an isolate from *B. napus* rhizosphere, is able to inhibit fungal growth on surfaces of rich medium containing high glucose independent of phenazines or GacA/GacS-regulated toxins but not on a complex medium with plant pectins and amino acids. In microfluidic interaction channels, this inhibitive potential has been quantified to 80 % growth reduction. An impact of a phenazine gene cluster on Verticillium growth on surface media could only be determined in a glucose environment. In microchannels filled with liquid pectins and amino acids, a phenazine gene cluster could increase the suppressive potential of the bacterium for about 30 %. An influence on Verticillium growth by genes responsible for single mycotoxins of a GacA/GacS regulation could not be proven. The sensor kinase GacS (a global regulator) as well as the response regulator GacA fulfill essential functions for fungal control especially on pectins and amino acids with an inhibition potential of approx. 30 %. In total, the entire regulation system leads to the strongest observed fungal suppression in this study of more than 90 %. Hyphal polarity has been altered in presence of the bacterium. The strongest effect was observed for *P. protegens* CHA0 potentially expressing a diverse mycotoxin cocktail resulting in more than 80 % curled hyphal tips compared to parallel hyphae in the fungal control without bacterium. This phenomenon might be interpreted as an evading strategy followed by Verticillium that tries to escape the bacterial impact. Fungal genetic response was addressed by sequencing the Verticillium transcriptome after co-cultivation with *P. protegens* CHA0. About one third of the total gene set was up-regulated in presence of the bacterium, including genes involved in detoxification possibly as a direct reaction to bacterial toxicity. The fungus presumably follows a detoxification and evasion strategy and drives back processes required for nutrient up-take like plant polysaccharide hydrolases associated to its reduced growth activity. In summary it can be considered, that in a static environment Verticillia have developed strategies to physically avoid fluorescent Pseudomonas by adapting their growth rates and by changing their growth direction. Transferring these findings gained from an artificial setup in a microfluidic confrontation design to the natural heterogeneous environment in the rhizosphere with areas of diverse suppressivness, Verticillium might potentially escape from a threatening to a more appropriate ecological niche for survival and to approach new host plant roots for infection. If evasion is no option for the fungus, like it is during artificial agitated co-cultivation or under natural conditions in the soil being located in a very widely spread Pseudomonas population, Verticillium possibly utilizes its capability to detoxify antifungal toxins to cope with bacterial antagonism.

Zusammenfassung

Bodenbürtige phytopathogene Verticillien führen zu enormen Ernteausfällen. Da bislang keine resistenten Kultursorten oder geeignete Fungizide zur Verfügung stehen, könnte die Verwendung von Biokontrollbakterien wie fluoreszierenden Pseudomonaden eine ökologische Alternative sein. Die Wirkung verschiedener Mykotoxine gegen Verticillium ist äußerst medienabhängig. *Pseudomonas fluorescens* DSM8569, ein natürliches Isolat aus der Rhizosphäre von *B. napus* ist in der Lage ohne Phenazine und GacA/GacS-regulierte Toxine das Pilzwachstum auf reichhaltigem Oberflächenmedium mit hohem Glukosegehalt zu inhibieren, allerdings nicht auf einem Komplexmedium mit Pektinen und Aminosäuren. In mikrofluidischen Interaktionskanälen konnte dieses Inhibitionspotential auf 80 % Wachstumsreduzierung quantifiziert werden. Ein signifikanter Einfluss eines Phenazine-Genclusters auf das Wachstum von Verticillium auf Oberflächenmedien konnte nur unter Glukosebedingungen bestimmt werden. In Mikrokanälen, gefüllt mit einem Pektin-Aminosäure-Medium, konnte das Phenazine-Gencluster das Hemmpotential des Bakteriums zusätzlich um ca. 30 % steigern. Gene für einzelne Mykotoxine, die durch ein GacA/GacS System reguliert werden, haben jeweils keinen individuellen Einfluss auf das Wachstum von Verticillium. Die Sensorkinase GacS (ein globaler Regulator) sowie der Antwortregulator GacA zeigen essentielle Funktionen für die Pilzkontrolle, vor allem auf einem Pektin-Aminosäure-Medium mit einem Hemmpotential von ca. 30 %. Insgesamt führt ein vollständiges Regulationssystem, zur stärksten beobachteten Pilzhemmung in dieser Studie von über 90 %. Auch die Polarität der Hyphen wurde unter Pseudomonaseinfluss verändert. Der stärkste Effekt wurde durch *P. protegens* CHA0 verursacht, mit mehr als 80 % gekräuselten Hyphenspitzen im Vergleich zu parallel wachsenden Hyphen der Pilzkontrolle ohne Bakterium. Dieses Phänomen könnte als Vermeidungsstrategie durch Verticillium interpretiert werden, welcher versucht dem intensiven Einfluss des Bakteriums zu entkommen um geeignetere Wurzeln zu infizieren. Pilzliche Antworten wurden durch Sequenzierung des Verticillium Transkriptoms nach Kokultivierung mit *P. protegens* CHA0 untersucht. Etwa ein Drittel aller Gene wurde in Anwesenheit des Bakteriums hochreguliert, inklusive der Gene, die an Detoxifizierung beteiligt sind. Dies könnte möglicherweise als direkte Antwort auf die bakterielle Toxizität interpretiert werden. Vermutlich verfolgt der Pilz eine Fluchtstrategie und fährt Prozesse zurück, die für die Nährstoffaufnahme entscheidend sind, wie etwas Pflanzen-Polysaccharid-Hydrolasen, und während reduzierter Wachstumsaktivität weniger benötigt werden. Zusammenfassend lässt sich festhalten, dass Verticillium unter statischen Bedingung Strategien entwickelt hat, um bestimmten fluoreszierenden Pseudomonaden räumlich auszuweichen, etwa durch Anpassung ihrer Wachstumsrate sowie Änderung Ihrer Wachstumsrichtung. Versucht man diese Erkenntnisse vom artifziellen Versuchsaufbau in einem mikrofluidischen Konfrontationsdesign auf die natürlichen heterogenen Bedingungen in der Rhizosphäre mit Bereichen unterschiedlicher Suppressivität zu übertragen, so lässt sich schlussfolgern, dass Verticillium potentiell versucht, lebensfeindliche Bereich zu verlassen und besser geeignete ökologische Lebensräume zu besetzten. Hier könnte der Pilz womöglich erhöhte Überlebenschancen vorfinden und somit die Möglichkeit neue

Pflanzenwurzeln zu infizieren. Wenn für den Pilz die Fluchtstrategie keine Möglichkeit darstellt, etwa während schwenkender Kokultivierung im Labor oder unter natürlichen Bedingung im Boden in großräumigen Bereichen hoher Pseudomonaskonzentration, könnte Verticillium möglicherweise seine Fähigkeit nutzen, um antimykotische Toxine zu detoxifizieren und somit zu versuchen, dem bakteriellen Antagonismus standzuhalten.

Chapter 1: Introduction

Fungal plant pathogens

Fungal plant pathogens rank as one of the most abundant and destructive pests in agriculture and lead to numerous complex diseases (Beckman, 1987; Atallah *et al.*, 2010; Rodriguez-Moreno *et al.*, 2018). Fungal infection can take place pre-harvest at growing plants with high yield losses estimated at more than US$ 200 billion (Birren *et al.*, 2002) or post-harvest with infestation and destruction of crop storage. Damage is even increased by production of mycotoxins during storage like aflatoxin by Aspergilli (Frisvad *et al.*, 2019) or deoxynivalenol and zearalenon secreted by *Fusarium* spp. (Khaneghah *et al.*, 2018) with harmful impact on human health. Thus, phytopathogenic fungi cause a considerable risk in human world food affairs in past as well as present and with increasing population probably also in future. A broad range of crops can be affected with a huge morphological and molecular variability in fungal pathogenic mode of infection (Horbach *et al.*, 2011; Jain *et al.*, 2019). Phytopathogenic fungi have different modes of trophic relationships to their host plants. There are several Basidiomycota that live biotrophicly like *Puccinia graminis* causing stem rust in cereals (Figueroa *et al.*, 2018). The biotrophic ascomycete *Blumeria graminis* is responsible for powdery mildew in many plants (Schnepf *et al.,* 2018). A large group of fungal plant pathogens that have huge agricultural impact live necrotrophicly, e.g. *Fusarium graminearum* (Wiemann *et al.*, 2013; Brodhun *et al.*, 2013; Bönninghausen *et al.*, 2019), *Botrytis cinerea* (Kretschmer *et al.,* 2009; Veloso and van Kan, 2018; Petrasch *et al.*, 2019), *Alternaria* spp. (Tralamazza *et al.*, 2018) or *Cochliobolus heterostrophus* (Kang *et al.*, 2018). The hemibiotrophic phytopathogenic fungi change the trophic mode during their life cycle in the plant from biotrophic to necrotrophic like *Magnaporthe grisea* (Park *et al.*, 2013; Figueroa *et al.*, 2018), *Phytophthora infestans* (Rodenburg *et al.*, 2018), *Colletotrichum* spp. (Yan *et al.*, 2018) or *Verticillium* spp. (Pegg and Brady, 2002; Tran *et al.,* 2013*;* Timpner *et al.,* 2013; Hoppenau *et al.*, 2014; Bui *et al*., 2019; Leonard et al., 2020).

Life cycle and taxonomy of the vascular plant pathogen Verticillium

Like the genus Trichoderma, the genus Verticillium belongs to the order of the Hypocreales of the ascomycetes. Verticillium consists of nine different haploid species as well as one amphidiploid species that is an interspecific hybrid out of two different haploid parents (*Verticillium longisporum*). These different Verticillium species are spread in temperate regions around the globe (Inderbitzin *et al.*, 2011; Carroll *et al.*, 2018). *V. dahliae* exhibits the broadest host range within the Verticillium genus causing wilt disease in more than 200 wooden and non-wooden plant species also covering many crops of agricultural interest e.g. cotton, olive, lettuce, potato and tomato (Pegg and Brady, 2002; Gordon *et al.*, 2006; Fradin and Thomma, 2006; Klostermann *et al.*, 2009; Depotter *et al.*, 2019a). In contrast to *V. dahliae*, *V. longisporum* has a narrow host range and mainly colonizes Brassicaceae like oilseed rape, cauliflower and horseradish (Heale and Karapapa, 1999; Zeise and von Tiedemann, 2001; Singh *et al.*, 2012; Zheng *et al.*, 2019). The symptoms can differ depending on the host plant. In oilseed rape *V. longisporum* infection can lead to stem striping as well as early senescence and stunting of the host plant (Depotter *et al.*, 2016 and 2017) whereas for cauliflower wilting symptoms similar to *V. dahliae* are described (Franca *et al.*, 2013). Simultaneously to the increasing relevance of oilseed rape as vegetable oil for nutrition and regenerative fuel production, also the ecological and economical relevance of *V. longisporum* as a fungal pathogen increases. With progressive global warming, the infection intensity of *V. longisporum* might increase (Siebold and von Tiedemann, 2012 and 2013). The intensity of a potential yield loss of oilseed rape due to *V. longisporum* infection depends on the inoculum level and varies from cultivar to cultivar but also individually between single plants of the same cultivar (Depotter *et al.*, 2019b). Due to its highly melanized resting structures, called microsclerotia, that can survive in the soil for many years, it is rather difficult to control the expansion of the filamentous soil borne fungus Verticillium (Wilhelm, 1955; Schnathorst, 1981; Heale and Karapapa, 1999; Yu *et al.,* 2019b; Bui *et al.*, 2019). Under appropriate environmental conditions, the microsclerotia can germinate towards the root and penetrate the root cortex (Figure 1.1).

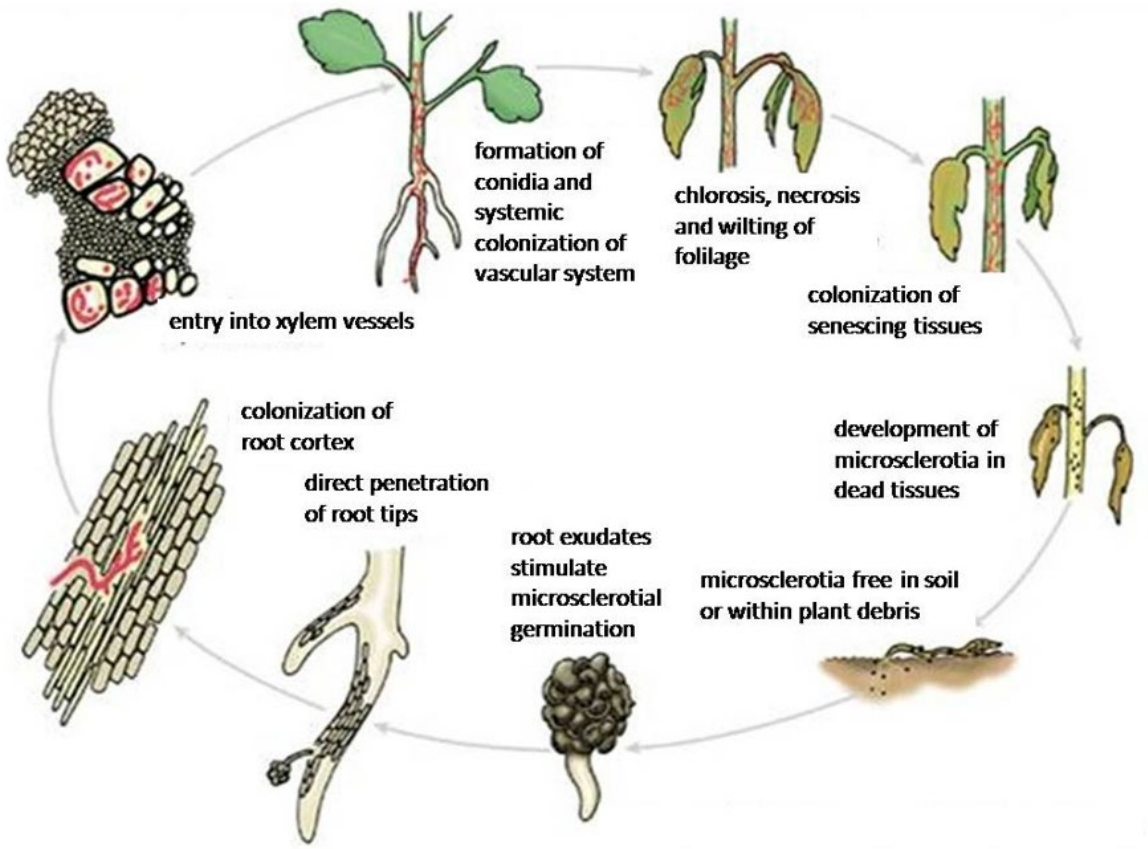

Figure 1.1: Life cycle of the soil borne phytopathogen Verticillium. The Verticillium resting structures, so-called microsclerotia, can survive free in the soil or in dead host plant material for a long period of time even under harsh climate conditions. They start germinating stimulated by root exudates that are specific for their respective host plant. The mycelium grows towards the host root and enters the plant by penetrating the rhizodermis. Subsequently, the root cortex is colonized and the hyphae enter the xylem vessels. This way conidia of the phytopathogenic fungus are transported with the transpiration flow within the vascular system spreading over the whole plant. First infection symptoms are visible by chlorotic and necrotic changes of the leaf surface and lead to a stunted plant phenotype. The disease symptoms can be summarized as early senescence of the plant development. In the dead plant material, the microsclerotia are formed and get into the soil again. There, they remain until a next stimulation via host plant root exudates takes place (from Berlanger and Powelson, 2000; drawing by Vickie Brewster, colored by Jesse Ewing).

The vascular pathogen Verticillium spreads all over the host by colonizing its xylem system (Pegg, 1989; Zhang *et al.*, 2018). Most of the infection time, the fungus lives biotrophically and colonizes the xylem vessels of the whole plant without any

apparent symptoms. Only in the later necrotrophic infection phase stem striping, early senescence and necrosis on leafs of stunted plants can be recognized sometimes in coincidence with substantial yield losses (Eynck *et al.*, 2007; Tyvaert *et al.*, 2019).

The amphidiploid *V. longisporum* is an interspecific hybrid of different haploid Verticillia

Understanding the evolution of *V. longisporum* is rather complex. *V. longisporum* is an interspecific hybrid of different haploid parental Verticillium species resulting in an amphidiploid genome (about 1.8x; Tran *et al*., 2013; Depotter *et al*., 2016, Fogelqvist *et al.*, 2018). *V. longisporum* is the only non-haploid species within the Verticillium genus. These hybridization events happened at least three times in various geographical regions with different parental lineages of *V. dahliae* and further unknown species resulting in three isolates of *V. longisporum*. Figure 1.2 shows all four single ancestors of *V. longisporum*, the two unknown species A1 and D1 as well as the two *V. dahliae* lineages D2 and D3.

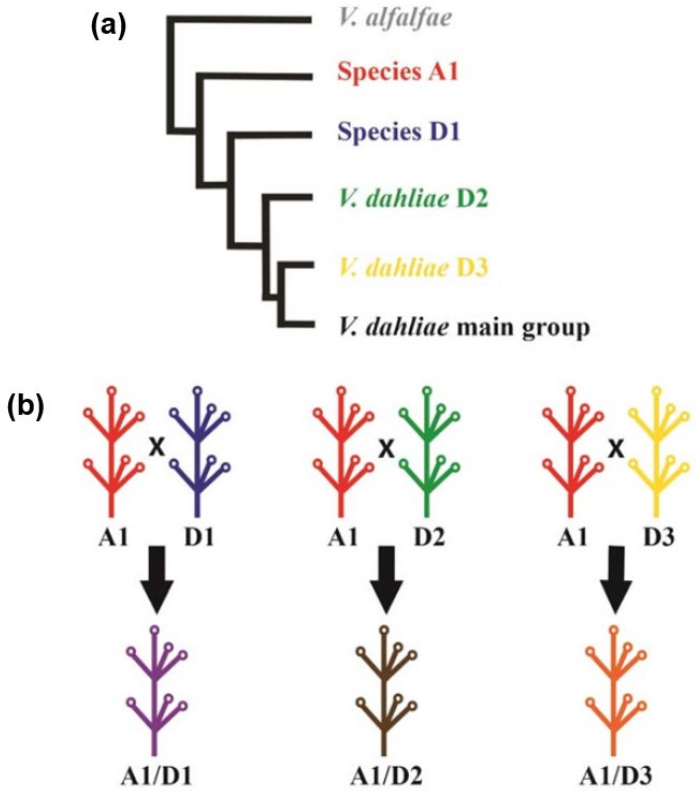

Figure 1.2: Evolution of *V. longisporum* as an interspecific hybrid of different Verticillium species. (a) Phylogenetic tree of respective progenitors of *V. longisporum*. Species A1 and D1 are regarded as unknown species, whereas D2 and D3 belong to two different lineages of *V. dahliae* that already have been described. (b) The four ancestors A1, D1, D2 and D3 shown in (a) hybridized in three individual hybridization events resulting in three different *V. longisporum* lineages. The unknown species A1 is present in all three hybrids as one parental strain: A1/D1, A1/D2 and A1/D3 (from Depotter *et al.*, 2016).

The hybrids can be differentiated into A1xD1, A1xD2 and A1xD3 (Tran *et al.*, 2013). The *V. longisporum* hybrids belonging to a combination of A1xD1 are considered to be virulent in Brassicaceae e.g. the lineage Vl43, that have been isolated in Mecklenburg, Germany, and further investigated in this study. The two lineages A1xD2, so far only proven to be located in North America (Inderbitzin *et al.*, 2011) as well as A1xD3 are not included in this study. The intensity of the symptoms depends different parameters like the species of the host plant, the nutrition conditions as well as on the specific isolate.

Conidia and resting structures of Verticillium species and their impact on plant infection

The different Verticillium isolates described above cannot only be discriminated genetically but also morphologically. All Verticillium species and lineages are characterized by asexual spore formation. Figure 1.3 shows differences in its physical shapes.

(a)

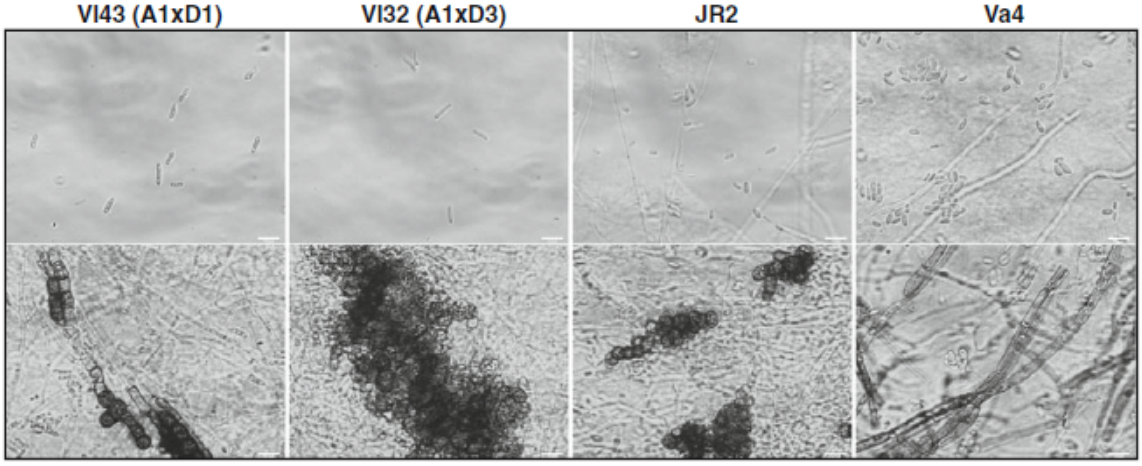

(b)

		V. longisporum A1xD1	*V. longisporum* A1xD3	*V. dahliae*	*V. nonalfalfae*
Long asexual conidia		+	+	rare	rare
Microsclerotia:	elongate	+	-	-	no microsclerotia
	compact	+	+	+	
	melanized	+	+	+	
	long cell	+	-	-	
	round cell	+	+	+	
Black mycelium (melanized and thickened cell wall)		-	-	-	+

Figure 1.3: Morphological comparison of selected Verticillium species and isolates with regard to asexual conidia as well as resting structures. (a) Morphological differences in conidia and microsclerotia formation of two *V. longisporum* hybrids A1xD1 (virulent strain VI43) and A1xD3 (avirulent strain VI32) as well as *V. dahliae* JR2 and *V. nonalfalfae* (*formerly named V. albo-atrum* strain Va4). (b) Overview about conidia shapes and melanized resting structures as differentiators between *V. longisporum* (A1xD1 and A1xD3), *V. dahliae* and *V. nonalfalfae* (from Tran *et al.*, 2013, modified).

Microscopy pictures from asexual spores of different Verticillia taken by *Tran et al.* (2013) show conidia from *V. dahliae* and *V. nonalfalfa (formerly named V. albo-atrum* strain Va4*)*, which have a round egg-shaped structure with a length of 3.5 to 5.5 µm. In contrast, the conidia from *V. longisporum* have a long shape that gives the species name, with a double length of 7.1 to 8.8 µm (Zeise and von Tiedemann, 2001). The asexual spores play an important role during plant infection. While initial stages of plant infection are dominated by hyphal growth during penetration of the root tip and colonization of the root cortex and the xylem vessels, the spores are

responsible for a systemic colonialization of the vascular system of the host plant. With the transpiration flow, the conidia are translocated throughout the whole plant. After spore germination, the hyphae infest increasing areas of the plant and the final necrotrophic phase starts causing typical infection symptoms (Eynck *et al.*, 2007; Depotter *et al.*, 2016).

When the host plant dies, the fungus starts to produce resting structures in the dead plant material. These so-called microsclerotia exhibit a highly increased content of melanin and are released to soil with plant debris. They are produced in the stem cortex beneath the epidermis in the oilseed rape plant (Depotter *et al.*, 2016). In contrast to the Verticillium conidia and hyphae that are predominantly present in the plant, the microsclerotia also occur in the soil. Since they are quite resistant against harsh ecological conditions, like frost, UV light, pH range or drought stress the melanized resting structures are able to survive in the soil for many years (Pegg and Brady, 2002; Harting *et al.*, 2020). *V. dahliae* and *V. longisporum* can form microsclerotia in high quantity depending on the nutrition composition (Tran *et al.*, 2013). The virulent A1xD1 lineage Vl43 that is investigated in this study, can form big microsclerotia complexes made out of melanized hyphae in multiple shapes as elongated, compact and also rounded cells (Figure 1.3). *V. nonalfalfae* does not produce any complex microsclerotia but instead the fungus is able to embed thick melanin layers in the hyphal cell wall, which is visible under the microscope as black mycelium.

Interactions in the plant rhizosphere

As a soil borne organism, Verticillium is part of the rhizosphere of several plant species. Plant rhizospheres represent highly heterogeneous habitats, which are the basis for diverse biocoenoses including complex microbiomes. The microbiota are of particular importance for plant growth, health and stress resilience (Compant *et al.*, 2019). Biochemical interactions are mainly driven by the secretion of secondary metabolites or signaling molecules from the different interaction partners as well as impacted by nutritional competition (Shaikh *et al.*, 2018). The majority of plant-microbe interactions is characterized by a beneficial ecological relationship as many microbes act as decomposer providing the plant with nutrients

and organic substances but also remove soil pollutants, and eliminate pathogens (Islam, 2018).

Rhizospheres consist of various bacteria and fungi dynamically interacting in an antagonistic or mutualistic way. Nazir *et al.* (2009) describes microbial communication in the rhizosphere as a crucial factor for the vitality of the ground substrate and calls it microbial fitness of the soil. In this context, beneficial effects of *Lyophyllum* spp. towards the development of *Burkholderia terrae* have been investigated. *Lyophyllum* spp. hyphae colonizing the surrounding of *Burkholderia terrae* support transportation and utilization of fungal exudates as nutrients for the bacterium (Warmink *et al*., 2011). In addition, competitive biocoenoses have been described. Toxin containing vesicles secreted by *Streptomyces lividans* result in significant growth suppression of *Aspergillus proliferans* and *Verticillium dahliae* (Schrempf and Merling, 2015).

Extended knowledge about the function of fungal-bacterial biocoenoses in the rhizosphere and their mechanisms of controlling each other may help to invent new strategies in using soil-microbes as biocontrol organisms against plant pathogens.

Natural rhizobacteria as antagonists of microbial pathogens

Agriculturists that are affected by soil borne pathogens in their cultivar can profit by the existing microbiota in the rhizosphere or even specifically improve the microbial composition in the soil (Gouda *et al.*, 2018; Orozco-Mosqueda *et al.*, 2018; Compant *et al.*, 2019). Unfortunately, the arsenal of opportunities to react to microbial infections in agriculture is rather limited. First, resistant cultivars can be chosen to avoid an infection per se. In many cases, resistant cultivars are not available or the pathogens can overcome the resistance. Therefore, pesticides are often applied resulting in severe ecological and health risks. Alternatively, natural rhizosphere microbes can be utilized against phytopathogenic organisms (Carmona-Hernandez *et al*., 2019). This way, a suppressive potential of the soil can be specifically build up to counteract the pathogen using existing biological capabilities (Sikora, 1992; Steinberg *et al.*, 2019).

Different microbes have been characterized as antagonists against pathogens. Many filamentous fungi can be utilized to suppress pathogenic growth (Baron *et al.*, 2019) like the beneficial rhizofungus *Coniothyrium minitans* that possesses activity against the phytopathogen *Sclerotinia sclerotiorum* (Zeng *et al.*, 2012). A suppressive activity has also been reported for the nematophage *Pochonia chlamydosporia* (formerly named *Verticillium chlamydosporia*) with strong antagonism against plant-pathogenic nematodes (Lin *et al.*, 2018; Uddin *et al.*, 2019). Also bacteria can be utilized as natural antagonists. Rhizobacteria like Bacilli have been identified as effective suppressors of fungal pathogens (Albayrak; 2019). *Bacillus subtilis* can be used to control the growth of several phytopathogens like *Ralstonia solanacearum* that can infect tomato plants leading to wilting symptoms (Chen *et al.*, 2013). *Bacillus subtilis* also acts against *Podosphaera fusca* causing powdery mildew diseases in cucurbit by activation of plants´s jasmonate- and salicylic acid-dependent defense response (Garcia-Gutierrez *et al.*, 2013). *Bacillus thuringiensis* and *B. weihenstephanensis* strains isolated from root-associated soil of field-grown tomatoes exhibit significant inhibition potential against the tomato pathogen *V. dahliae* JR2 but also against the oilseed rape pathogen *V. longisporum* Vl43 (Hollensteiner *et al*., 2017). Against Verticillium wilt in olive *Paenibacillus alvei* has been identified to be an effective antagonist against *V. dahliae* also in field experiments (Martinez-Garcia *et al.*, 2015; Markakis *et al.*, 2016).

During this interplay, the plant, the pathogen and the biocontrol organism are intensively communicating and interacting with each other (Figure 1.4).

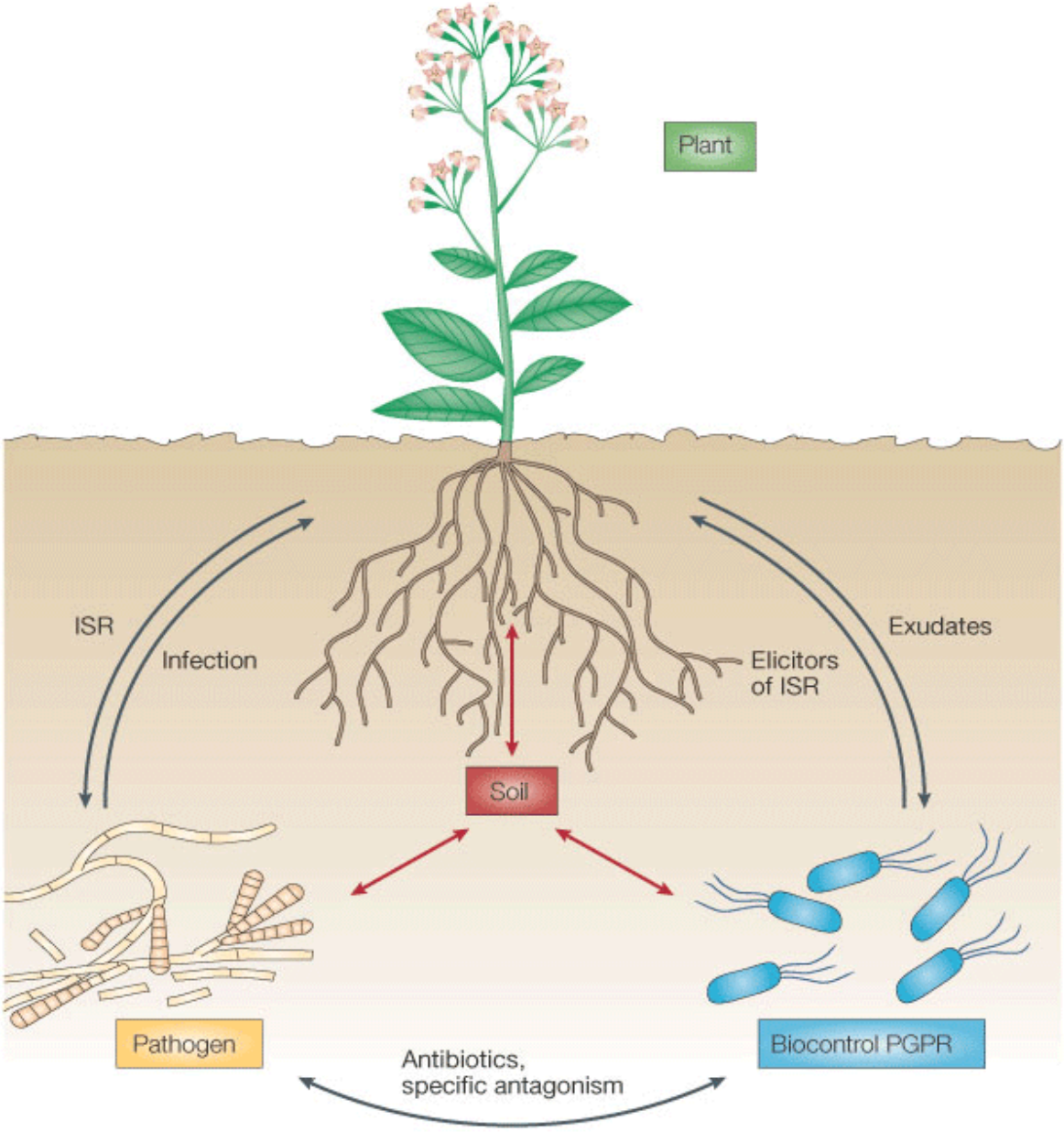

Figure 1.4: Interactions between growth-promoting rhizobacterium, plant, pathogen and soil. The interplay of diverse organisms colonizing the soil is rather complex and can influence their development directly and indirectly. A plant has to cope with a variety of soil born pathogenic species that possess a direct infection potential towards the root of specific host plants. The plant itself is able to induce systemic resistance (ISR) to repel the infection process. Antagonistic bacteria as fluorescent pseudomonads or Bacilli can also be stimulated by root exudates and even promote plant growth rate. Plant-beneficial rhizobacteria can also directly interact with the plant-pathogenic organisms, often in an antagonistic manner by the secretion of toxic metabolites. If the growth-promoting rhizobacteria (PGPR) successfully suppress the growth of the pathogen, this has an additional indirect plant supporting effect by decreasing the infection intensity of the pathogen (from Haas and Défago, 2005).

Bacterial and fungal biocontrol organisms can protect host plants against fungal pathogens by diverse mechanisms. Many beneficial microorganisms have a direct plant growth promotion effect (Khan *et al.*, 2019). Additionally, they are able to prime the host plant by inducing systemic resistance with specific secreted elicitors like siderophores or O-antigens before a putative pathogen has the chance to invade the plant (Conrath *et al.*, 2002; Haas and Défago, 2005; Abuamsha *et al.*, 2010; Berendsen *et al.*, 2012; Goh *et al.*, 2013; Kupferschmied *et al.*, 2013; Kannojia *et al.*, 2019). Besides growth promotion effects, also parasitism of the pathogen (mycoparasitism in case of fungal pathogens) plays an important role to suppress its infection intensity. A direct competition between the pathogen and the biocontrol organism for nutrients or infection spots on the plant surface can lead to a suppression of pathogenicity towards the host plant. By secretion of bioactive compounds like antibiotics, reactive oxygen species, cyanides, lipopeptides or siderophores, the antagonist can also control the growth of the phytopathogen (Weller, 2007; Yu *et al.*, 2019a). There is a wide range of organisms with putative suppressive properties against pathogens. *Bacillus thuringiensis* and *B. licheniformis* for example generate their antifungal potential by the production of the cell wall degrading enzyme chitinase (Gomaa, 2012). *Clonostachys rosea* detoxifies the mycotoxin zearalenone of *Fusarium graminearum* by the production of zearalenone hydrolases (Kosawang *et al*., 2014).

Many different fluorescent pseudomonad species from the group of □-proteobacteria have been discovered as antagonistic rhizobacteria that can install a suppressive potential in the rhizosphere expressed by a diverse arsenal of bioactive substances (Sahu *et al.*; 2018; Mishra and Arora, 2018). *Pseudomonas protegens* CHA0 is one of the best characterized antifungal strains and has been intensively investigated by different groups (Haas and Défago, 2005; Weller, 2007; Flury *et al.*, 2019). A multiple range of antibiotic secondary metabolites like 2,4-diacetylphloroglucinol (DAPG), biosurfactants, pyoluteorin and hydrogen cyanide (HCN) can be secreted by *P. protegens* CHA0 that are regulated by the two-component system GacA/GacS (Haas and Défago, 2005; Mazzola, 2007; Yan *et al.*, 2018).

The GacA/GacS two-component system is part of a complex posttranscriptional signal-transduction pathway, that has been discovered in *Pseudomonas protegens* strain CHA0 (Figure 1.5). GacA/GacS initiates the translation of pathogenicity related genes. The consequence is synthesis and secretion of bioactive secondary metabolites in a stress dependent manner. Key target genes controlled by this signal pathway are involved in the synthesis of specific bioactive compounds like DAPG (operon *phlA,F*), HCN (operon *hcnABC* and *anr*) or pyoluteorin (*plt*), are constitutively expressed. These operons are constitutively expressed but the transcripts are not translated because of the translational repressors RsmA and RsmE, which bind to the ribosomal binding site. The GacS sensor kinase is located in the membrane and is stimulated by the perception of appropriate environmental stress stimuli. This results in phosphorylation of the response regulator GacA, which activates the formation of the small regulatory RNAs *rsmX, rsmY* and *rsmZ*. The regulatory RNAs bind the translational repressors RsmA and RsmE and allow the translation of the mRNAs of the target genes (Figure 1.5). Under stress-induced derepression, the translation of the target genes *phlA,F*, *hcnABC*, *anr* or *plt* are activated and the resulting enzymes produce the corresponding secondary metabolites, which are released by the cell (Laville *et al.*, 1992; Zuber *et al.*, 2003; Heeb *et al*., 2005; Gonzalez *et al*., 2008; Brencic *et al*. 2009; Wei *et al*., 2013; Nandi *et al.*, 2015; Traxler and Kolter, 2015; Yan *et al.*, 2018).

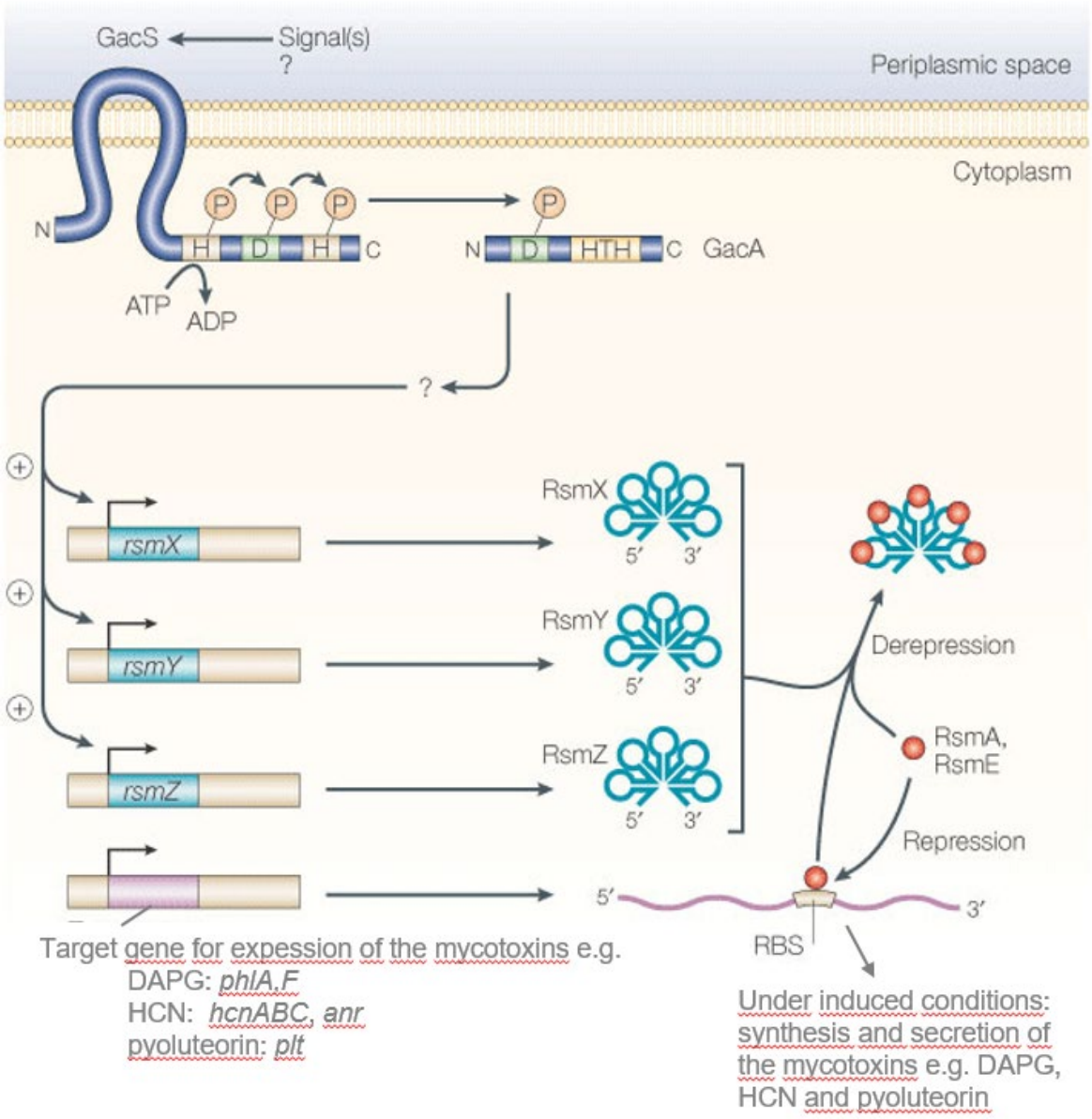

Figure 1.5: Model of the GacA/GacS signal-transduction pathway in *Pseudomonas protegens* strain CHA0. A diverse pattern of genes coding for antifungal compounds, in the figure called 'target genes', are constantly expressed: the operon *phlA,F* codes for the enzymes to form 2,4-diacetylphloroglucinol (DAPG); the operon *hcnABC* codes for the enzymes to form hydrogen cyanide (HCN); the gene *plt* codes for pyoluteorin producing enzymes. The respective mRNAs are post-transcriptionally inhibited by the small proteins RsmA and RsmE binding at the ribosome-binding site (RBS). Stimulated by external signals, e.g. specific root exudates, the sensor kinase GacS, an integrated membrane protein, is phosphorylated. Along the signal transduction, the phosphate is transferred to the response regulator GacA. In this induced form, GacA activates the expression of the small RNAs rsmX, rsmY and rsmZ that act as derepressors of RsmA and RsmE. This way the translation inhibition of the target mRNAs is nullified under inducing conditions caused by the external signal. The synthesis of the bioactive toxins as well as their secretion takes place (from Haas and Défago, 2005).

Besides the DAPG producer *P. protegens* CHA0, also the phenazine producer *P. synxantha* 2-79 (formerly named *P. fluorescens* 2-79) is further investigated in this study. Phenazines show a broad-range antibiotic spectrum against many different microbial pathogens (Biessy and Filion, 2018). Different phenazine derivates are synthesized during the phenazine pathway. *P. synxantha* 2-79 is capable of the production of the well-characterized and highly effective antibiotic phenazine-1-carboxylic acid (PCA). Figure 1.6 shows the pathway of PCA with multiple steps catalyzed by the seven-gene operon *phzABCDEFG* (Mavrodi *et al.*, 1998 and 2006; Biessy and Filion, 2018).

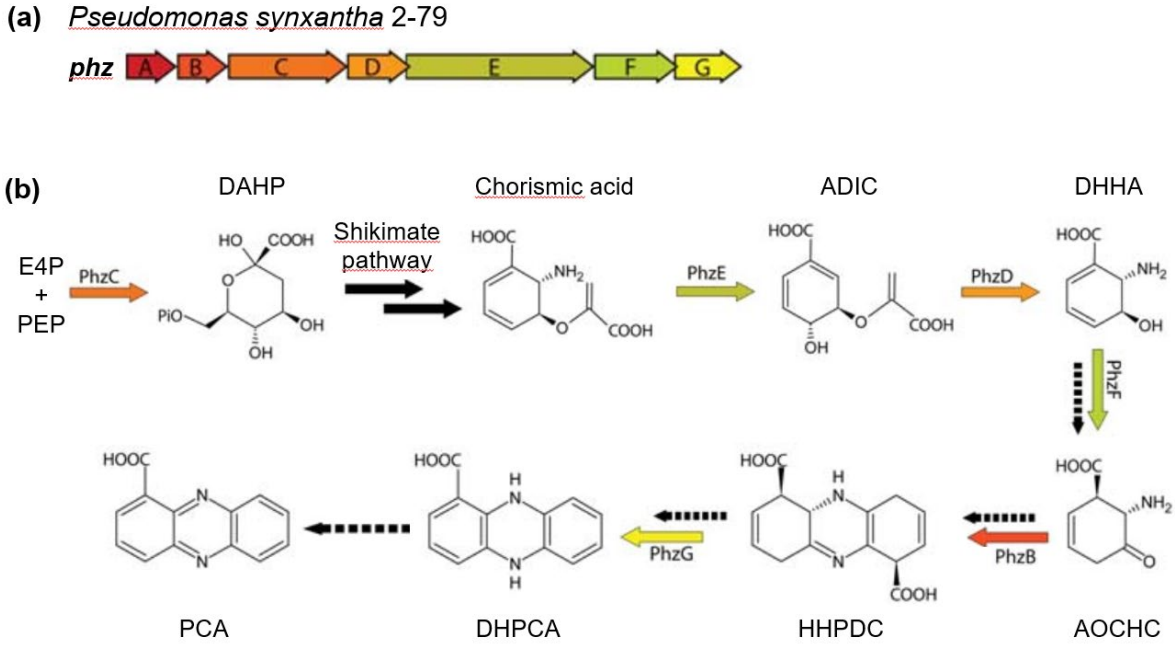

Figure 1.6: Phenazin seven-gene operon and pathway in phenazine-secreting *Pseudomonas* spp. (a) Arrangement of the seven genes phzA-G coding for enzymes involved in the phenazine biosynthesis inter alia of *P. synxantha* 2-79 (formerly named *P. fluorescens* 2-79). (b) Function of the seven enzymes PhzA-G during the phenazine pathway resulting in the phenazine derivate phenazine-1-carboxylic acid (PCA). Colored arrows correspond to the gene color of the respective phenazine gene from (a) and mark a catalyzed reaction. Dotted black arrows symbolize spontaneous and uncatalyzed conversions. Solid black arrows during the shikimate pathway indicate further unpresented reactions from 3-deoxy-D-arabinoheptulosonate-7-phosphate (DAHP) to chorismate. Further abbreviations: E4P: erythrose-4-phosphate; PEP: phosphoenolpyruvate; ADIC: 2-amino-4-deoxychorismic acid; DHHA: trans-2,3-dihydro-3-hydroxyanthranlic acid; AOCHC: 6-amino-5-oxo-cyclohex-2-ene-1-carboxylic acid; HHPDC: hexahydrophenazine-1,6-dicarboxylic acid; DHPCA: 5,10-dihydrophenazine-1-carboxylic acid (from Biessy and Filion, 2018; modified).

The formation of the secondary metabolite phenazine is connected to the primary metabolism of the shikimate pathway, which produces the aromatic amino acids phenylalanine, tyrosine and tryptophan. The initial step of the shikimate pathway is the conjunction of erythrose 4-phosphate (E4P) from the pentose phosphate pathway and phosphoenolpyruvate (PEP) from glycolysis to 3-deoxy-D-arabinoheptulosonate-7-phosphate (DAHP) catalyzed by the enzyme PhzC. Aromatic amino acid biosynthesis continues through shikimate to chorismate. Already 1972, shikimate has been described as precursor for phenazine synthesis (Longley *et al.*, 1972). In five subsequent enzymatic reactions catalyzed by PhzE, PhzD, PhzF, PhzB and PhzG the antibiotic phenazine metabolite phenazine-1-carboxylic acid (PCA) is formed which is secreted by *P. synxantha* 2-79 (Mavrodi *et al.*, 1998; Biessy and Filion, 2018). The phenazine deficient 2-79 stain used in this study lacks the full seven-gene locus and is generally impaired in the expression of any phenazine (Mavrodi *et al.*, 1998).

Aims and structure of this study

The major goal of this study was to compare the mutual impact on growth of phytopathogenic fungal Verticillia and fluorescent pseudomonads as soil bacteria during co-cultivation in different settings and with different nutrition. Possible suppressive impacts of the bacterium due to different antifungal strain-specific capabilities towards fungal growth rate, morphology and expression patterns should be analyzed on solid or liquid media with and without spatial limitations.
Starting point of the thesis was the determination of the genomic potential of two selected bacteria (chapters 2 & 3), followed by co-cultivations of Verticillia and wildtype and mutant bacterial strains during different nutritional conditions on agar plates (chapter 4) and finally in liquid media including a microfluidic confrontation assay (chapter 5).

In chapter 2 (Nesemann *et al.,* 2015a) the draft genomic sequence of the beneficial rhizobacterium *Pseudomonas fluorescens* DSM8569 is presented. *P. fluorescens* DSM8569 have been isolated in Rostock, Germany, and have initially been

described by Berg and Ballin in 1994. This strain has been selected as a putative candidate for growth inhibition of *V. longisporum* Vl43, infecting oil seed rape, as it is a natural isolate of the same rhizosphere. This is why in this study *P. fluorescens* DSM8569 is called P_rhizo.

In chapter 3 (Nesemann *et al.,* 2015b) the draft genome sequence of *P. synxantha* 2-79 is presented. *P. synxantha* 2-79 (formerly named *P. fluorescens* 2-79; Weller and Cook; 1983) is capable of the synthesis of phenazines. It was analyzed for its potential in growth suppression of *V. longisporum* Vl43. Mazurier *et al.* (2009) showed that *P. synxantha* 2-79 is capable of secreting antifungal phenazines but not of DAPG. This is why in this study *P. synxantha* 2-79 is called P_phen.

In chapter 4 (Nesemann *et al.,* 2018), virulent phytopathogenic Verticillium strains have been selected for co-cultivation with potential natural antagonistic rhizobacteria. It was analyzed whether a soil bacterium, derived from a specific plant´s rhizosphere (oilseed rape; P_rhizo), differs in its impact on growth towards the corresponding fungal plant pathogen of the same plant rhizosphere (*V. longisporum* on oilseed rape) compared to pathogens of other hosts (*V. dahliae* on tomato). Further, it was analyzed, whether different growth conditions as high glucose environment or restricted nutrition on a complex pectin containing plant medium change the potential biocontrol of fungal growth by bacteria. Various co-culture experiments of three different Pseudomonas strains combined with two fungal pathogens were performed. *P. fluorescens* DSM8569 (P_rhizo), derived from the rhizosphere of oilseed rape. *P. synxantha* 2-79 produces phenazines (P_phen), whereas *P. protegens* CHA0 (P_DAPG) possesses no genes for enzymes for phenazines, but for different other antifungal secondary metabolites, including 2,4-diacetylphloroglucinol (DAPG). The haploid fungus *V. dahliae* JR2 infects tomato, whereas the amphidiploid *V. longisporum* Vl43 hybrid fungus infects oilseed rape.

In chapter 5, the mutualistic interaction of Verticillium and Pseudomonas was analyzed in a microfluidic interaction device with embedded interaction channels. The fungus and the bacteria were inoculated on opposite sides of the channels.

The narrow microchannels limit the amount of hyphae accessing the channel. They were filled with a liquid medium rich in pectins and amino acids. This improves the microscopic observance by physically restricting hyphae to grow only in one direction. The impact of respective bacterial strains on Verticillium growth was quantified and the hyphal growth distance was measured under microscopic magnification. This method also allows deeper insights into fungal morphological adaption to bacterial impact. The Verticillium transcriptome in interaction with the DAPG-producing *P. protegens* CHA0 (P_DAPG) in liquid media was sequenced to gain further information about activated and deferred fungal pathways during bacterial co-cultivation.

Finally, chapter 6 is a general discussion regarding the topics presented in the single chapters above.

Chapter 2: Draft genome sequence of the beneficial rhizobacterium *Pseudomonas fluorescens* DSM8569

Kai Nesemann[a], Susanna A. Braus-Stromeyer[a], Andrea Thuermer[b], Rolf Daniel[b], Gerhard H. Braus[a#]

[a]Institute of Microbiology and Genetics, Department of Molecular Microbiology and Genetics, Georg-August-Universität, Göttingen, Germany.
[b]Göttingen genomics laboratory (G2L) at the Institute of Microbiology and Genetics, Department of Genomic and Applied Microbiology, Georg-August-Universität, Göttingen, Germany.

[#]Corresponding author: Gerhard H. Braus; Telephone: +49-551-3933771; Fax: +49-551-3933330; E-mail: gbraus@gwdg.de

Author contributions:

Culturing and harvesting of Pseudomonas biomass: KN
DNA extraction and measurement: KN
Preparation of sequencing setup: KN
Further DNA sample preparation for sequencing: AT
Generation of a shotgun-sequencing library: AT
Sequencing of the whole genome: AT
De novo assembly of shotgun reads: AT
Draft genome annotation: AT
Data interpretation: KN
Supervision: GB; RD; SB
Manuscript: GB, RD, SB, AT, KN

genomeA
Journals.ASM.org

Draft Genome Sequence of the Beneficial Rhizobacterium *Pseudomonas fluorescens* DSM 8569, a Natural Isolate of Oilseed Rape (*Brassica napus*)

Kai Nesemann,[a] Susanna A. Braus-Stromeyer,[a] Andrea Thuermer,[b] Rolf Daniel,[b] Gerhard H. Braus[a]

Department of Molecular Microbiology and Genetics, Institute of Microbiology and Genetics, Georg-August Universität, Göttingen, Germany[a]; Department of Genomic and Applied Microbiology & Göttingen Genomics Laboratory, Institute of Microbiology and Genetics, Georg-August Universität, Göttingen, Germany[b]

***Pseudomonas fluorescens* DSM 8569 represents a natural isolate of the rhizosphere of oilseed rape (*Brassica napus*) in Germany and possesses antagonistic potential toward the fungal pathogen *Verticillium*. We report here the draft genome sequence of strain DSM 8569, which comprises 5,914 protein-coding sequences.**

Received 4 February 2015 **Accepted** 18 February 2015 **Published** 26 March 2015

Citation Nesemann K, Braus-Stromeyer SA, Thuermer A, Daniel R, Braus GH. 2015. Draft genome sequence of the beneficial rhizobacterium *Pseudomonas fluorescens* DSM 8569, a natural isolate of oilseed rape (*Brassica napus*). Genome Announc 3(2):e00137-15. doi:10.1128/genomea.00137-15.

Address correspondence to Gerhard H. Braus, gbraus@gwdg.de.

Pseudomonas represents an abundant bacterial genus in many antagonistic root-associated communities (1). *Pseudomonas fluorescens* DSM 8569 was isolated from the rhizosphere of the *Verticillium* host oilseed rape (*Brassica napus*) in Rostock, Germany (2). The phytopathogenic fungus *Verticillium* requires an activator of adhesion for systemic infection of plant roots (3). The bacterium revealed a strong antimycotic effect on the phytopathogenic fungus *Verticillium* (4). A variety of secreted secondary metabolites with antimycotic impact were described in fluorescent pseudomonads, such as 2,4-diacetylphloroglucinol (DAPG), pyoluteorin, HCN, or pyrrolnitrin. A two-component system, *gacA-gacS*, was discovered in *Pseudomonas protegens* CHA0, which posttranscriptionally regulates the synthesis and secretion of these compounds (1). The synthetic pathway of phenazines in *P. fluorescens* 2-79 was investigated previously (5, 6). The chemical group of phenazines causes oxidative stress by accumulating toxic superoxide radicals and hydrogen peroxide in the target cell (7). Currently, it is unknown which suppressive mechanisms are responsible for the antagonistic potential of *P. fluorescens* DSM 8569. Genomic sequencing will be helpful in understanding the plant-promoting and antagonistic potentials of fluorescent pseudomonads.

The biocontrol strain *P. fluorescens* DSM 8569 was obtained from the DSMZ (Braunschweig, Germany). The genomic DNA was isolated using the MasterPure complete DNA and RNA purification kit (Epicentre, Madison, WI, USA). A shotgun sequencing library was generated, employing the Nextera DNA sample preparation kit, according to the manufacturer's instructions. The whole genome of DSM 8569 was sequenced with the Genome Analyzer IIx (Illumina, San Diego, CA, USA). In total, 8.3 million paired-end reads of 112 bp were generated. The *de novo* assembly of all shotgun reads using SPAdes 3.0.0 (8) resulted in 135 contigs >3 kb and 119-fold coverage. The draft genome sequence comprises 6.6 Mb and a G+C content of 61.01%. Genome annotation was performed by the use of Prokka (9). The draft genome was found to harbor 2 rRNA clusters, 43 tRNA genes, 4,560 protein-coding genes with a predicted function, and 1,354 genes coding for hypothetical proteins.

The proteins involved in secondary metabolism were analyzed. The genes necessary for pyoluteorin synthesis (GenBank accession numbers 15560761, 15560764, 15560758, 15560774, and 15560768) and the entire phenazine operon described for *P. fluorescens* 2-79 (L48616.1) are absent. At least one gene (*phlG* [15563823]) required for the regulation of 2,4-diacetylphloroglucinol synthesis is missing in DSM 8569. In contrast, the genes responsible for HCN synthesis (15560558 and 15559866) are present in DSM 8569.

Nucleotide sequence accession numbers. This whole-genome shotgun project has been deposited at DDBJ/EMBL/GenBank under the accession no. JXOE00000000. The version described in this paper is the first version, JXOE01000000.

ACKNOWLEDGMENTS

This work was supported by the Federal Ministry of Education and Research (BMBF) BioFung project and the DFG through grants awarded to G.H.B.

REFERENCES

1. **Haas D, Défago G.** 2005. Biological control of soil-borne pathogens by fluorescent pseudomonads. Nat Rev Microbiol 3:307–319. http://dx.doi.org/10.1038/nrmicro1129.
2. **Berg G, Ballin G.** 1994. Bacterial antagonists to *Verticillium dahliae* Kleb. J Phytopathol 141:99–110. http://dx.doi.org/10.1111/j.1439-0434.1994.tb01449.x.
3. **Tran VT, Braus-Stromeyer SA, Kusch H, Reusche M, Kaever A, Kühn A, Valerius O, Landesfeind M, Aßhauer K, Tech M, Hoff K, Pena-Centeno T, Stanke M, Lipka V, Braus GH.** 2014. *Verticillium* transcription activator of adhesion Vta2 suppresses microsclerotia formation and is required for systemic infection of plant roots. New Phytol 202:565–581. http://dx.doi.org/10.1111/nph.12671.
4. **Berg G, Opelt K, Zachow C, Lottmann J, Götz M, Costa R, Smalla K.** 2006. The rhizosphere effect on bacteria antagonistic towards the pathogenic fungus *Verticillium* differs depending on plant species and site. FEMS Microbiol Ecol 56:250–261. http://dx.doi.org/10.1111/j.1574-6941.2005.00025.x.

5. **Mavrodi DV, Ksenzenko VN, Bonsall RF, Cook RJ, Boronin AM, Thomashow LS.** 1998. A seven-gene locus for synthesis of phenazine-1-carboxylic acid by *Pseudomonas fluorescens* 2-79. J Bacteriol **180:**2541–2548.
6. **Mavrodi DV, Peever TL, Mavrodi OV, Parejko JA, Raaijmakers JM, Lemanceau P, Mazurier S, Heide L, Blankenfeldt W, Weller DM, Thomashow LS.** 2010. Diversity and evolution of the phenazine biosynthesis pathway. Appl Environ Microbiol **76:**866–879. http://dx.doi.org/10.1128/AEM.02009-09.
7. **Hassett DJ, Woodruff WA, Wozniak DJ, Vasil ML, Cohen MS, Ohman DE.** 1993. Cloning and characterization of the *Pseudomonas aeruginosa* *sodA* and *sodB* genes encoding manganese- and iron-cofactored superoxide dismutase: demonstration of increased manganese superoxide dismutase activity in alginate-producing bacteria. J Bacteriol **175:**7658–7665.
8. **Bankevich A, Nurk S, Antipov D, Gurevich AA, Dvorkin M, Kulikov AS, Lesin VM, Nikolenko SI, Pham S, Prjibelski AD, Pyshkin AV, Sirotkin AV, Vyahhi N, Tesler G, Alekseyev MA, Pevzner PA.** 2012. SPAdes: a new genome assembly algorithm and its applications to single-cell sequencing. J Comput Biol **19:**455–477. http://dx.doi.org/10.1089/cmb.2012.0021.
9. **Seemann T.** 2014. Prokka: rapid prokaryotic genome annotation. Bioinformatics **30:**2068–2069. http://dx.doi.org/10.1093/bioinformatics/btu153.

Chapter 3: Draft genome sequence of the phenazine producing *Pseudomonas fluorescens* 2-79

Kai Nesemann[a], Susanna A. Braus-Stromeyer[a], Andrea Thuermer[b], Rolf Daniel[b], Dmitri Mavrodi[c], Linda S. Thomashow[c], Gerhard H. Braus[a#]

[a]Institute of Microbiology and Genetics, Department of Molecular Microbiology and Genetics, Georg-August-Universität, Göttingen, Germany.
[b]Göttingen genomics laboratory (G2L) at the Institute of Microbiology and Genetics, Department of Genomic and Applied Microbiology, Georg-August-Universität, Göttingen, Germany.
[c]Department of Plant Pathology, USDA-ARS Root Disease and Biocontrol Research Unit, Washington State University, Pullmann, WA, USA.
[#]Corresponding author: Gerhard H. Braus; Telephone: +49-551-3933771; Fax: +49-551-3933330; E-mail: gbraus@gwdg.de

Author contributions:

Providing Pseudomonas strain: DM, LT
Culturing and harvesting of Pseudomonas biomass: KN
DNA extraction and measurement: KN
Preparation of sequencing setup: KN
Further DNA sample preparation for sequencing: AT
Generation of a shotgun-sequencing library: AT
Sequencing of the whole genome: AT
De novo assembly of shotgun reads: AT
Draft genome annotation: AT
Data interpretation: KN
Supervision: GB, RD, SB
Manuscript: GB, RD, SB, AT, KN

genomeA
Journals.ASM.org

Draft Genome Sequence of the Phenazine-Producing *Pseudomonas fluorescens* Strain 2-79

Kai Nesemann,[a] Susanna A. Braus-Stromeyer,[a] Andrea Thuermer,[b] Rolf Daniel,[b] Dmitri V. Mavrodi,[c] Linda S. Thomashow,[d] David M. Weller,[d] Gerhard H. Braus[a]

Department of Molecular Microbiology and Genetics, Institute of Microbiology and Genetics, Georg-August Universität, Göttingen, Germany[a]; Department of Genomic and Applied Microbiology and Göttingen Genomics Laboratory, Institute of Microbiology and Genetics, Georg-August Universität, Göttingen, Germany[b]; Department of Biological Sciences, University of Southern Mississippi, Hattiesburg, Mississippi, USA[c]; USDA-ARS Root Disease and Biological Control Research Unit, Washington State University, Pullman, Washington, USA[d]

***Pseudomonas fluorescens* strain 2-79, a natural isolate of the rhizosphere of wheat (*Triticum aestivum* L.), possesses antagonistic potential toward several fungal pathogens. We report the draft genome sequence of strain 2-79, which comprises 5,674 protein-coding sequences.**

Received 4 February 2015 **Accepted** 18 February 2015 **Published** 26 March 2015

Citation Nesemann K, Braus-Stromeyer SA, Thuermer A, Daniel R, Mavrodi DV, Thomashow LS, Weller DM, Braus GH. 2015. Draft genome sequence of the phenazine-producing *Pseudomonas fluorescens* strain 2-79. Genome Announc 3(2):e00130-15. doi:10.1128/genomeA.00130-15.

Address correspondence to Gerhard H. Braus, gbraus@gwdg.de.

The concentration and composition of antibiotic-producing, root-colonizing organisms are important factors that partially determine the suppressiveness of soils toward certain soil-borne diseases (1).

Fluorescent pseudomonads play a major role in suppressing take-all disease of wheat caused by the fungal pathogen *Gaeumannomyces graminis* var. *tritici* (Sacc.) (2). In 1979, Weller and Cook isolated bacteria from roots of wheat plants grown in take-all suppressive soils in Washington state, USA (3). *Pseudomonas fluorescens* 2-79 (NRRL B-15132) was characterized as a strong biological control agent suppressing *G. graminis* in vitro and *in planta*. Wheat plants infected with *G. graminis* var. *tritici* and additionally treated with *P. fluorescens* 2-79 resulted in taller plants, more heads, and fewer symptoms of root disease compared to the control plants without bacterial treatment. Bacterial treatment could increase the yield up to 147% in soils fumigated with methyl bromide and up to 27% in natural soils (3). *P. fluorescens* 2-79 produces phenazines, which represent a diverse chemical group of nitrogen-containing heterocyclic pigments possessing broadly inhibitory properties toward bacteria and fungi (4). Phenazines undergo redox reactions with NADH/NADPH, leading to an increase of toxic superoxide radicals and hydrogen peroxide in the target cells (5). Mavrodi et al. investigated the biosynthesis pathway of phenazines in *P. fluorescens* 2-79 (6).

Genomic DNA of *P. fluorescens* 2-79 was isolated by using the MasterPure Complete DNA and RNA purification kit (Epicentre, Madison, WI, USA). A shotgun sequencing library was generated employing the Nextera DNA sample preparation kit following the manufacturer's instructions. The whole genome of *P. fluorescens* 2-79 was sequenced with the Genome Analyzer IIx (Illumina, San Diego, CA, USA). In total, 8.5 million paired-end reads of 112 bp were generated. *De novo* assembly of all shotgun reads using SPAdes version 3.0.0 (7) resulted in 143 contigs >3 kb and 123-fold coverage. The draft genome sequence comprises 6.4 Mb and a GC content of 59.83%. Genome annotation was performed by using Prokka (8). The draft genome harbored 1 rRNA cluster, 47 tRNA genes, 4,286 protein-encoding genes with function prediction, and 1,388 genes coding for hypothetical proteins.

Proteins involved in secondary metabolism were analyzed. The gene *hcnA* (GenBank accession no. 15560558) involved in HCN synthesis and the phenazine operon (GenBank accession no. L48616.1) are present in *P. fluorescens* 2-79. The gene *phlD* (GenBank accession no. 15563828) necessary for the synthesis of 2,4-diacetylphloroglucinol (DAPG) is absent in 2-79.

Nucleotide sequence accession numbers. This whole-genome shotgun project has been deposited at DDBJ/EMBL/GenBank under the accession number JXCQ00000000. The version described in this paper is the first version, JXCQ01000000.

ACKNOWLEDGMENTS

This work was supported by the Federal Ministry of Education and Research (BMBF) BioFung project and the DFG through grants awarded to G.H.B. We also are grateful for support provided by USDA-NRI grant no. 2011-67019-30212 from the USDA-NIFA Soil Processes program.

REFERENCES

1. **Haas D, Défago G.** 2005. Biological control of soil-borne pathogens by fluorescent pseudomonads. Nat Rev Microbiol 3:307–319. http://dx.doi.org/10.1038/nrmicro1129.
2. **Cook RJ, Rovira AD.** 1976. The role of bacteria in the biological control of *Gaeumannomyces graminis* by suppressive soils. Soil Biol Biochem 8:269–273. http://dx.doi.org/10.1016/0038-0717(76)90056-0.
3. **Weller DM, Cook RJ.** 1983. Suppression of take-all of wheat by seed treatments with fluorescent pseudomonads. Phytopathology 73:463–469. http://dx.doi.org/10.1094/Phyto-73-463.
4. **Mavrodi DV, Blankenfeldt W, Thomashow LS.** 2006. Phenazine compounds in fluorescent *Pseudomonas* spp. biosynthesis and regulation. Annu Rev Phytopathol 44:417–445. http://dx.doi.org/10.1146/ annurev-.phyto.44.013106.145710.
5. **Hassett DJ, Woodruff WA, Wozniak DJ, Vasil ML, Cohen MS, Ohman DE.** 1993. Cloning and characterization of the *Pseudomonas aeruginosa sodA* and *sodB* genes encoding manganese- and iron-cofactored superoxide

dismutase: demonstration of increased manganese superoxide dismutase activity in alginate-producing bacteria. J Bacteriol 175:7658–7665.
6. **Mavrodi DV, Peever TL, Mavrodi OV, Parejko JA, Raaijmakers JM, Lemanceau P, Mazurier S, Heide L, Blankenfeldt W, Weller DM, Thomashow LS.** 2010. Diversity and evolution of the phenazine biosynthesis pathway. Appl Environ Microbiol 76:866–879. http://dx.doi.org/10.1128/AEM.02009-09.
7. **Bankevich A, Nurk S, Antipov D, Gurevich AA, Dvorkin M, Kulikov AS, Lesin VM, Nikolenko SI, Pham S, Prjibelski AD, Pyshkin AV, Sirotkin AV, Vyahhi N, Tesler G, Alekseyev MA, Pevzner PA.** 2012. SPAdes: a new genome assembly algorithm and its applications to single-cell sequencing. J Comput Biol 19:455–477. http://dx.doi.org/10.1089/cmb.2012.0021.
8. **Seemann T.** 2014. Prokka: rapid prokaryotic genome annotation. Bioinformatics 30:2068455–2069. http://dx.doi.org/10.1093/bioinformatics/btu153.

Chapter 4: Fluorescent pseudomonads pursue media-dependent strategies to inhibit growth of pathogenic *Verticillium* fungi

Kai Nesemann[1], Susanna A. Braus-Stromeyer[1], Rebekka Harting[1], Annalena Höfer[1], Harald Kusch[1,2], Alinne Batista Ambrosio[1], Christian Timpner[1], Gerhard H. Braus[1*]

[1]Institute of Microbiology and Genetics and Göttingen Center for Molecular Biosciences (GZMB), Georg-August-Universität Göttingen, Germany.

[2]present address: Department of Medical Informatics, Georg-August-Universität Göttingen, Germany.

* Corresponding author: Gerhard H. Braus, Grisebachstraße 8, 37077 Göttingen, Germany, Telephone: +49-551-3933771; Fax: +49-551-3933330; E-mail: gbraus@gwdg.de

Author contributions:

Fig 1: AA, KN

Fig 2: AA, KN

Fig 3: AA, KN

Fig 4: AA, KN

Fig 5: AA, KN

Fig 6: RH, AH

Fig 7: RH, AH

Fig S1: RH, CT

Table 1: KN

Table: 2: RH, AH

Table S1: RH, AH, KN

Table S2: RH, CT

Table S3: RH, CT

Table S4: KN

Supervision and scientific advice: GB, SB, RH, HK

Manuskript: GB, RH, AH, KN

Appl Microbiol Biotechnol
https://doi.org/10.1007/s00253-017-8618-5

APPLIED GENETICS AND MOLECULAR BIOTECHNOLOGY

Fluorescent pseudomonads pursue media-dependent strategies to inhibit growth of pathogenic *Verticillium* fungi

Kai Nesemann[1] · Susanna A. Braus-Stromeyer[1] · Rebekka Harting[1] · Annalena Höfer[1] · Harald Kusch[1,2] · Alinne Batista Ambrosio[1] · Christian Timpner[1] · Gerhard H. Braus[1]

Received: 9 August 2017 / Revised: 30 October 2017 / Accepted: 30 October 2017

Abstract *Verticillium* species represent economically important phytopathogenic fungi with bacteria as natural rhizosphere antagonists. Growth inhibition patterns of *Verticillium* in different media were compared to saprophytic *Aspergillus* strains and were significantly more pronounced in various co-cultivations with different *Pseudomonas* strains. The *Brassica napus* rhizosphere bacterium *Pseudomonas fluorescens* DSM8569 is able to inhibit growth of rapeseed (*Verticillium longisporum*) or tomato (*Verticillium dahliae*) pathogens without the potential for phenazine or 2,4-diacetylphloroglucinol (DAPG) mycotoxin biosynthesis. Bacterial inhibition of *Verticillium* growth remained even after the removal of pseudomonads from co-cultures. Fungal growth response in the presence of the bacterium is independent of the fungal control genes of secondary metabolism *LAE1* and *CSN5*. The phenazine producer *P. fluorescens* 2-79 (P_phen) inhibits *Verticillium* growth especially on high glucose solid agar surfaces. Additional phenazine-independent mechanisms in the same strain are able to reduce fungal surface growth in the presence of pectin and amino acids. The DAPG-producing *Pseudomonas protegens* CHA0 (P_DAPG), which can also produce hydrogen cyanide or pyoluteorin, has an additional inhibitory potential on fungal growth, which is independent of these antifungal compounds, but which requires the bacterial GacA/GacS control system. This translational two-component system is present in many Gram-negative bacteria and coordinates the production of multiple secondary metabolites. Our data suggest that pseudomonads pursue different media-dependent strategies that inhibit fungal growth. Metabolites such as phenazines are able to completely inhibit fungal surface growth in the presence of glucose, whereas GacA/GacS controlled inhibitors provide the same fungal growth effect on pectin/amino acid agar.

Keywords Phenazines · 2,4-diacetylphloroglucinol · gacA/gacS-two component system · *Verticillium* · *Pseudomonas*

Introduction

The dynamic microbiome of the plant rhizosphere comprises various bacteria and fungi with mutual interactions. Biocontrol of fungal plant pathogens requires the understanding of fungal-bacterial biocoenosis and the investigation of antagonistic mechanisms. Hemibiotrophic pathogens of the genus *Verticillium* enter the endosphere of host plants from the rhizosphere through the roots and colonize the xylem vessels (Pegg 1989). Three main pathogenic *Verticillium* species are distributed within temperate world regions (Inderbitzin et al. 2011). *Verticillium dahliae* and *Verticillium albo-atrum* exhibit a host range of more than 200 plant species, including important crops such as cotton, olive, and tomato (Pegg and Brady 2002; Fradin and Thomma 2006). *Verticillium longisporum* is an amphidiploid hybrid of *Verticillium dahliae* and unknown haploid *Verticillium* species, which mainly infects Brassicaceae such as oil-containing rapeseed (Singh et al. 2012; Tran et al. 2013; Depotter et al. 2016). The ecological and economical relevance of the fungal pathogen

Electronic supplementary material The online version of this article (https://doi.org/10.1007/s00253-017-8618-5) contains supplementary material, which is available to authorized users.

✉ Gerhard H. Braus
gbraus@gwdg.de

[1] Institute of Microbiology and Genetics and Goettingen Center for Molecular Biosciences (GZMB), University of Goettingen, Grisebachstraße 8, 37077 Goettingen, Germany

[2] Present address: Department of Medical Informatics, University of Goettingen, Goettingen, Germany

Published online: 18 November 2017

V. longisporum increased with the utilization of rapeseed oil for nutrition and regenerative fuel production.

The use of naturally occurring microorganisms from the rhizosphere with antagonistic biocontrol activity is an approved alternative to chemical treatment of plants in agriculture. Antagonists with a suppressive potential towards pathogens in the soil include fungi as well as bacteria (Sikora 1992). The beneficial rhizofungus *Coniothyrium minitans* for example is commercially produced (Bayer CropScience Biologics GmbH 2017) and exhibits biocontrol activity against the plant pathogenic fungus *Sclerotinia sclerotiorum* (Zeng et al. 2012). The rhizobacterium *Bacillus subtilis* exhibits antagonism, mediated by biofilm formation on plant roots, towards several phytopathogenic organisms such as *Ralstonia solanacearum*, which causes tomato wilt (Chen et al. 2013). Tomato root-associated *Bacillus* strains were able to inhibit *V. dahliae* growth on plate (Hollensteiner et al. 2017).

Fluorescent pseudomonads represent a diverse group of γ-proteobacteria that interact with plants and possess well-characterized beneficial properties (Weller et al. 2002). They secrete diffusible and volatile bioactive compounds, which act antagonistically towards fungal pathogens (Bender et al. 1999; Traxler and Kolter 2015). Phenazines are common colored bacterial secondary metabolites, which interact synergistically with biosurfactants (Perneel et al. 2008). Biosurfactants permeabilize host membranes, allowing phenazines to enter the cells and inhibit mitochondrial electron transport (Perneel 2006; Mavrodi et al. 2010). The mycotoxins 2,4-diacetylphloroglucinol (DAPG), pyoluteorin, pyrrolnitrin, hydrogen cyanide (HCN), as well as exoproteases are regulated by the translational GacA/GacS-two-component system. Still unknown external signals trigger the autophosphorylation of the GacS sensor kinase and the phosphate transfer to the GacA response regulator, which induces translational repression of target mRNAs (Haas and Défago 2005; Nandi et al. 2015). The 2,4-diacetylphloroglucinol producing *Pseudomonas protegens* CHA0 from the rhizosphere has been identified as an organism possessing one of the broadest biocontrol repertoires (Weller 2007).

The media-dependent interplay between fluorescent pseudomonads, which differ in their genetic potential to produce secreted bioactive metabolites and the growth potential of various fungal *Verticillium* spp. strains was compared. Bacteria reduced fungal growth by distinct different strategies when nutritional conditions change from glucose to pectin/amino acids. The bacterial GacA/GacS-two-component system, which controls numerous metabolites, is important for bacterial-meditated inhibition of fungal growth, whereas the fungal control of metabolites by regulators as Lael or Csn5 are not relevant for the bacterial-fungal interaction under the tested conditions. Bacterial inhibition of fungal growth was so efficient that removal of pseudomonads from a co-culture did not allow *V. dahliae* to resume growth. The inhibition potential of pseudomonads towards saprophytic *Aspergillus* species is significantly reduced in comparison to plant pathogenic *Verticillium* species.

Materials and methods

Bacterial and fungal strains are listed in Table S1, primers in Table S2 and plasmids in Table S3. Figure artwork has been performed with Adobe Illustrator, Adobe Photoshop, GIMP (The GIMP team, version 2.8) and ChemDraw (® PerkinElmer Informatics).

Cultivation and co-cultivation of bacteria and fungi

The media for fungal cultivation included potato dextrose agar (PDA; from Roth, Karlsruhe, Germany) consisting of potato starch, as well as the pectin and amino acids-containing simulated xylem medium (SXM; casein hydrolysate from Oxoid, Hamphire, England; Pectin from citrus peel from Sigma-Aldrich Chemie GmbH, St. Louis, USA). The latter was based on the recipe from (Neumann and Dobinson 2003) and modified as follows: 0.4% casein; 0.2% pectin; 2% 50× AspA (3.5 M $NaNO_3$, 350 mM KCL, 550 mM KH_2PO_4); 0.2% 1 M $MgSO_4$; and 1× trace elements (Scott and Kafer 1982). For cultivation in liquid medium, 1×10^6 spores were inoculated in 150 ml medium in 500 ml Erlenmeyer flasks, which were incubated on a shaker at 150 rpm. Plates contained 2% agar and were inoculated with 1×10^5 spores, which were spread using glass beads. Fungal cultures were incubated for 6 days at 25 °C. SXM cultures were filtered through Miracloth (EMD Millipore Corp., Billerica, USA) to harvest spores. The filtrate was centrifuged for 3 min at 3500 rpm and washed twice with sterile water. The spores were stored in a physiological solution (0.96% NaCl, 0.05% Tween 80) at 4 °C. The number of spores was determined with a particle counter (Beckman Coulter, Brea, CA USA) and adjusted to a concentration of 1×10^6 spores ml^{-1}.

Bacteria were cultivated in Lysogeny broth (Bertani 1951) or SXM medium overnight at 30 °C. The concentration was determined by photometry and converted to colony-forming units (CFU; $OD_{600nm} = 1$ or $\approx 5 \times 10^8$ CFU ml^{-1}) (Cui 2005). For co-cultivations on solid medium, spores were plated, a hole of 1 cm in diameter was excised in the center of the plate and 60 µl of a bacterial suspension ($OD_{600nm} = 1$) were used for inoculation. Plates were incubated for 7 days at 25 °C. The diameter of the resulting cyclic inhibition zone was measured and documented. Comparative co-cultivation experiments on solid media with *V. dahliae*, *Aspergillus nidulans* and *Aspergillus fumigatus* were conducted on PDA and pectin and amino acids containing SXM as described before. Plates were incubated for 4 days at 25 °C.

For co-cultivations in liquid medium, 100 µl of a bacterial suspension (OD_{600nm} = 1) were used for inoculation of SXM or potato dextrose medium (PDM; potato dextrose glucose broth from Roth, Karlsruhe, Germany) together with 1×10^6 *V. dahliae* spores. Co-cultures were grown under constant agitation. After 0, 12, 24, 48, 72, and 96 h, 3 × 10 µl of the culture were plated on SXM or PDA plates containing kanamycin (final concentration 50 µg ml^{-1}; from AppliChem GmbH, Maryland Heights, USA); cefotaxime (final concentration 300 µg ml^{-1}; from Wako Pure Chemical Industries, Osaka, Japan), and doxycycline (final concentration 40 µg ml^{-1}; from Sigma-Aldrich Chemie GmbH, St. Louis, USA). Plates were incubated for 3 days at 25 °C. Bacterial survival was tested after 96 h of co-cultivation. Then, 10 µl of the culture were plated on LB medium and incubated at 25 °C for 3 days.

Construction of *V. dahliae* deletion and gene disruption strains

For construction of a gene disruption cassette, 5′ and 3′ flanking regions of the *LAE1* gene were amplified by PCR with primers VD*LAE*F1Lc/VD*LAE*F1Rc and VD*LAE*F2Lc/VD*LAE*F2Rc, respectively. The 3′ flanking region of LAE1 was inserted 3′ of the nourseotricin resistance cassette into the pKO2 vector (Timpner et al. 2013) using *Bam*HI/*Pst*I restriction sites. Next, the 5′ flanking region of the gene was inserted into the vector using *Eco*RI/*Eco*RV restriction sites, placing it 5′ of the nourseotricin resistance marker. The resulting plasmid pME3990 (Table S3) was used for *Agrobacterium tumefaciens*-mediated transformation (Bundock et al. 1995) of *V. dahliae* JR2 (Fradin et al. 2009). For the deletion of *CSN5*, the flanking regions of the gene were amplified with the primers *CSN5* P1, *CSN5* P2, *CSN5* P3, and *CSN5* P4. The fragments were inserted into the pKO2 vector using *Eco*RI/*Eco*RV or *Xba*I/*Hin*dIII restriction sites, respectively. The resulting plasmid pME4412 (Table S3) was used for *A. tumefaciens*-mediated transformation of *V. dahliae* JR2. Transformants were verified by Southern hybridization using the AlkPhos Direct Labeling and Detection System (GE healthcare life sciences, Buckinghamshire, UK).

Analysis of *Pseudomonas* genome data

The genomes of the *Pseudomonas* wild-type strains used in this study were searched for secondary metabolism related genes, which might be involved in the antagonistic activity of the isolate. Genome sequences of P_phen and P_rhizo (Nesemann et al. 2015a, b) were further analyzed by biblast search using the sequence of P_DAPG (Jousset et al. 2014) as reference.

Results

Pseudomonas fluorescens DSM8569 isolated from the *Brassica* rhizosphere exhibits a similar inhibition potential for the rapeseed pathogen *V. longisporum* as for the tomato pathogen *V. dahliae*

Fluorescent pseudomonads can inhibit the growth of fungal pathogens and are therefore used as biocontrol organisms (Weller et al. 2002). *Pseudomonas fluorescens* DSM8569 (P_rhizo) colonizes the rhizosphere of the plant *Brassica napus* and was isolated in northern Germany (Berg and Ballin 1994). The genome of P_rhizo does not contain the gene cluster for the production of the mycotoxic phenazines, which are secreted by other pseudomonads. The DAPG gene cluster for the production of the antifungal compound 2,4-diacetylphloroglucinol is only partially conserved in this strain (Table 1, S4) (Nesemann et al. 2015a).

It was examined whether this bacterium is able to affect the growth of the *B. napus* pathogen *V. longisporum*. The 1×10^5 *Verticillium* spores were distributed on a D-glucose rich medium plate (PDA), containing a central hole filled with 7×10^7 CFU of P_rhizo. An inhibition zone without fungus of 8 mm was visible after 7 days of incubation (Fig. 1a), indicating that the bacteria inhibit growth of the *B. napus* pathogen *V. longisporum*. The observed growth inhibition on PDA medium was compared to co-cultivation on SXM plates, which contain pectins and amino acids. On this medium, no inhibition zone was observed. Fungal control plates in the presence of *Escherichia coli* (DH5α) or in the absence of any bacteria were unaffected in growth (Fig. 1a). The lack of a phenazine cluster and the presence of an incomplete DAPG cluster in the P_rhizo genome suggest that bacterial inhibition of fungal growth in the presence of glucose requires neither phenazines nor DAPG.

P_rhizo was isolated from the *Brassica* rhizosphere (Berg and Ballin 1994). We analyzed whether related fungal pathogens, which are pathogens in rhizospheres of other plant hosts, are similarly affected in growth. Co-cultivation experiments of P_rhizo with the tomato pathogen *V. dahliae* JR2 (Fradin et al. 2009) revealed a similar inhibition potential to the rapeseed pathogen *V. longisporum* on high glucose medium (inhibition zone 9.3 mm ± 0.8) and a slight inhibition on pectin/amino acid agar (inhibition zone 2.3 mm ± 0.5) (Fig. 1b). Thus, the antifungal activity of P_rhizo is not limited to fungal pathogens from its natural habitat.

Fungi produce numerous bioactive secondary metabolites (Bayram and Braus 2012), which could influence fungal-bacterial interactions. It was examined whether genes that control secondary metabolism of model fungi influence the suppressive effect of pseudomonads against *V. dahliae*. The *A. nidulans* methyltransferase LaeA represents a conserved global regulator of secondary metabolism in many

Table 1 Comparison of genome potentials of *P. fluorescens* DSM8569 (P_rhizo), *P. fluorescens* 2–79 (P_phen), and *P. protegens* CHA0 (P_DAPG)

Organism	Phenazine cluster	DAPG cluster	HCN cluster	Pyoluteorin-cluster	GacA/GacS-system	GacA/GacS-regulation
P_rhizo	–	o	+	–	+	o
P_phen	+	–	o	–	+	o
P_DAPG	–	+	+	+	+	+

Gene clusters for bioactive compounds as phenazines, DAPG, HCN, pyoluteorin, or the GacA/GacS control system are indicated: gene cluster completely present: +; partial gene cluster: o; gene cluster absent: –

ascomycetes (Bok and Keller 2004; Bayram et al. 2008; Sarikaya-Bayram et al. 2010). A *V. dahliae LAE1* deletion strain (Vd*ΔLAE1*) was constructed (Fig. S1) to investigate whether growth of the fungal mutant is further reduced in the presence of the P_rhizo bacterium. Vd*ΔLAE1* displayed a similar growth inhibition as the wild type during co-

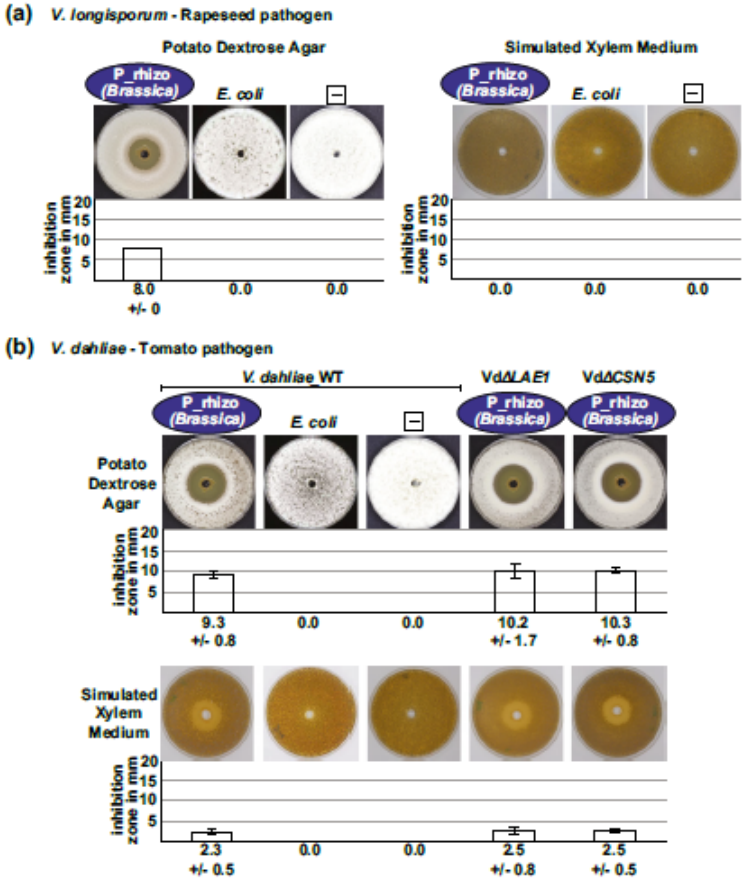

Fig. 1 Inhibition zone during co-cultivation of the rapeseed pathogen *Verticillium longisporum* Vl43 or the tomato pathogen *V. dahliae* JR2 with the *Brassica* rhizosphere isolate *P. fluorescens* DSM8569 (P_rhizo). Co-cultivations were performed on solid potato dextrose medium (containing glucose) and simulated xylem medium (containing pectin and amino acids). 1×10^5 fungal spores were homogeneously inoculated on the plates. Then, 7×10^7 colony-forming units of a bacterial culture were inoculated into a central hole in the agar plate. The diameter of the hyphae-free inhibition zone in millimeters was determined after 7 days of incubation at 25 °C. Example plates are depicted. The graph includes data of two biological (including each three technical) replicates. An inhibition zone was defined as an area where no hyphae could be monitored and fungal growth was completely suppressed. The mean values and standard deviations are given beneath the graph. **a** Co-cultivation of *Brassica*-hosting *V. longisporum* Vl43 in the presence (P_rhizo; *Brassica*) and absence (−) of the *Brassica* rhizosphere isolate P_rhizo (*P. fluorescens* DSM8569), as well as in the presence of *E. coli* (strain DH5α). **b** Co-cultivation of the tomato-hosting *V. dahliae* JR2 in the presence and absence of P_rhizo, as well as in the presence of *E. coli* (strain DH5α) and *V. dahliae* JR2 deletion strains lacking *LAE1* (Vd*ΔLAE1*) or *CSN5* (Vd*ΔCSN5*)

cultivation with P_rhizo on glucose rich PDA medium (inhibition zone 10.2 mm ± 1.7) and pectin-containing SXM (inhibition zone 2.5 mm ± 0.8) (Fig. 1b), suggesting that Lae1 controlled fungal secondary metabolites are not relevant for fungal growth during the *Verticillium-Pseudomonas* interaction.

The fungal COP9 signalosome controls cellular ubiquitination and protein degradation and is required for coordinated secondary metabolism (Nahlik et al. 2010). In the absence of the COP9 deneddylase subunit, the secondary metabolism of *A. nidulans* is misregulated. The *V. dahliae CSN5* gene, which encodes the deneddylase subunit, was deleted (Fig. S1). Growth of the Vd*ΔCSN5* strain was similar to wild type during co-cultivation with P_rhizo (inhibition zone 10.3 mm ± 0.8 for cultivation on PDA and 2.5 mm ± 0.8 for cultivation on SXM) (Fig. 1b). This suggests that neither Lae1 nor Csn5 controlled fungal secondary metabolism is relevant for *Pseudomonas* fungal interactions.

In summary, the *B. napus* rhizosphere bacterium *P. fluorescens* DSM8569 (P_rhizo), is not only able to inhibit the growth of a rapeseed pathogenic fungus, but also that of a tomato pathogen, without having the potential to synthesize typical *Pseudomonas* mycotoxins such as phenazines or DAPG. Fungal growth response in the presence of the bacterium is independent of fungal control genes of secondary metabolism such as *LAE1* or *CSN5*.

Phenazine-mediated growth inhibition of *Verticillium* species on solid agar surfaces is increased in high glucose medium

Pseudomonas fluorescens P_rhizo does not require an intact phenazine gene cluster to reduce fungal growth (Nesemann et al. 2015a) (Table 1, S4). Surface growth of *V. longisporum* or *V. dahliae* was analyzed in the presence of *Pseudomonas* strains secreting phenazines to monitor whether the fungal strains are sensitive. The phenazine producer *P. fluorescens* 2–79 (P_phen) has been isolated from wheat roots suppressive to the plant disease "take-all" (Weller and Cook 1983). Significant surface growth inhibition of *V. longisporum* and *V. dahliae* was caused by the phenazine producer P_phen on high glucose agar (inhibition zone 7.7 mm ± 0.8 for *V. longisporum* and 5.8 mm ± 0.8 for *V. dahliae*). In the presence of pectin and amino acids, bigger inhibition zones of 13.0 mm ± 0.6 for *V. longisporum* and 15.0 mm ± 0.9 for *V. dahliae* were visible (Fig. 2). Co-cultivation with the isogenic phenazine-deficient mutant strain P_phen*Δphz* (Khan et al. 2005) revealed that growth inhibition of *V. longisporum* (inhibition zone 13.2 mm ± 1.8) and *V. dahliae* (inhibition zone 15.0 mm ± 0.6) on pectin/amino acid agar is independent of the phenazine cluster. These genes are only required for fungal growth inhibition on high glucose agar as on this medium an inhibition zone was neither visible for *V. longisporum* nor for *V. dahliae* (Fig. 2).

Co-cultivation with *V. dahliae* Vd*ΔLAE1* and Vd*ΔCSN5* strains suggested that there is no significant function of the fungal *LAE1* or *CSN5* control genes of secondary metabolism for bacterial-fungal interactions (Fig. 3). On high-glucose medium, the inhibition zone of co-cultures with the P_phen wildtype was 6.2 mm ± 0.8 for the *LAE1* deletion strain and 4.7 mm ± 1.5 for the *CSN5* deletion strain, which is very similar to the effects observed for the wild type (inhibition zone 5.8 mm ± 0.8). For the phenazine-deficient bacterial mutant strain, no inhibition of the *LAE1* and the *CSN5* deletion strain could be observed on PDA medium. The inhibition zones on SXM ranged between 14 and 16 mm for the two deletion strains, which is comparable to that of the wild-type strain (inhibition zone 15 mm ± 0.9) (Fig. 2). Our experiments support a media-dependent fungal growth inhibition by phenazines on high glucose agar. Additional phenazine-independent mechanisms in the phenazine-deficient P_phen*Δphz* strain are able to reduce fungal surface growth in the presence of pectin and amino acids.

Bacterial inhibition of *Verticillium* surface growth on pectin/amino acid medium is independent of an intact gene cluster for 2,4-diacetylphloroglucinol

Several fluorescent pseudomonads produce the antifungal secondary metabolite

2,4-diacetylphloroglucino (DAPG) (Meyer et al. 2009; Kwak et al. 2011). The genome of P_rhizo encodes only a partial DAPG cluster and it is therefore unlikely that this bacterium produces DAPG (Table 1, S4). A DAPG secreting *P. protegens* strain CHA0 (P_DAPG) was isolated from tobacco rhizosphere suppressive against the fungal disease black root rot (Stutz et al. 1986; Schnider-Keel et al. 2000). The impact of CHA0 (P_DAPG) on *Verticillium* growth was analyzed by co-cultivation on agar plates. Co-cultivations with P_DAPG and *V. longisporum* or *V. dahliae* resulted in a clear inhibitory effect on pectin/amino acid as well as on high glucose agar (Fig. 4). When *V. longisporum* was co-cultured with P_DAPG on potato dextrose medium, an inhibition zone of 9.3 mm ± 2.3 was observed. The effect of the bacterium on *V. dahliae* on this medium was similar with an area without fungal growth of 7.2 mm ± 1.7. On simulated xylem medium, the effect on *V. longisporum* (inhibition zone 7.7 mm ± 1.6) and *V. dahliae* (inhibition zone 8.0 mm ± 0.9) was also comparable.

Fungal co-cultivations with *P. protegens* strains lacking or overproducing DAPG (P_DAPG*ΔphlA* and P_DAPG*ΔphlF*, respectively) resulted in a similar inhibition of fungal growth as observed for the *P. protegens* wild type on pectin/amino acid medium. Respective inhibition zones averaged 7.7 mm ± 0.5 for cultivation of P_DAPG*ΔphlA* and 7.2 mm ± 0.4 for P_DAPG*ΔphlF* together with *V. longisporum*. For co-cultivation with *V. dahliae*, the areas without fungal growth

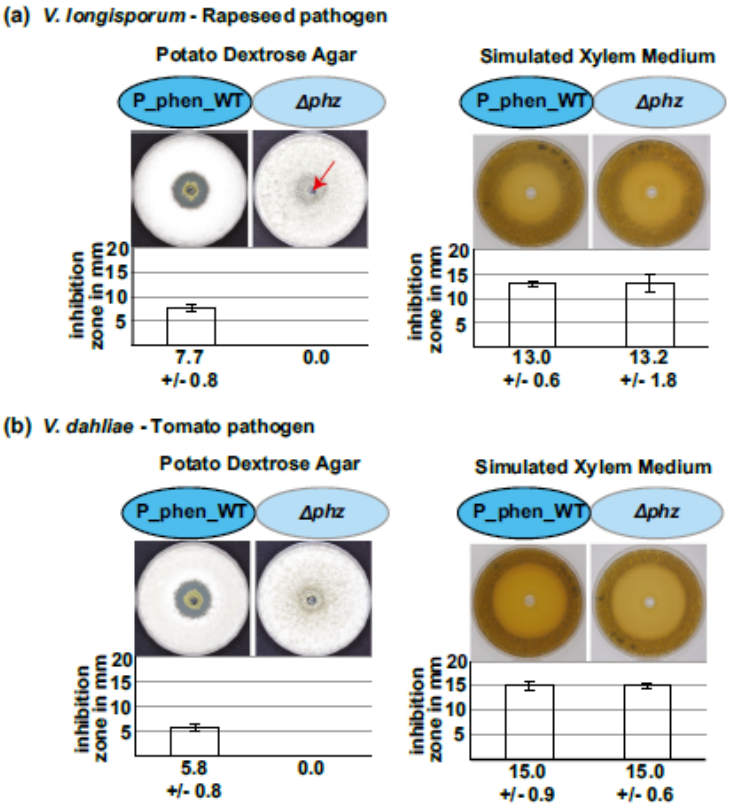

Fig. 2 Inhibition zone during co-cultivation of *V. longisporum* Vl43 or *V. dahliae* JR2 with phenazine-producing *P. fluorescens* 2-79. Co-cultivation of 1×10^5 fungal spores and 7×10^7 colony-forming units of bacterial culture was performed on potato dextrose agar and simulated xylem medium as described in Fig. 1. Diameters of hyphae-free inhibition zones in millimeter were determined after 7 days of incubation at 25 °C as described in Fig. 1. Co-cultivation of *Verticillium* spp. in the presence of the phenazine-producing P_phen wild type (WT: *P. fluorescens* 2–79), as well as in presence of a phenazine-deficient deletion strain (Δ*phz*). **a** Co-cultivation with *Brassica*-infecting *V. longisporum* VL43. **b** Co-cultivation with tomato-infecting *V. dahliae* JR2

were 8.3 mm ± 0.5 for P_DAPGΔ*phlA* and 8.5 mm ± 0.8 for P_DAPGΔ*phlF*. On high glucose agar, a contribution of DAPG on the size of inhibition zones was observed. Deletion of *phlA* slightly reduced the inhibitory effect (inhibition zone 7.0 mm ± 0.6 for *V. longisporum* and 6.3 mm ± 1.5 for *V. dahliae*). Overproduction of DAPG in the *phlF* deletion strain had the opposite effect. Whereas the inhibitory potential of the bacterium is slightly increased towards *V. longisporum* (inhibition zone 11.7 mm ± 0.8), the area without fungal growth is approximately doubled in co-cultures with *V. dahliae* (inhibition zone 14.5 ± 2.1) compared to the inhibition zone of the fungus with the bacterial wild type. This suggests that DAPG production contributes to the inhibitory effect of the bacterium on fungal growth on high glucose medium but there is a DAPG-independent fungal growth inhibition mechanism on both media (Fig. 4).

The P_DAPG strain secretes a number of additional bioactive metabolites. Hydrogen cyanide (HCN) acts by blocking the oxygen-binding site in the respiratory chain (Hamel 2011). Bacterial mutant strains with deletions in HCN-producing genes (P_DAPGΔ*hcn*, Δ*anr*) resulted in fungal inhibition zones ranging between 7 and 9 mm, which are similar in size compared to the inhibition of the bacterial wild type on both tested media (Fig. 4). Antifungal pyoluteorin composed of a bichlorinated pyrrole ring (Nowak-Thompson et al. 1999) is produced by P_DAPG. A pyoluteorin deficient mutant strain (P_DAPGΔ*plt*) still reduced *V. longisporum* or *V. dahliae* growth c.f. wild type (inhibition zones of 8.7 mm ± 2.3 and 6.7 mm ± 2.0 on PDA and 6.7 mm ± 0.8 and 8.3 mm ± 1.4 on SXM, respectively) (Fig. 4).

These data indicate that *P. protegens* CHA0 (P_DAPG) has the potential to inhibit fungal growth using mechanisms that are independent of the production of antifungal compounds such as DAPG, hydrogen cyanide or pyoluteorin.

The bacterial GacA/GacS control system coordinating multiple secondary metabolites is required for fungal growth inhibition on pectin agar surfaces

The *P. protegens* CHA0 (P_DAPG) genome lacks the phenazine gene cluster but possesses genes of the GacA/GacS-two-component system (Table 1, S4). The sensor kinase GacS is autophosphorylated by external signals and transfers the phosphate to the response regulator GacA. Deletion of either *gacA* or *gacS* leads to loss of secretion of bioactive metabolites including DAPG, hydrogen cyanide and pyoluteorin (Laville

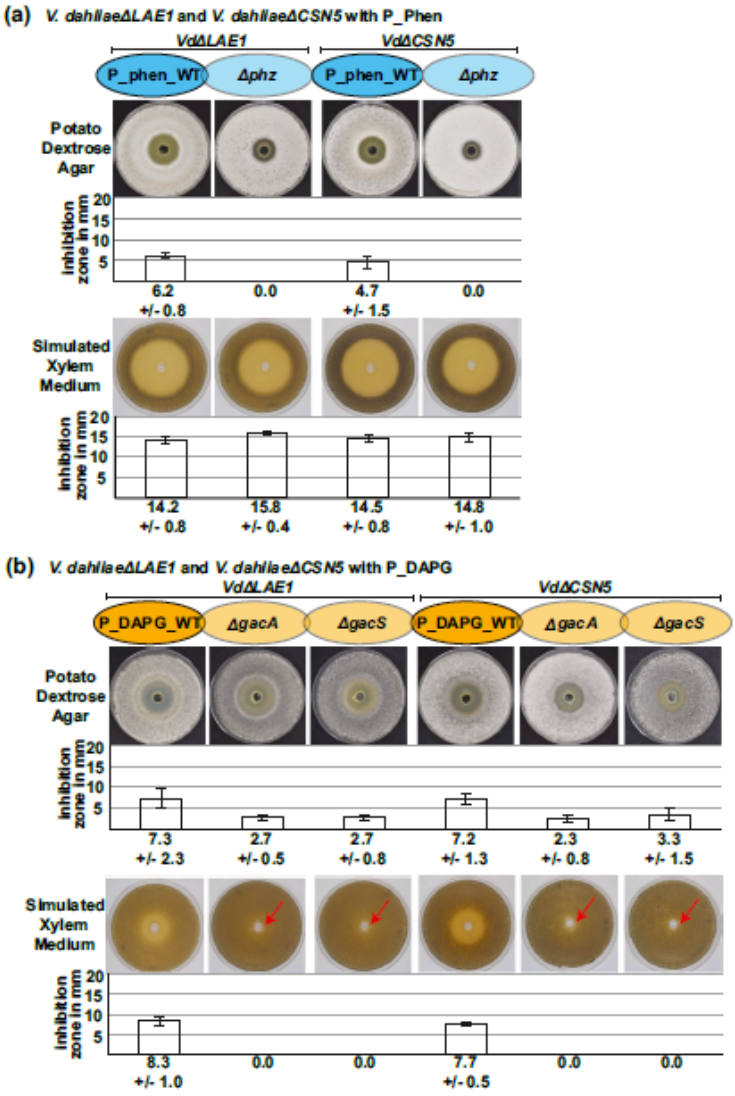

Fig. 3 Inhibition zone during co-cultivation of *V. dahliae* JR2 *LAE1* and *CSN5* deletion strains with phenazine-producing *P. fluorescens* 2-79 or DAPG-producing *P. protegens* CHA0. Co-cultivation of 1×10^5 fungal spores and 7×10^7 colony-forming units of bacterial culture was performed on potato dextrose agar and simulated xylem medium as described in Fig. 1. The diameter of the hyphae-free inhibition zone in mm was determined after 7 days of incubation at 25 °C as described in Fig. 1. a Co-cultivation of *V. dahliae* JR2 deletion strains lacking *LAE1* (VdΔ*LAE1*) or *CSN5* (VdΔ*CSN5*) in presence of the phenazine-producing P_phen wild type (WT: *P. fluorescens* 2–79), as well as in presence of a phenazine deficient deletion strain (Δ*phz*). b Co-cultivation of *V. dahliae* JR2 deletion strains lacking *LAE1* (VdΔ*LAE1*) or *CSN5* (VdΔ*CSN5*) in the presence of the DAPG-producing P_DAPG wild type (WT: *P. protegens* CHA0), and deletion strains restricted in multiple mycotoxin production: Δ*gacA* and Δ*gacS* in which one of the two units for the regulation of multiple toxin production is deleted

et al. 1992; Zuber et al. 2003). The constitutively expressed target genes of the GacA/GacS-system are post-transcriptionally repressed by RsmA and RsmE (Haas and Défago 2005). Phosphorylated GacA activates the expression of derepressors, which inhibit RsmA and RsmE (Laville et al. 1992; Brencic et al. 2009).

Deletion mutants P_DAPGΔ*gacA* and P_DAPGΔ*gacS* co-cultivated with *V. longisporum* or *V. dahliae* were unable to inhibit fungal wild-type growth on agar plates with media of pectin and amino acids (Fig. 5). Similarly, *V. dahliae CSN5* and *LAE1* deletion strains were not inhibited (Fig. 3). The bacterial mutant strains P_DAPGΔ*gacA* and P_DAPGΔ*gacS* were still able to inhibit *V. longisporum* or *V. dahliae* growth on glucose medium agar but with reduced intensity (Fig. 5). The inhibition zones were reduced by more than 50% when *V. longisporum* was co-cultured with the *gacA* or *gacS* deletion strain (inhibition zones 3.2 mm ± 0.4 and 4.3 mm ± 0.5, respectively) when compared to cultivations with the wild-type isolate P_DAPG. The inhibitory potential of P_DAPG towards *V. dahliae* was almost completely lost when *gacA* or *gacS* were deleted in the bacterium (inhibition zone of 1.2 mm ± 1.3 for P_DAPGΔ*gacA* and 1 mm ± 0.9 for P_DAPGΔ*gacS*).

This suggests distinct media-dependent strategies of pseudomonads in the control of fungal growth. Metabolites such as phenazines control fungal surface growth with glucose, whereas GacA/GacS provides inhibitors of fungal growth on pectin/amino acid agar.

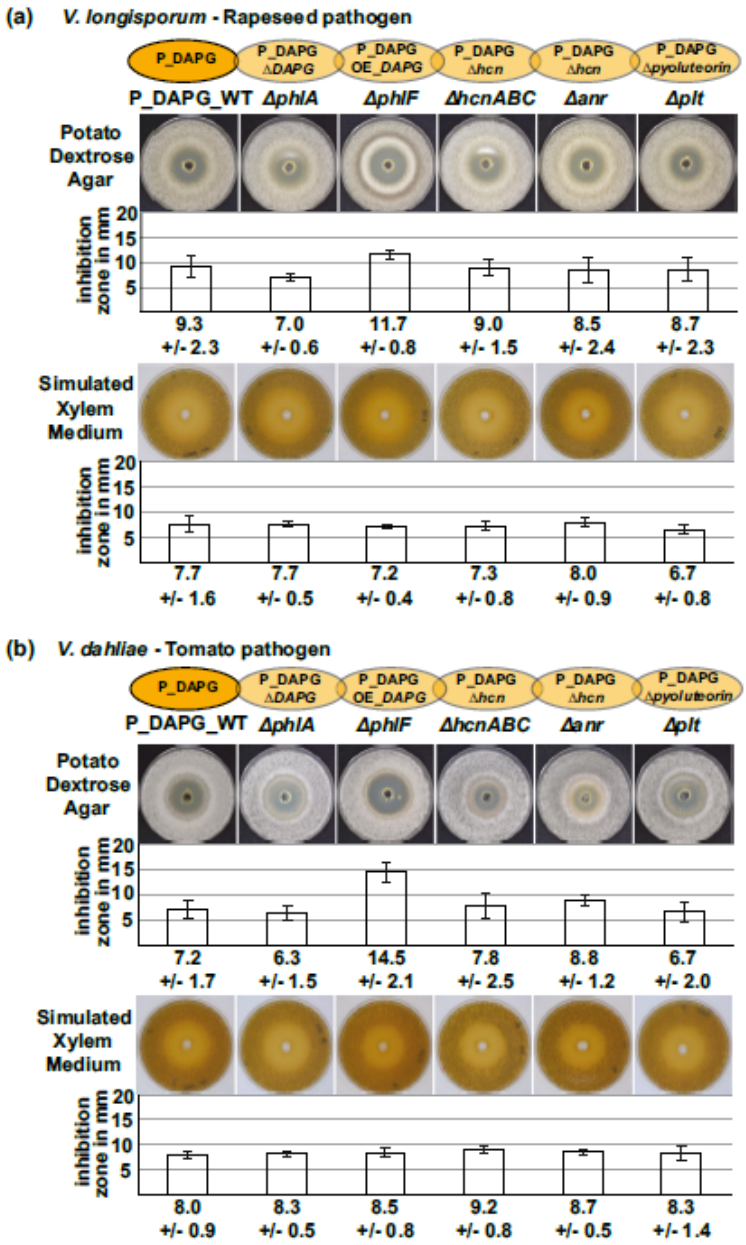

Fig. 4 Inhibition zone during co-cultivation of *V. longisporum* VL43 and *V. dahliae* JR2 with DAPG-producing *P. protegens* CHA0. Co-cultivation of 1×10^5 fungal spores and 7×10^7 colony-forming units of bacterial culture was performed on potato dextrose agar and simulated xylem medium as described in Fig. 1. The diameter of the hyphae-free inhibition zone in millimeters was determined after 7 days of incubation at 25 °C as described in Fig. 1. Co-cultivation of *Verticillium* spp. in the presence of DAPG-producing P_DAPG wild type (WT: *P. protegens* CHA0), or one of the following bacterial deletion strains: Δ*phlA* - lacking one essential gene for DAPG synthesis, without DAPG production; Δ*phlF* - lacking the inhibitor of DAPG production, leading to increased DAPG secretion (Schnider-Keel et al. 2000); Δ*hcnABC* - essential gene for HCN production deleted; Δ*anr* - HCN regulator anr deleted with deficient HCN secretion; Δ*plt* - essential gene for pyoluteorin synthesis deleted strain (Δ*phz*). **a** Co-cultivation with *Brassica*-infecting *V. longisporum* VL43. **b** Co-cultivation with tomato-infecting *V. dahliae* JR2

Efficient fungal growth inhibition of *Brassica* rhizosphere and of phenazine-producing bacteria depends on the nutrient source

All tested bacterial wild-type strains showed a similar inhibitory effect towards both *V. dahliae* and *V. longisporum*, when co-cultivated on solid agar surfaces, which was dependent on nutrition. Co-cultivation experiments of fungal spores together with bacterial cells were performed in liquid medium to further analyze the effect of the different pseudomonads on *V. dahliae*, pectin/amino acid SXM, and high-glucose PDM were used as in the experiments on plates. Culture aliquots were plated on antibiotic containing agar plates after 0, 12, 24, 48, 72, and 96 h of incubation to remove the bacterial cells and to monitor whether the fungus is able to regain growth. Fungal spores cultivated in the absence of pseudomonads or together with *E. coli* cells served as controls. The strongest effect of P_rhizo on fungal growth was observed in high glucose medium

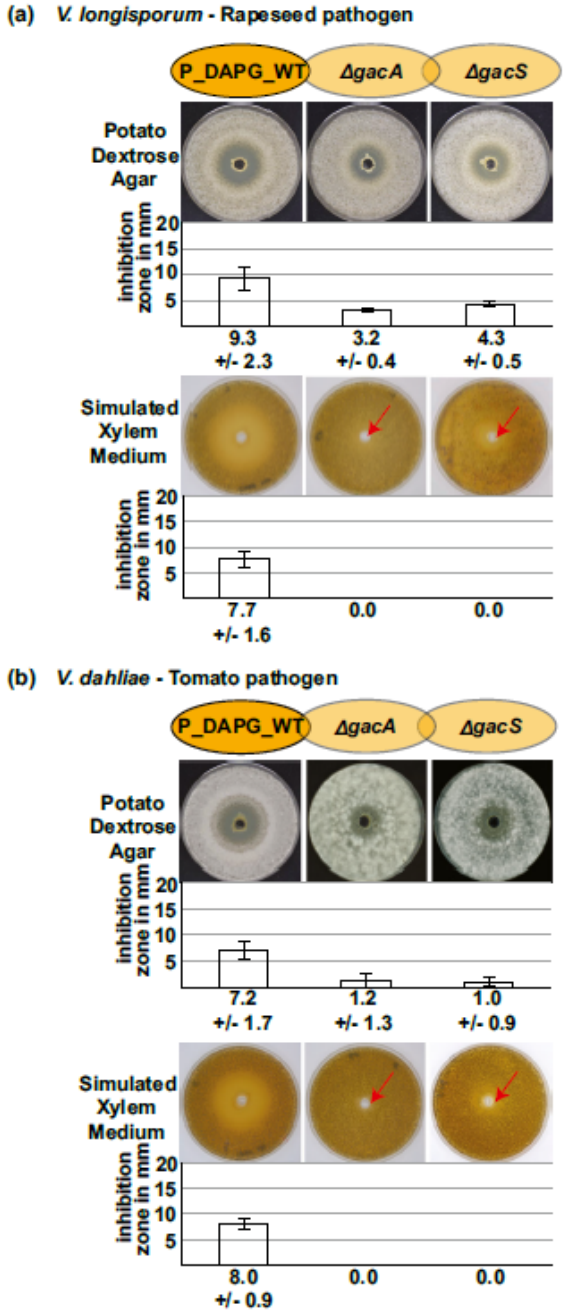

◀ **Fig. 5** Inhibition zone during co-cultivation of *V. longisporum* VL43 and *V. dahliae* JR2 with bacterial *gacA* and *gacS* deletion strains. Co-cultivation of 1×10^5 fungal spores and 7×10^7 colony-forming units of bacterial culture was performed on potato dextrose agar and simulated xylem medium as described in Fig. 1. The diameter of the hyphae-free inhibition zone in millimeters was determined after 7 days of incubation at 25 °C as described in Fig. 1. Co-cultivation of *Verticillium* spp. in presence of DAPG-producing P_DAPG wild type (WT: *P. protegens* CHA0) and corresponding deletion strains restricted in multiple mycotoxin production: Δ*gacA* and Δ*gacS* in which one of the two units for the regulation of multiple toxin production is deleted. **a** Co-cultivation with *Brassica*-infecting *V. longisporum* VL43. **b** Co-cultivation with tomato-infecting *V. dahliae* JR2

(Table 2). The fungus was unable to form colonies after co-cultivation for 48 h when the bacterium was removed by the antibiotic cocktail. This was different for the other tested pseudomonads. For P_DAPG and P_phen fungal growth inhibition in some cultivations was only visible after 72 or 96 h of co-cultivation, respectively, suggesting that these bacteria need more time in co-culture to persistently inhibit fungal growth. When cultured together with *E. coli*, no effects on *V. dahliae* growth could be observed. All bacterial cells were able to form colonies on LB agar plates after 96 h of cultivation with the fungus, supporting our previous observations that the fungus does not compromise bacterial growth. In pectin-/amino acid-containing medium, the strongest effect on the fungus was observed for P_phen: after 24 h of co-cultivation, fungal growth could only be observed on some plates and after 48 h, no fungal growth could be detected. *E. coli*, P_DAPG and P_rhizo did not show significant effects on fungal growth after co-cultivation for up to 96 h and all bacteria formed colonies on LB medium. Our results are in accordance with the observation of the

Table 2 Influence of *P. fluorescens* 2-79 (P_phen), *P. protegens* CHA0P_DAPG, and *P. fluorescens* DSM8569 (P_rhizo) on *V. dahliae* growth after co-cultivation in liquid medium. Bacterial strains were co-cultivated with *V. dahliae* JR2 spores in liquid pectin/amino acid simulated xylem medium or liquid high glucose potato dextrose medium for 0, 12, 24, 48, 72, and 96 h, respectively. Aliquots were plated on antibiotics containing medium and fungal growth was observed after 3 days of incubation at 25 °C. Fungal cultures without bacteria (w/o bacteria) served as control. Data were derived from two independent experiments with three replications each

	w/o bacteria	*E. coli*	P_phen	P_DAPG	P_rhizo
JR2 potato dextrose medium					
0 h	+	+	+	+	+
12 h	+	+	+	+	+
24 h	+	+	+	+	+
48 h	+	+	+	+	–
72 h	+	+	+/–	+	–
96 h	+	+	+/–	+/–	–
JR2 simulated xylem medium					
0 h	+	+	+	+	+
12 h	+	+	+	+	+
24 h	+	+	+/–	+	+
48 h	+	+	–	+	+
72 h	+	+	–	+	+
96 h	+	+	–	+	+

+ = growth in all replicates; – = no growth in all replicates; +/– = growth in some replicates but not all

inhibitory potential on agar surfaces: P_rhizo had the strongest effect on high glucose medium, whereas P_phen is most effective on pectin/amino acid medium. This bacterial inhibition of fungal growth is persistent because the fungus was unable to resume growth, even after the bacterium had been removed.

The inhibition potential of pseudomonads towards saprophytic *Aspergillus* species is reduced in comparison to plant pathogenic *V. dahliae*

Bacteria in the rhizosphere encounter not only plant-pathogenic fungi as *V. longisporum* or *V. dahliae* but also soilborne saprophytic fungi as *Aspergillus* species. We performed co-cultivation experiments with *A. nidulans* or the opportunistic human pathogen *A. fumigatus* with all three bacterial wild-type strains to investigate the specificity of the inhibitory potential on fungal growth. The inhibition effects of all tested pseudomonads towards the *Aspergillus* strains are decreased when compared to the effects on *V. dahliae* (Fig. 6).

On high-glucose PDA medium, there was only a minimal effect (approx. 1-mm inhibition) observed for the co-cultivation of P_DAPG with *A. fumigatus* but not for co-cultures of P_phen and P_rhizo with this fungus. None of the three bacterial isolates showed any restriction of *A. nidulans*. This is in contrast to the observations made for *V. dahliae* where all three bacterial strains reduced fungal growth with inhibition zones of approximately 5.8 mm (P_phen), 7.2 mm (P_DAPG), and 9.3 mm (P_rhizo).

The inhibitory potential towards both *Aspergillus* species was stronger on pectin/amino acid containing SXM than on high-glucose medium. Co-cultivations with *V. dahliae* usually resulted in a zone without or a minimum of fungal growth whereas we could observe two different areas in co-cultivation experiments with *Aspergillus* species on this medium: in addition to zones without fungal growth, in some co-cultures, sectors with a reduced amount of hyphae and conidiophores could be observed. On pectin/amino acid medium P_phen had the strongest inhibition effect on *V. dahliae*

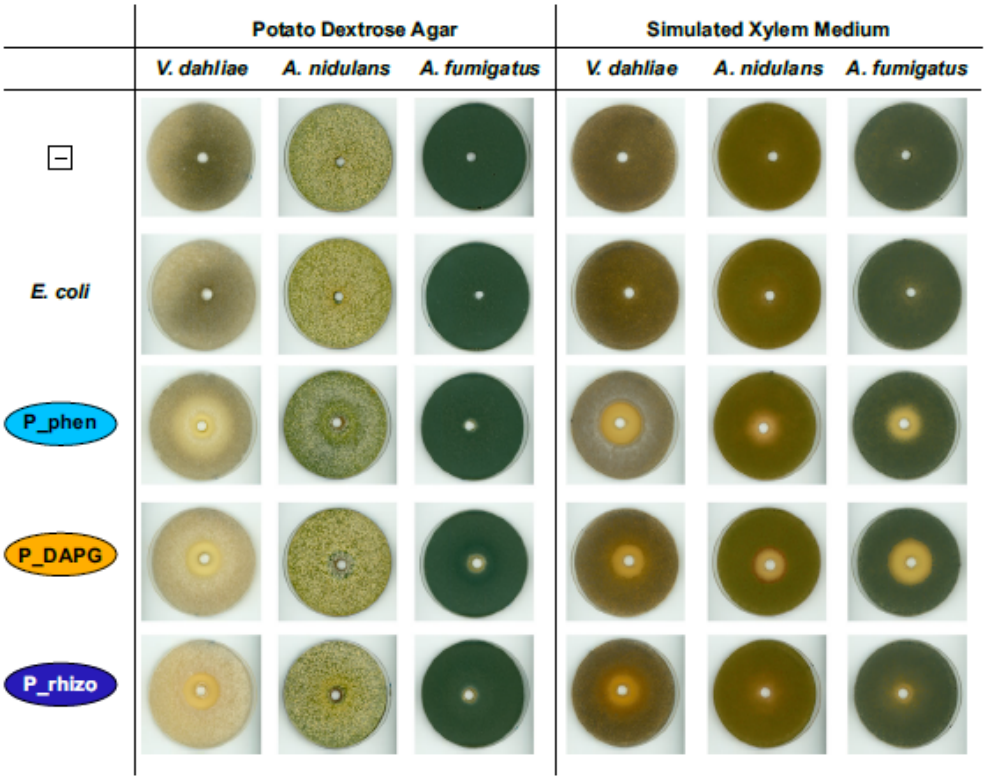

Fig. 6 Inhibition potential of *P. fluorescens* 2–79 (p_phen), *P. protegens* CHA0 (p_DAPG) and *P. fluorescens* DSM8569 (P_rhizo) on *V. dahliae*, *A. nidulans*, and *A. fumigatus*. Co-cultivation of 1×10^5 fungal spores and 7×10^7 colony-forming units of bacterial culture was performed on simulated xylem medium and potato dextrose agar. Plates were incubated for 4 days at 25 °C. Two biological replicates were performed, each having three technical replicates. *V. dahliae* wild type JR2, the *A. nidulans* wild type A4, and the *A. fumigatus* strain AfS35 were co-cultivated with phenazine-producing P_phen (*P. fluorescens* 2–79), DAPG-producing P_DAPG (*P. protegens* CHA0) and *Brassica* rhizosphere isolate P_rhizo (*P. fluorescens* DSM8569). *E. coli* (DH5α) as well as untreated fungus (−) served as controls

(inhibition zone approximately 15 mm). The effect on both *Aspergillus* species is reduced, as we could observe hyphae and conidiophores in the area surrounding the bacterial application site but no zones without fungal growth. This area of growth reduction was 3 mm ± 0.5 for *A. nidulans* and 7 mm ± 0.5 for *A. fumigatus*. In co-cultures of *V. dahliae* with P_DAPG, an inhibition zone of approximately 8 mm was observed, whereas this area without fungal growth was reduced to 3 mm ± 0.4 when the bacterium was cultured together with *A. nidulans*. For *A. fumigatus* incubated with P_DAPG, we observed a sector of 9 mm ± 1.5 in which the fungus was affected. However, a complete inhibition was only observed in the inner 3.6 mm ± 0.6 around the bacteria application site whereas in the rest of the sector some hyphae and conidiophores could be detected.

This suggests that pseudomonads have a specific and highly efficient effect on the growth of plant-pathogenic fungi as *V. dahliae* or *V. longisporum*, but only a minor inhibitory impact on fungi as saprophytic *Aspergillus* species.

Discussion

Verticillium and pseudomonads are part of the microbiome of the plant rhizosphere. The fungus *Verticillium* has to face and compete with the rhizosphere microbiome, which might be densely populated during different seasons under varying ecological or nutritional conditions. Root exudates of an appropriate host induce germination of *Verticillium* microsclerotia and hyphal growth towards host plant roots (Zhou et al. 2006; Eynck et al. 2007). Microsclerotia are fungal resting structures, which are formed to survive during winter after the death of the host plant in the soil (Pegg 1989; Pegg and Brady 2002; Tran et al. 2014). We have analyzed the *Verticillium-Pseudomonas* growth interference in a simplified model and found as a common feature that bacterial growth was never significantly compromised by the fungus. By contrast, fungal growth was inhibited by the bacterium on different solid media surfaces. The potential of pseudomonads to reduce fungal growth was not restricted to fungi living in the rhizosphere, where the bacterium had originally been identified. Liquid co-cultivation of fungal spores with bacteria led also to an inhibitory effect on *V. dahliae*, which was so persistent in some cases that the fungus was even unable to regain the potential to grow after removal of the bacterium from the co-culture. This suggests that pseudomonads can damage or destroy fungal spores or germinating hyphae. The inhibitory potential of the pseudomonas strains was significantly milder towards saprophytic fungi such as *A. nidulans* or *A. fumigatus*. Plant-pathogens have to deal in a significant part of their life cycle with plant immune responses, whereas saprophytes might be specifically adapted in their hyphal growth mode to acquire competitively nutrients in the habitat soil.

Another finding was that the presence of general regulatory genes for the coordinated fungal expression of numerous specific secondary metabolism genes as the epigenetic Lae1 methyltransferase (Sarikaya-Bayram et al. 2015) or the Csn5 deneddylase for specific protein turnover regulation (Braus et al. 2010) are not relevant for bacterial-fungal interaction during co-cultivation. Specific inductions of secondary metabolites had been described for some *Streptomyces-Aspergillus* interactions (Schroeckh et al. 2009; Nützmann et al. 2011).

We found only under specific conditions that a single bacterial compound was responsible for fungal growth inhibition. Phenazine, which had been described as fungal inhibitor (Kerr et al. 1999), specifically reduced fungal growth when nutrients as high amounts of glucose are provided, which would allow faster growth in the absence of bacteria. Phenazines are not required for fungal growth control on pectin/amino acid medium, where a lack of phenazine synthesis can be compensated by a plethora of genes encoding for a cocktail of other antifungal metabolites. Fungal colonies develop more rapidly on a high glucose medium than on pectin amino acid agar surfaces. Bacterial phenazine producers interfere and reduce this faster fungal growth.

Pseudomonads, which do not possess phenazine biosynthetic genes, are highly capable to reduce fungal growth as well in an environment of slower fungal growth in a pectin/amino acids medium or in the presence of high glucose. A combination of genes for several bacterial metabolites or mycotoxins rather than a single gene for a single toxin is presumably responsible for the *Pseudomonas*-mediated effects on vegetative *Verticillium* growth (Fig. 7). The GacA/GacS genetic network regulates the formation of mycotoxins, such as 2,4-diacetylphloroglucinol, pyoluteorin, and hydrogen cyanide (Heeb and Haas 2001). This system is robust to control fungal growth because the deletions for the genes for GacA/GacS regulators had a significant impact on fungal growth but not single deletions of biosynthetic genes of single antifungal compounds.

The fungus might follow distinct nutrient-dependent growth strategies. Nutritional conditions can induce the option to respond to the presence of the phenazine-producing bacterium by growing in other directions. Alternatively, attractive carbon sources might induce a "wait and see" behavior, where the fungus reduces the growth rate of vegetative hyphae. Wait and see fungal responses have been described in *A. fumigatus* in nutrient-rich but hostile environments as human blood (Irmer et al. 2015). The distribution of secreted bacterial metabolites depends on the specific location of the organisms in a particular set-up (i.e., agar). On solid agar medium, the fungus is inoculated throughout the whole petri dish and the bacterium starts to grow at a single inoculation point. The bacterium inoculated in the center produces a metabolite gradient (decreasing concentration of

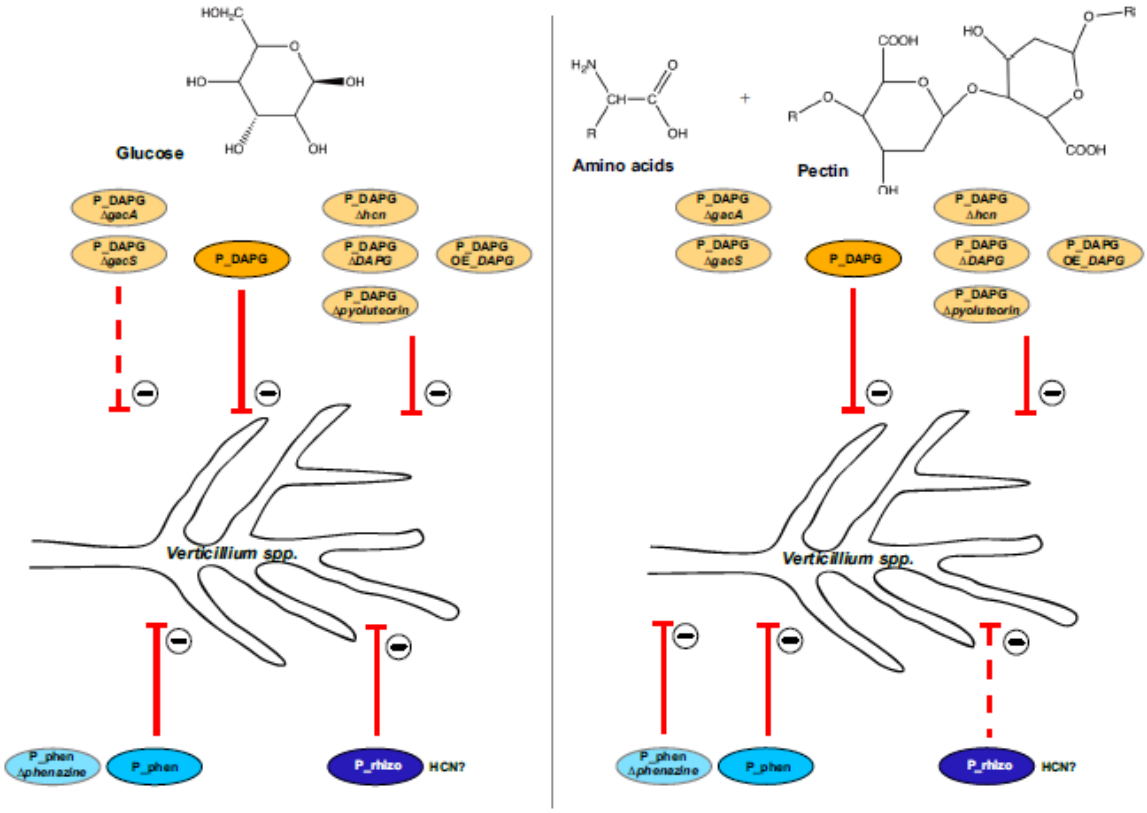

Fig. 7 Model summarizing the effects of different fluorescent pseudomonads to inhibit *V. longisporum* or *V. dahliae* growth. All *Pseudomonas* wild-type strains (P_DAPG (dark orange); P_phen (dark turquois); P_rhizo (dark blue)) were able to inhibit *V. longisporum* and *V. dahliae* growth (marked with red connectors and minus). The inhibition potential of strains with deletions in different genes coding for proteins involved in the production of metabolites is summarized. Corresponding mutants of the P_DAPG strain are depicted in light orange and the mutant of the P_phen strain is depicted in light turquois. Left: on glucose-containing medium the inhibitory effect of the P_DAPG wild type was similar to strains carrying deletions in genes coding for proteins involved in the production of HCN (P_DAPG Δ*hcn*), DAPG (P_DAPG Δ*DAPG*) and pyoluteroin (P_DAPG Δ*pyoluteroin*). Also, overexpression of DAPG (P_DAPG OE_*DAPG*) did not change the inhibition potential. Strains with deletions in the genes coding for gacA (P_DAPG Δ*gacA*) or gacS (P_DAPG Δ*gacS*), respectively, which are involved in the control of several metabolites, showed slightly decreased inhibitory effects on the fungi (dashed line). The ability of P_phen to inhibit *Verticillium* spp. growth was dependent on an intact phenazine gene cluster. The mutant strain (P_phen Δ*phenazine*) did not show any impact on the fungus. The role of HCN production of P-rhizo remains elusive. Right: on pectin/amino acid containing medium, the inhibitory potential of P_DAPG was comparable to P_DAPG Δ*hcn*, P_DAPG Δ*DAPG*, P_DAPG OE_*DAPG*, and P_DAPG Δ*pyoluteroin*. In contrast, P_DAPG Δ*gacA* and P_DAPG Δ*gacS* were not able to inhibit *Verticillium* spp. growth. The inhibitory effect of P_phen on fungal growth was independent from an intact phenazine cluster. P_rhizo showed slight inhibitory effects towards *V. dahliae* but not towards *V. longisporum* (dashed line)

metabolites further away from the center), which can be perceived by the fungus. Secreted bacterial metabolites might cause a negative chemotaxis in the petri dish format, which results in fungal branching and colony formation thus avoiding the bacterium to a certain extent.

Co-cultivations of different fluorescent pseudomonads with *Verticillium* species revealed an interesting potential for biocontrol protection of crops against these emerging pathogens. Plants can specifically induce the production of bacterial metabolites with antifungal properties in the rhizosphere upon fungal infection (Jousset et al. 2011). Pseudomonads primarily produce a cocktail of bioactive compounds, which reduces fungal growth. Both an intact phenazine cluster as well as an intact GacA/GacS-system are important for the antagonistic activities of the bacteria towards the fungus. A combination of different fluorescent pseudomonads for biocontrol might be an interesting path for a wider antimycotic spectrum in the rhizosphere. An improved biocontrol of *Verticillium* by *Pseudomonas* spp. requires a more detailed understanding of mutual fungal and bacterial actions and responses in the rhizosphere. Such an endeavor might be worthwhile, because these fungi are of increasing interest to agriculture.

Acknowledgements The authors thank Linda Thomashow for strain Pf2-79Δ*phz*, Dieter Haas for PfCHA-mutants, and Tuan Tran for plasmid pKO2. We are grateful to Josua Schinke and Bastian Joehnk for proofreading and Sarah Zunken for technical support.

Funding This study was funded by the Deutsche Forschungsgemeinschaft (DFG) grant BR1502/15–1 and by the Federal Ministry of Education and Research (BMBF) BioFung project.

Compliance with ethical standards

Conflict of interest The authors declare that they have no competing interests.

Ethical approval This article does not contain any studies with human participants or animals performed by any of the authors.

References

Bayram Ö, Braus GH (2012) Coordination of secondary metabolism and development in fungi: the velvet family of regulatory proteins. FEMS Microbiol Rev 36(1):1–24. https://doi.org/10.1111/j.1574-6976.2011.00285.x

Bayram O, Krappmann S, Ni M, Bok JW, Helmstaedt K, Valerius O, Braus-Stromeyer S, Kwon N-J, Keller NP, J-H Y, Braus GH (2008) VelB/VeA/LaeA complex coordinates light signal with fungal development and secondary metabolism. Science 320(5882): 1504–1506. https://doi.org/10.1126/science.1155888

Bayer CropScience Biologics GmbH Contans WG for control of Sclerotinia spp. http://www.biologics.bayer.com/. Accessed 5 May 2017

Bender C, Rangaswamy V, Loper J (1999) Polyketide production by plant-associated pseudomonads. Annu Rev Phytopathol 37(1): 175–196. https://doi.org/10.1146/annurev.phyto.37.1.175

Berg G, Ballin G (1994) Bacterial antagonists to *Verticillium dahliae* Kleb. J Phytopathol 141(1):99–110. https://doi.org/10.1111/j.1439-0434.1994.tb01449.x

Bertani G (1951) Studies on Lysogenesis I. The mode of phageliberation by lysogenic *Escherichia coli*. J Bacteriol 62:293–300

Biologics Bayer Bayer CropScience Biologics GmbH Contans WG for control of *Sclerotinia* spp. http://www.biologics.bayer.com/. Accessed 5 May 2017

Bok JW, Keller NP (2004) LaeA, a regulator of secondary metabolism in *Aspergillus* spp. Eukaryot Cell 3(2):527–535. https://doi.org/10.1128/EC.3.2.527-535.2004

Braus GH, Irniger S, Bayram Ö (2010) Fungal development and the COP9 signalosome. Curr Opin Microbiol 13(6):672–676. https://doi.org/10.1016/j.mib.2010.09.011

Brencic A, McFarland KA, McManus HR, Castang S, Mogno I, Dove SL, Lory S (2009) The GacS/GacA signal transduction system of *Pseudomonas aeruginosa* acts exclusively through its control over the transcription of the RsmY and RsmZ regulatory small RNAs. Mol Microbiol 73(3):434–445. https://doi.org/10.1111/j.1365-2958.2009.06782.x

Bundock P, den Dulk-Ras A, Beijersbergen A, Hooykaas PJ (1995) Trans-kingdom T-DNA transfer from *Agrobacterium tumefaciens* to *Saccharomyces cerevisiae*. EMBO J 14(2):3206–3214. https://doi.org/10.1016/j.fgb.2006.07.006

Chen Y, Yan F, Chai Y, Liu H, Kolter R, Losick R, Guo J (2013) Biocontrol of tomato wilt disease by *Bacillus subtilis* isolates from natural environments depends on conserved genes mediating biofilm formation. Environ Microbiol 15(3):848–864. https://doi.org/10.1111/j.1462-2920.2012.02860.x

Cui J (2005) Pseudomonas syringae manipulates systemic plant defenses against pathogens and herbivores. Proc Natl Acad Sci U S A 102(5): 1791–1796. https://doi.org/10.1073/pnas.0409450102

Depotter JRL, Deketelaere S, Inderbitzin P, Von TA, Hofte M, Subbarao KV, Wood TA, Thomma BPHJ (2016) *Verticillium longisporum*, the invisible threat to oilseed rape and other brassicaceous plant hosts. Mol Plant Pathol 17(7):1004–1016. https://doi.org/10.1111/mpp.12350

Eynck C, Koopmann B, Grunewaldt-Stoecker G, Karlovsky P, von Tiedemann A (2007) Differential interactions of *Verticillium longisporum and V. dahliae with Brassica napus* detected with molecular and histological techniques. Eur J Plant Pathol 118(3):259–274. https://doi.org/10.1007/s10658-007-9144-6

Fradin EF, Thomma BPHJ (2006) Physiology and molecular aspects of Verticillium wilt diseases caused by *V. dahliae* and *V. albo-atrum*. Mol Plant Pathol 7(2):71–86. https://doi.org/10.1111/j.1364-3703.2006.00323.x

Fradin EF, Zhang Z, Juarez Ayala JC, Castroverde CDM, Nazar RN, Robb J, Liu C-M, Thomma BPHJ (2009) Genetic dissection of Verticillium wilt resistance mediated by tomato Ve1. Plant Physiol 150(1):320–332. https://doi.org/10.1104/pp.109.136762

Haas D, Défago G (2005) Biological control of soil-borne pathogens by fluorescent pseudomonads. Nat Rev Microbiol 3(4):307–319. https://doi.org/10.1038/nrmicro1129

Hamel J (2011) A review of acute cyanide poisoning with a treatment update. Crit Care Nurse 31(1):72–82. https://doi.org/10.4037/ccn2011799

Heeb S, Haas D (2001) Regulatory roles of the GacS/GacA two-component system in plant-associated and other gram-negative bacteria. Mol Plant-Microbe Interact 14(12):1351–1363. https://doi.org/10.1094/MPMI.2001.14.12.1351

Hollensteiner J, Wemheuer F, Harting R, Kolarzyk AM, Diaz Valerio SM, Poehlein A, Brzuszkiewicz EB, Nesemann K, Braus-Stromeyer SA, Braus GH, Daniel R, Liesegang H (2017) *Bacillus thuringiensis* and *Bacillus weihenstephanensis* inhibit the growth of Phytopathogenic *Verticillium* species. Front Microbiol 7:2171. https://doi.org/10.3389/fmicb.2016.02171

Inderbitzin P, Bostock RM, Davis RM, Usami T, Platt HW, Subbarao KV (2011) Phylogenetics and taxonomy of the fungal vascular wilt pathogen *Verticillium*, with the descriptions of five new species. PLoS One 6(12):e28341. https://doi.org/10.1371/journal.pone.0028341

Irmer H, Tarazona S, Sasse C, Olbermann P, Loeffler J, Krappmann S, Conesa A, Braus GH (2015) RNAseq analysis of *Aspergillus fumigatus* in blood reveals a just wait and see resting stage behavior. BMC Genomics 16(1):640. https://doi.org/10.1186/s12864-015-1853-1

Jousset A, Rochat L, Lanoue A, Bonkowski M, Keel C, Scheu S (2011) Plants respond to pathogen infection by enhancing the antifungal gene expression of root-associated bacteria. Mol Plant-Microbe Interact 24(3):352–358. https://doi.org/10.1094/MPMI-09-10-0208

Jousset A, Schuldes J, Keel C, Maurhofer M, Daniel R, Scheu S, Thuermer A (2014) Full-genome sequence of the plant growth-promoting bacterium *Pseudomonas protegens* CHA0. Genome Announc 2. https://doi.org/10.1128/genomeA.00322-14

Kerr JR, Taylor GW, Rutman A, Høiby N, Cole PJ, Wilson R (1999) *Pseudomonas aeruginosa* pyocyanin and 1-hydroxyphenazine inhibit fungal growth. J Clin Pathol 52(5):385–387. https://doi.org/10.1136/jcp.52.5.385

Khan SR, Mavrodi DV, Jog GJ, Suga H, Thomashow LS, Farrand SK (2005) Activation of the phz operon of *Pseudomonas fluorescens* 2-79 requires the LuxR homolog PhzR, N-(3-OH-Hexanoyl)-L-

homoserine lactone produced by the LuxI homolog PhzI, and a cis-acting phz box. J Bacteriol 187(18):6517–6527. https://doi.org/10.1128/JB.187.18.6517-6527.2005

Kwak YS, Han S, Thomashow LS, Rice JT, Paulitz TC, Kim D, Weller DM (2011) *Saccharomyces cerevisiae* genome-wide mutant screen for sensitivity to 2,4-diacetylphloroglucinol, an antibiotic produced by *Pseudomonas fluorescens*. Appl Environ Microbiol 77(5):1770–1776. https://doi.org/10.1128/AEM.02151-10

Laville J, Voisard C, Keel C, Maurhofer M, Défago G, Haas D (1992) Global control in *Pseudomonas fluorescens* mediating antibiotic synthesis and suppression of black root rot of tobacco. Proc Natl Acad Sci U S A 89(5):1562–1566. https://doi.org/10.1073/pnas.89.5.1562

Mavrodi DV, Peever TL, Mavrodi OV, Parejko JA, Raaijmakers JM, Lemanceau P, Mazurier S, Heide L, Blankenfeldt W, Weller DM, Thomashow LS (2010) Diversity and evolution of the phenazine biosynthesis pathway. Appl Environ Microbiol 76(3):866–879. https://doi.org/10.1128/AEM.02009-09

Meyer SLF, Halbrendt JM, Carta LK, Skantar AM, Liu T, Abdelnabby HME, Vinyard BT (2009) Toxicity of 2,4-diacetylphloroglucinol (DAPG) to plant-parasitic and bacterial-feeding nematodes. J Nematol 41(4):274–280

Nahlik K, Dumkow M, Bayram Ö, Helmstaedt K, Busch S, Valerius O, Gerke J, Hoppert M, Schwier E, Opitz L, Westermann M, Grond S, Feussner K, Goebel C, Kaever A, Meinicke P, Feussner I, Braus GH (2010) The COP9 signalosome mediates transcriptional and metabolic response to hormones, oxidative stress protection and cell wall rearrangement during fungal development. Mol Microbiol 78(4):964–979. https://doi.org/10.1111/j.1365-2958.2010.07384.x

Nandi M, Selin C, Brassinga AKC, Belmonte MF, Fernando WGD, Loewen PC, de Kievit TR (2015) Pyrrolnitrin and hydrogen cyanide production by *Pseudomonas chlororaphis* strain PA23 exhibits nematicidal and repellent activity against *Caenorhabditis elegans*. PLoS One 10(4):e0123184. https://doi.org/10.1371/journal.pone.0123184

Nesemann K, Braus-Stromeyer SA, Thuemmer A, Daniel R, Braus GH (2015a) Draft genome sequence of the beneficial Rhizobacterium *Pseudomonas fluorescens* DSM 8569, a natural isolate of oilseed rape (*Brassica napus*). Genome Announc 3(2):e00137–e00115. https://doi.org/10.1128/genomeA.00137-15

Nesemann K, Braus-Stromeyer SA, Thuemmer A, Daniel R, Mavrodi DV, Thomashow LS, Weller DM, Braus GH (2015b) Draft genome sequence of the Phenazine-producing *Pseudomonas fluorescens* strain 2-79. Genome Announc 3(2):e00130–e00115. https://doi.org/10.1128/genomeA.00130-15

Neumann MJ, Dobinson KF (2003) Sequence tag analysis of gene expression during pathogenic growth and microsclerotia development in the vascular wilt pathogen *Verticillium dahliae*. Fungal Genet Biol 38(1):54–62. https://doi.org/10.1016/S1087-1845(02)00507-8

Nowak-Thompson B, Chaney N, Wing JS, Gould SJ, Loper JE (1999) Characterization of the pyoluteorin biosynthetic gene cluster of *Pseudomonas fluorescens* Pf-5. J Bacteriol 181(7):2166–2174

Nützmann H-W, Reyes-Dominguez Y, Scherlach K, Schroeckh V, Horn F, Gacek A, Schümann J, Hertweck C, Strauss J, Brakhage AA (2011) Bacteria-induced natural product formation in the fungus *Aspergillus nidulans* requires Saga/Ada-mediated histone acetylation. Proc Natl Acad Sci U S A 108(34):14282–14287. https://doi.org/10.1073/pnas.1103523108

Pegg GF (1989) Pathogenesis in vascular diseases of plants. In: Tjamos EC, Beckman CH (eds) Vascular wilt diseases of plants. Springer Berlin Heidelberg, Berlin, Heidelberg, pp 51–94. https://doi.org/10.1007/978-3-642-73166-2_4

Pegg GF, Brady BL (2002) Verticillium wilts. CABI Pub, Wallingford. https://doi.org/10.1079/9780851995298.0000

Perneel M (2006) The root rot pathogen *Pythium myriotylum* on cocoyam (*Xanthosoma sagittifolium* (L.) Schott): intraspecific variability and biological control. Proefschrift Universiteit Gent

Perneel M, D'hondt L, De Maeyer K, Adiobo A, Rabaey K, Höfte M (2008) Phenazines and biosurfactants interact in the biological control of soil-borne diseases caused by *Pythium spp*. Environ Microbiol 10(3):778–788. https://doi.org/10.1111/j.1462-2920.2007.01501.x

Sarikaya-Bayram O, Bayram O, Valerius O, Park HS, Irniger S, Gerke J, Ni M, Han K-H, J-H Y, Braus GH (2010) LaeA control of velvet family regulatory proteins for light-dependent development and fungal cell-type specificity. PLoS Genet 6(12):e1001226. https://doi.org/10.1371/journal.pgen.1001226

Sarikaya-Bayram Ö, Palmer JM, Keller N, Braus GH, Bayram Ö (2015) One Juliet and four Romeos: VeA and its methyltransferases. Front Microbiol 6:1–7. https://doi.org/10.3389/fmicb.2015.00001

Schnider-Keel U, Seematter A, Maurhofer M, Blumer C, Duffy B, Gigot-Bonnefoy C, Reimmann C, Notz R, Défago G, Haas D, Keel C (2000) Autoinduction of 2,4-diacetylphloroglucinol biosynthesis in the biocontrol agent *Pseudomonas fluorescens* CHA0 and repression by the bacterial metabolites salicylate and pyoluteorin. J Bacteriol 182(5):1215–1225. https://doi.org/10.1128/JB.182.5.1215-1225.2000

Schroeckh V, Scherlach K, Nutzmann H-W, Shelest E, Schmidt-Heck W, Schuemann J, Martin K, Hertweck C, Brakhage AA (2009) Intimate bacterial-fungal interaction triggers biosynthesis of archetypal polyketides in *Aspergillus nidulans*. Proc Natl Acad Sci 106(34):14558–14563. https://doi.org/10.1073/pnas.0901870106

Scott BR, Kafer E (1982) *Aspergillus nidulans*: an organism for detecting a range of genetic damage. In: Chemical mutagens. pp 447–479. https://doi.org/10.1007/978-1-4615-6625-0_11

Sikora RA (1992) Management of the antagonistic potential in agricultural ecosystems for the biological control of plant parasitic nematodes. Annu Rev Phytopathol 30(1):245–270. https://doi.org/10.1146/annurev.py.30.090192.001333

Singh S, Braus-Stromeyer SA, Timpner C, Valerius O, von Tiedemann A, Karlovsky P, Druebert C, Polle A, Braus GH (2012) The plant host *Brassica napus* induces in the pathogen *Verticillium longisporum* the expression of functional catalase peroxidase which is required for the late phase of disease. Mol Plant-Microbe Interact 25(4):569–581. https://doi.org/10.1094/MPMI-08-11-0217

Stutz EW, Défago G, Kern H (1986) Naturally occurring fluorescent pseudomonads involved in suppression of black root rot of tobacco. Phytopathology 76(2):181–185. https://doi.org/10.1094/Phyto-76-181

Timpner C, Braus-Stromeyer SA, Tran VT, Braus GH (2013) The Cpc1 regulator of the cross-pathway control of amino acid biosynthesis is required for pathogenicity of the vascular pathogen *Verticillium longisporum*. Mol Plant-Microbe Interact 26(11):1312–1324. https://doi.org/10.1094/MPMI-06-13-0181-R

Tran VT, Braus-Stromeyer SA, Timpner C, Braus GH (2013) Molecular diagnosis to discriminate pathogen and apathogen species of the hybrid *Verticillium longisporum on the oilseed crop Brassica napus*. Appl Microbiol Biotechnol 97(10):4467–4483. https://doi.org/10.1007/s00253-012-4530-1

Tran V-T, Braus-Stromeyer SA, Kusch H, Reusche M, Kaever A, Kühn A, Valerius O, Landesfeind M, Aßhauer K, Tech M, Hoff K, Pena-Centeno T, Stanke M, Lipka V, Braus GH (2014) *Verticillium* transcription activator of adhesion Vta2 suppresses microsclerotia formation and is required for systemic infection of plant roots. New Phytol 202(2):565–581. https://doi.org/10.1111/nph.12671

Traxler MF, Kolter R (2015) Natural products in soil microbe interactions and evolution. Nat Prod Rep 32(7):956–970. https://doi.org/10.1039/c5np00013k

Weller DM (2007) *Pseudomonas* biocontrol agents of soilborne pathogens: looking back over 30 years. Phytopathology 97(2):250–256. https://doi.org/10.1094/PHYTO-97-2-0250

Weller DM, Cook RJ (1983) Supression of take-all of wheat by seed treatments with fluorescent pseudomonads. Phytopathology 73(3): 463–469. https://doi.org/10.1094/Phyto-73-463

Weller DM, Raaijmakers JM, Gardener BBM, Thomashow LS (2002) Microbial populations responsible for specific soil suppressiveness to plant pathogens. Annu Rev Phytopathol 40(1):309–348. https://doi.org/10.1146/annurev.phyto.40.030402.110010

Zeng W, Wang D, Kirk W, Hao J (2012) Use of *Coniothyrium minitans* and other microorganisms for reducing *Sclerotinia sclerotiorum*. Biol Control 60(2):225–232. https://doi.org/10.1016/j.biocontrol.2011.10.009

Zhou L, Hu Q, Johansson A, Dixelius C (2006) *Verticillium longisporum and V. dahliae*: infection and disease in *Brassica napus*. Plant Pathol 55:137–144. https://doi.org/10.1111/j.1365-3059.2005.01311.x

Zuber S, Carruthers F, Keel C, Mattart A, Blumer C, Pessi G, Gigot-Bonnefoy C, Schnider-Keel U, Heeb S, Reimmann C, Haas D (2003) GacS sensor domains pertinent to the regulation of exoproduct formation and to the biocontrol potential of *Pseudomonas fluorescens* CHA0. Mol Plant-Microbe Interact 16(7):634–644. https://doi.org/10.1094/MPMI.2003.16.7.634

Chapter 5: Pathogenic Verticillia Follow Evasion and Detoxification Strategies during Confrontation with Fluorescent Pseudomonads

Kai Nesemann[1], Rebekka Harting[1], Annalena Höfer[1], Harald Kusch[2], Claire E. Stanley[3], Martina Stöckli[4], Manuel Landesfeind[1], Alexander Kaever[1], Katharina Hoff[5], Mario Stanke[5], Andrew J. deMello[3], Markus Künzler[4], Markus Aebi[4], Susanna A. Braus-Stromeyer[1], Gerhard H. Braus[1]

[1]Institute of Microbiology and Genetics and Göttingen Center for Molecular Biosciences (GZMB), Georg-August-Universität Göttingen, Germany.

[2]Department of Medical Informatics, Georg-August-Universität Göttingen, Germany.

[3]Institute of Chemical and Bioengineering, ETH Zürich, Switzerland.

[4]Institute of Microbiology, ETH Zürich, Switzerland.

[5]Institute of Mathematics and Computer Science, Ernst-Moritz-Arndt-Universität Greifswald, Germany.

* Corresponding author: Gerhard H. Braus, Grisebachstraße 8, 37077 Göttingen, Germany, Telephone: +49-551-3933771; Fax: +49-551-3933330; E-mail: gbraus@gwdg.de

Author contributions:

Table 5.1: KN
Fig 5.1: CS, MS, AdM, MK, MA
Fig 5.2: CS, MS, KN
Fig 5.3: CS, MS, KN
Fig 5.4: CS, MS, KN
Fig 5.5: SB, RH, AH, HK, ML, AK, KH, MS, KN
Table 5.2: SB, RH, AH, HK, ML, AK, KH, MS, KN
Table S5: SB, RH, AH, HK, ML, AK, KH, MS, KN
Table S6: SB, RH, AH, HK, ML, AK, KH, MS, KN
Table S7: SB, RH, AH, HK, ML, AK, KH, MS, KN
Supervision and scientific advice: GB, SB, RH, HK
Manuscript: GB, SB, RH, KN

Abstract

Verticillia are phytopathogenic fungi responsible for increasing yield losses in numerous economical important crops. The impact of different fluorescent pseudomonads on fungal growth was analyzed in microfluidic interaction channels. A Brassica-rhizosphere derived *Pseudomonas fluorescens*, which neither carries the genes for phenazine nor 2,4-diacetyphloroglucinol (DAPG) synthesis, reduces Verticillium polar hyphal growth by almost 60 % in comparison to *E. coli* as control in a confrontation assay in microfluidic interaction channels filled with a liquid pectin and amino acid medium. A *Pseudomonas synthaxa* with an intact phenazine cluster reduces fungal growth by 30 % more than a corresponding mutant strain. A DAPG producing *Pseudomonas protegens* strain can reduce fungal microfluidic growth by 90 %. The contribution for this inhibition of the two-component system GacA/GacS control system for a response regulator and a sensor kinase corresponds to 30 % and includes a 10 % inhibition provided by an intact DAPG cluster. An intact phenazine or GacA/GacS system induces in addition a strong change in hyphal polarity. This suggests that the fungus attempts to evade the confrontation with corresponding bacteria. During liquid media co-cultivation, *P. protegens* alters transcriptional profiles of *V. longisporum* genes after two hours with one third up-regulated genes including detoxification related genes and a decrease of a comparable portion of fungal transcripts involved in protein biosynthesis, plant infection or nutrition. The fungus presumably follows an evasion strategy to escape from bacterial toxicity, which includes avoiding contact by changing growth direction through morphological adaption combined with intensifying expression of genes coding for detoxifying enzymes.

Key words: Verticillium, fluorescent pseudomonads, GacA/GacS two-component system, DAPG, phenazines, microfluidics, transcriptome analysis

Introduction

Soil is a highly diverse habitat with complex relationships between multiple inhabitant species. In particular, bacterial-fungal interactions play a major role for microbial fitness in soils (Nazir *et al.*, 2009). The heterogeneous microbiota of the rhizosphere of a plant can contain different phytopathogenic species with negative impact on agricultural yields. The ascomycete *Verticillium longisporum* is an interspecific hybrid of two haploid parental strains and contains an amphidiploid genome. The soil-born pathogen mainly infects Brassicaceae and can survive in the soil for many years due to highly melanized resting structures, so called microsclerotia (Pegg and Brady, 2002; Harting *et al*., 2020). After germination in the soil, Verticillium hyphae enter the root cortex and colonizes the vascular system of its host plant (Eynck *et al.*, 2007; Tran *et al.*, 2014; *Zhang et al.*, 2018). In the absence of appropriate fungicides or resistant cultivars, there are hardly any strategies available to control the infection process of vascular plant pathogens. Besides chemical treatments, it is an approved method in agriculture to use natural microorganisms with antagonistic activity from the rhizosphere as biological control organisms. By the application of specific bacterial or fungal antagonists as biocontrol agents, a suppressive potential towards pathogens can be installed in the soil (Sikora, 1992).

One of the largest groups of biocontrol organisms are fluorescent pseudomonads that belong to □-proteobacteria and possess well-characterized and distinct beneficial properties in the interaction with plants (Haas and Défago, 2005). Several compounds secreted by fluorescent pseudomonads with crucial antagonistic impact against fungal pathogens could be identified in the recent years including 2,4-diacetylphloroglucinol (DAPG), phenazines, biosurfactants, pyoluteorin, pyrrolnitrin, hydrogen cyanide (HCN), pyoverdine siderophore, indole-acetic acid and exoproteases (Haas and Défago, 2005; Mazzola, 2007). *P. protegens* CHA0 has been identified as a biocontrol agent exhibiting one of the broadest repertoires of potential antagonistic and plant growth-promoting mechanisms so far (Weller, 2007).

Pseudomonas spp. have been described as an appropriate biocontrol agent against Verticillium wilt in literature (Martinez-Garcia *et al.*, 2015; Markakis *et al.*,

2016; Deketelaere *et al.*, 2017). Fluorescent pseudomonads can cause suppressive effects on the growth of different Verticillium species in co-cultivation studies on different agar-containing media (Nesemann *et al.*, 2018). The presence of a phenazine gene cluster coding for a single component is sufficient to suppress fungal growth under high glucose growth conditions. In a complex pectin medium the genetic potential for the secretion of different substances regulated by the two-component regulatory system GacA/GacS is essential for inhibition. *P. protegens* CHA0 genes controlled by the GacA/GacS signal-transduction pathway include *phlA* and *phlF* (for DAPG synthesis), *hcnABC* and *anr* (for HCN) and *plt* (for pyoluteorin). Corresponding mRNAs are constitutively expressed and are under non-inducing conditions posttranscriptionally inhibited by repressors RsmA and RsmE, which block translation, synthesis and finally secretion of bioactive metabolites. Environmental stress signals trigger autophosphorylation of the membrane sensor protein GacS, which transfers subsequently the phosphate group to the response regulator GacA. This activates the expression of the small RNAs *rsmXYZ* acting as derepressors of RsmA and RsmE, which bind to the ribosomal binding sites of the transcripts for the secondary metabolite producing enzymes and prevent translation during non-stress conditions. As a result, the translation of enzymes, and subsequently synthesis and secretion of the respective toxins can take place (Laville *et al.*, 1992; Zuber *et al.*, 2003; Heeb *et al.*, 2005; Gonzalez *et al.*, 2008; Brencic *et al.* 2009; Wei *et al.*, 2013; Nandi *et al.*, 2015; Traxler and Kolter, 2015; Yan *et al.*, 2018; Zhang *et al.*, 2020).

In this study, the plant pathogen *Verticillium longisporum* strain Vl43 was analyzed with different rhizobacteria in a liquid confrontation assay for better morphological observations and compared to previous surface studies for the same fungus (Nesemann *et al.*, 2018). These surface studies revealed differences in the bacteria-fungus interplay for fluorescent pseudomonads with different potential to synthesize bioactive compounds. Verticillium mutant strains deficient in secondary metabolism by deleting the global regulator of secondary metabolism *LAE1* (Bok and Keller, 2004; Bayram *et al.,* 2008; Sarikaya-Bayram *et al.,* 2010) or the deneddylase subunit *CSN5* resulting in derepressed secondary metabolism (Nahlik *et al.*, 2010) showed the same inhibition patterns as wildtype on agar surfaces. An inhibitory effect on fungal spore germination was also described

recently after co-cultivation of *V. dahliae* with different fluorescent pseudomonads in two liquid media types (Nesemann *et al.*, 2018). In microfluidic interaction channels, the growth response of Verticillium hyphae was monitored in presence of three distinct Pseudomonas species with differences in their genetic potential. The *P. synthaxa* strain (P_phen) carries genes for phenazine and *P. protegens* (P_DAPG) for DAPG production, respectively. The *P. fluorescens* strain derives from the rhizosphere of oilseed rape (P_rhizo) and carries neither an intact phenazine nor DAPG cluster. P_rhizo could suppress Verticillium polar growth in confrontation microchannels independently of the presence of phenazines or DAPG producing genes. A contribution of 30 % fungal growth inhibition is provided by an intact phenazine cluster or as well when the genetic information for a complex combination of different GacA/GacS-regulated metabolites including DAPG is present in the bacterial genome. The genetic potential for GacA/GacS-controlled metabolites or phenazines leads to an altered morphology of Verticillium hyphae with a polarity change to avoid bacteria. *P. protegens* induces after two hours of co-cultivation alterations in *V. longisporum* gene expression including up-regulation of detoxification related genes as well as decreased levels of transcripts for protein biosynthesis and degradation of plant polysaccharides. Taken together, Verticillium rather follows an evasion and detoxification strategy to avoid contact to Pseudomonas.

Material and Methods

Organisms used in this study

Bacterial and fungal strains used in this study are listed in table 5.1.

Table 5.1 Organisms and strains used in this study.

*DSMZ - Leibniz Institute - German Collection of Microorganisms and Cell Cultures GmbH, Braunschweig, Germany

organism	characteristics	reference
Verticillium longisporum		
V. longisporum 43	wild type - isolated from oilseed rape in Mecklenburg, Germany	Zeise and von Tiedemann, 2001
V. longisporum 43_Gfp	green fluorescent Vl43	Tran *et al.*, 2014
Pseudomonas fluorescens		
P_rhizo (DSM8569)	wild type - natural isolate from oilseed rape rhizosphere	DSMZ*
Pseudomonas synxantha		
P_phen (2-79)	wild type, producing phenazines (formerly named *P. fluorescens*)	Weller and Cook, 1983
P_phen∆*phz*	production of phenazines blocked	Mavrodi *et al.*, 1998
Pseudomonas protegens		
P_DAPG (CHA0)	wild type, producing e.g. DAPG, HCN, pyoluteorin	Stutz *et al.*, 1986
P_DAPG_mCherry	red fluorescent CHA0	Rochat *et al.*, 2010
P_DAPG∆*gacA*::ΩKm^r	key enzyme in biosynthesis of several antibiotics; no production of 2,4-DAPG, HCN, pyoluteorin	Laville *et al.*, 1992
P_DAPG∆*gacS*	key enzyme in biosynthesis of several antibiotics; no production of 2,4-DAPG, HCN, pyoluteorin	Zuber *et al.*, 2003
P_DAPG∆*gacS_mCherry*	red fluorescent CHA0	Keel, unpublished
P_DAPG∆*hcnABC*	almost no production of HCN	Laville *et al.*, 1998
P_DAPG∆*anr::ΩHg*^{r}	transcription factor for HCN-production; 8 % HCN production compared to wild type	Laville *et al.*, 1998
P_DAPG∆*plt::Tn5*	no production of pyoluteorin	Maurhofer *et al.*, 1994
P_DAPG∆*phlA*	gene in phl-operon for 2,4-DAPG synthesis; no production of 2,4-DAPG	Schnider-Keel *et al.*, 2000
P_DAPG∆*phlF::ΩKm*^{r}	repressor gene for 2,4-DAPG synthesis; enhanced production of 2,4-DAPG	Schnider-Keel *et al.*, 2000
Escherichia coli		
DH5α	wild type	Meselson and Yuan, 1968

Cultivation conditions of bacteria and fungi

Fungi and bacteria were inoculated and cultivated as described in Nesemann *et al.,* 2018.

Microfluid device system

Detailed interaction studies with Verticillium and Pseudomonas were performed in microfluidic interaction devices. Microfluidic applications facilitate miniaturized analytics of physical processes in micrometer scale to control pl-µl liquid volumes, in this case cultural medium (deMello, 2006). Thus, we were able to follow their interaction *in vivo* on single cell level under the microscope. The devices were developed by Stanley *et al.*, 2014.

Verticillium was pre-cultivated on SXM plates, and inoculated with hyphae on an agar block at the one side of the device. After the hyphae passed a narrow bridge of 10 µm diameter about 10 to 20 hyphae can grow into an interaction channel. In total, 28 parallel channels exist with a diameter of 100 µm and a length of 6650 µm. As soon as the hyphal tips reach the beginning of the channel, 40 µl of bacterial suspension out of the exponential phase (OD_{600nm} = 1; $5x10^7$ CFU) was applied at the opposite site of the channel. A fluid inlet hole is connected to the interaction channels. This way, the bacterial cells can distribute within the device. Fungal growth behavior and morphology was documented every 24 hours. For better optical illustration we used a green-fluorescent-protein(Gfp)-expressing strain of *V. longisporum* Vl43 (Eynck *et al.*, 2007) and *P. protegens CHA0* mCherry expressing strains P_DAPG (Rochat *et al.*, 2010) and P_DAPG∆*gacS* (Zuber *et al.*, 2003).

Furthermore, growth tests using the supernatant of *P. fluorescens* were performed in the microfluid device system. For the non-induced supernatant a bacterial culture with OD_{600nm} = 1 in SXM was sterile filtered. As the induction of secondary metabolite secretion might require the presence of Verticillium, *V. longisporum*_Gfp was pre-cultured in 150 ml liquid SXM for 6 days and *P. fluorescens* culture with OD_{600nm} = 1 in 50 ml SXM. The fungal mycelium was filtered by Miracloth and transferred to 120 ml of fresh SXM. Additionally, 30 ml of

the overnight Pseudomonas culture was added to a total volume of 150 ml. A co-cultivation period of 3 hours at 25 °C with agitation at 150 rpm followed. Afterwards, the co-culture was filtered again by Miracloth membrane and sterile filtered (Filtropur S 0.2, Sarstedt, Nümbrecht, Germany). After the pre-growth of Verticillium in the device, the medium was exchanged to 40 µl of the non-induced or induced supernatant, respectively.

The Zeiss Axio Observer Z.1 system (Carl Zeiss AG, Germany) in combination with the Laser Lunch System (Model 3iL32, Intelligent Imaging Innovations Inc, Colorado, USA) was used to obtain fluorescence microscopy applied with Zeiss PlanAPOCHROMAT 40x/1,4oil or Zeiss PlanAPOCHROMAT 100x/1,4oil objective, respectively. Pictures were taken with the QuantEM:512SC camera (Photometrics, Arizona, USA) and the Slide Book 5.0 imaging software (Intelligent Imaging Innovations Inc.) with an exposure time of 150 ms for Gfp and 500 ms for mCherry.

Transcriptome sequencing and analysis

Nine cultures of *Verticillium longisporum* 43 have been precultivated for five days with $1x10^6$ spores in 150 ml of liquid SXM at 25 °C with 150 rpm. The total amount of 1.350 ml of fungal culture was pooled and slightly sedimented. The top 350 ml medium was discarded and the remaining 1000 ml culture was equally distributed to eight 500 ml flasks with 125 ml of culture each. Additionally, six cultures of *Pseudomonas protegens* CHA0 were grown at the same conditions (in 150 ml SXM at 25 °C with 150 rpm) up to an OD_{600nm} = 1 ($5x10^7$ CFU). The single cultures were pooled and concentrated to an OD_{600nm} = 3 by centrifuging at 5000 g and resuspended in fresh SXM. Six of the eight flasks filled with 125 ml fungal culture were immediately mixed with 25 ml of bacterial culture (OD_{600nm} = 3), leading to a co-culture of *V. longisporum* Vl43 and *P. protegens* CHA0 with a final OD_{600nm} = 0,5. At the same time the two remaining flasks with 125 ml fungal culture were mixed with 25 ml fresh SXM and served as an untreated control. The six co-cultures and the two pure fungal cultures were further incubated at the same conditions as described before. The co-cultures as well as the fungal control cultures without bacteria were harvested after 120 min by filtering the cultures

through Miracloth filters and directly shock-frozen in liquid N_2. RNA extraction was performed by using the RNeasy Plant Mini Kit from Qiagen (Hilden, Germany). RNA sequencing was performed by GATC Biotech AG (Konstanz, Germany). The sequences are released at NCBI under the Accession-number SRP068348; http://www.ncbi.nlm.nih.gov/sra/?term=SRP068348. By selecting the poly-A^+-part of the eukaryotic mRNA, only the fungal RNA was sequenced. All *V. longisporum* Vl43 transcripts have been mapped against *V. dahliae* JR2 (VDAG_JR2v.4.0; de Jounge *et al.*, 2012; deposited at www.fungi.ensembl.org/Verticillium_dahliaejr2/Info/Index; Howe *et al.*, 2019). A filter and cluster analysis of all transcripts was performed using the MarVis-Cluster interface (Kaever *et al.*, 2009) within the MarVis-Suite software (Kaever *et al.*, 2015; http://marvis.gobics.de) into three groups representing the down-, non- and up-regulated fungal genes when the bacterium is present. The complete transcriptomic dataset has been automatically annotated by Ensembl- (Howe *et al.*, 2019) and Gene Ontology (GO; Ashburner *et al.*, 2000; Gene Ontology Consortium, 2019) database. For subsequent functional characterization only transcripts with adjusted p-values (padj) of < 0,01 were chosen to ensure that only candidates are included with highest probability that Verticillium gene regulation reflects Pseudomonas treatment. To identify most up- and down-regulated genes for further analysis, transcripts with Log_2_Fold_Change > 4 were regarded as most up-regulated and transcripts with Log_2_Fold_Change < -3 were regarded as most down-regulated ones. This selected dataset was manually annotated by amino-acid sequence BLAST for domain prediction in SMART (http://smart.embl-heidelberg.de/; Letunic *et al.,* 2015 and 2018). Based on this annotation the candidates have been manually assigned to functional categories.

Results

90 % of Verticillia polar hyphal growth can be reduced by fluorescent pseudomonads in confrontation assays.

Growth of Verticillia within microchannels is unaffected by *E. coli.* Fungal growth inhibition by bacteria in SXM containing pectin and amino acids was analyzed when single polar hyphae were grown in microchannels filled with liquid SXM. Confrontation assays with single hyphae of *V. longisporum*, which constitutively express green fluorescent protein (Gfp; Tran *et al*., 2014) and different Pseudomonas strains were performed in microfluidic devices. The length of labeled hyphae growing within these interaction channels was measured after 7 days using fluorescence microscopy. Fungi and bacteria were inoculated at opposing ends of the device. After 7 days the hyphae reached the end of the channel when bacteria are absent. The fungal growth rate of approximately 950 µm per day (µm d-1) did not change substantially upon inoculation with *E. coli* cells or cell free supernatants of *Pseudomonas* spp. Hyphae cultivated in physiological salt solution instead of SXM showed poor growth, suggesting a rather low nutrition effect by the agar inoculation block (Figure 5.1).

Verticillia polar hyphal microchannel growth is reduced by almost 60 % by rhizosphere fluorescent pseudomonads without intact phenazine or DAPG gene cluster. Confrontation assays in microfluidic devices of *V. longisporum* with the rhizosphere isolate of rapeseed (*P. fluorescens* DSM8569, P_rhizo) lacking a phenazine or DAPG cluster reduced the fungal growth rate by more than half to 397 µm d^{-1} in comparison to 950 µm d^{-1} of *V. longisporum* hyphae grown without inhibition. These data suggest a strong potential of rhizosphere pseudomonads to inhibit fungal growth in a confrontation assay with physical constraints in a liquid pectin amino acid medium, which is independent of the genetic potential to produce either phenazines or DAPG.

Verticillia polar hyphal microchannel growth is reduced by 70 % due to rhizosphere fluorescent pseudomonads with intact phenazine gene cluster.

The presence of an intact phenazine cluster (*P. synxantha* 2-79, P_phen), reduced the fungal growth rate in microchannels containing pectin amino acid to almost a third (hyphae grew 286 µm d^{-1} compared to 950 µm d^{-1} without bacteria). The analysis of the phenazine cluster deletion strain P_phen∆*phz* resulted in fungal growth of 546 µm d^{-1} (approximately 60 % of wildtype fungal growth) and revealed that an intact phenazine cluster can contribute to about 30 % of fungal growth reduction caused by the bacteria (Figure 5.1).

Verticillia polar hyphal microchannel growth is reduced by 90 % due to rhizosphere fluorescent pseudomonads with intact compared to defective DAPG gene cluster. The presence of an intact DAPG cluster (*P. protegens* CHA0, P_DAPG, constitutively expressing the red fluorescent protein, Rfp) only enabled the fungus to grow 67 µm d^{-1} corresponding to less than 10 % of the wildtype fungus resulting in the largest observed reduction in Verticillium growth rate (more than 90 %) of the conditions tested using the microfluidic assay. A mutant strain defective in the DAPG cluster (∆*phlA* deletion) improved fungal growth from 67 µm d^{-1} to 182 µm d^{-1} (compared to 950 µm per day without bacteria) and revealed that the DAPG cluster contributes to about 10 % of the bacteria-induced fungal growth inhibition (Figure 5.1).

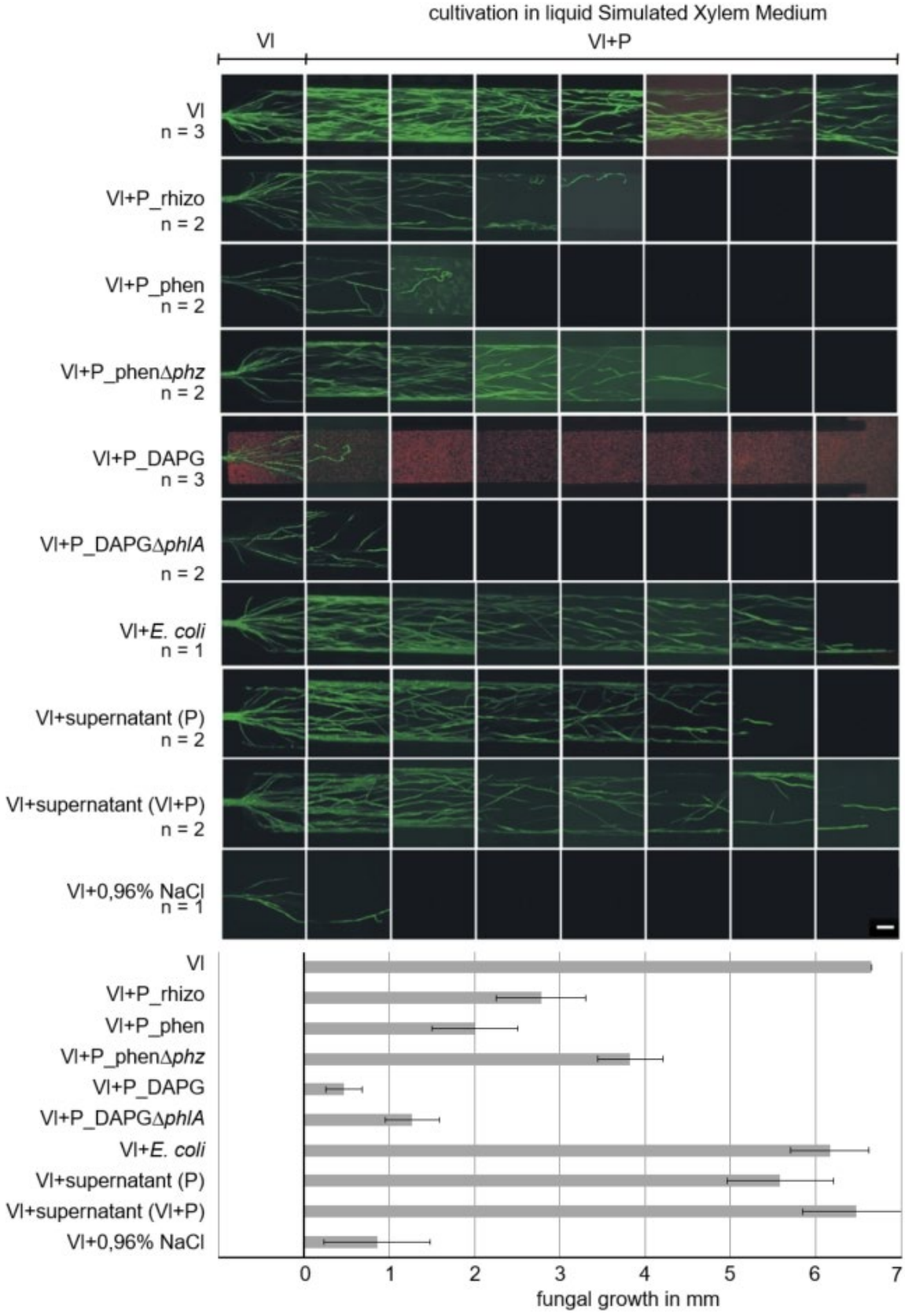
cultivation in liquid Simulated Xylem Medium
Vl
Vl+P
Vl
n = 3
Vl+P_rhizo
n = 2
Vl+P_phen
n = 2
Vl+P_phenΔphz
n = 2
Vl+P_DAPG
n = 3
Vl+P_DAPGΔphlA
n = 2
Vl+E. coli
n = 1
Vl+supernatant (P)
n = 2
Vl+supernatant (Vl+P)
n = 2
Vl+0,96% NaCl
n = 1
Vl
Vl+P_rhizo
Vl+P_phen
Vl+P_phenΔphz
Vl+P_DAPG
Vl+P_DAPGΔphlA
Vl+E. coli
Vl+supernatant (P)
Vl+supernatant (Vl+P)
Vl+0,96% NaCl
0
1
2
3
4
5
6
7
fungal growth in mm

Figure 5.1: Co-cultivation in microfluidic devices of *V. longisporum* VI43 and different wild type fluorescent pseudomonads as well as deletion strains lacking genomic potential for phenazine or DAPG. Co-cultivation was performed in liquid simulated xylem medium containing complex plant molecules such as pectin. *V. longisporum* VI43 (VI) was inoculated at the fungal inoculation site. The device was incubated until the hyphae entered the microchannels. As soon as the fungal hyphae reached the beginning of the interaction channels fluorescent pseudomonads were inoculated at the opposite end of the channel. Bacteria spread throughout the device. Hyphal growth is displayed in mm (scale bar = 10 µm). The diagram shows the arithmetic average of all measured values. The amount of biological replicates (n) is given, respectively. *V. longisporum* expressing the green fluorescent protein was co-cultivated with: the Brassica rhizosphere isolate P_rhizo (*P. fluorescens* DSM8569); the phenazine-producing P_phen wild type (WT: *P. synxantha* 2-79) and the phenazine deficient deletion strain (Δ*phz*); the DAPG-producing P_DAPG (WT: *P. protegens* CHA0), expressing the red fluorescent protein and deletion strains lacking one essential gene for DAPG synthesis *phlA* (Δ*phlA*). Further, *V. longisporum* was treated with sterile supernatant of P_DAPG mono-culture (P), sterile supernatant of P_DAPG and *V. longisporum* co-culture (VI+P) as well as 0.96 % NaCl. Co-cultivation with *E. coli* served as a neutral control.

An intact GacA/GacS regulatory system of fluorescent pseudomonads can contribute to 30 % bacterial inhibition potential against Verticillia hyphal growth in microchannels.

An intact DAPG cluster compared to an intact phenazine cluster can contribute to the growth inhibition of fluorescent pseudomonades in microchannels to 10 % and 30 %, respectively. Increased DAPG secretion by deleting the Δ*phlF* gene for the inhibitor PhlF did not result in a further reduction of the fungal growth rate (P_DAPGΔ*phlF*; Figure 5.2). An additional contribution of 50 % of fungal growth inhibition (as in P_rhizo) can be independent of the presence of either an intact DAPG or phenazine cluster. Several bacterial mycotoxin gene clusters including the DAPG cluster are under control of the bacterial GacA/GacS two component system. Deletion in *P. protegens* CHA0 (P_DAPG) of either the *gacA* or *gacS* gene leads to a recovery in the hyphal growth rate of Verticillium from 67 µm d^{-1} to 336 µm d^{-1} (P_DAPGΔ*gacA*) or 299 µm d^{-1} (P_DAPGΔ*gacS*) compared to approximately 950 µm per day fungal growth without bacterial inhibition (Figure 5.2). This suggests that the two-component system coordinates a substantial portion of 30 % of the bacterial potential to inhibit fungal growth. Several additional

bacterial mutant strains revealed GacA/GacS mediated contributions of the genes for HCN-production (Δ*hcnABC* lacks three essential genes for formation of HCN and Δ*anr* deficient in HCN secretion) and for pyoluteorin synthesis (Δ*plt*) lacking the essential gene for pyoluteorin synthesis (Figure 5.2).

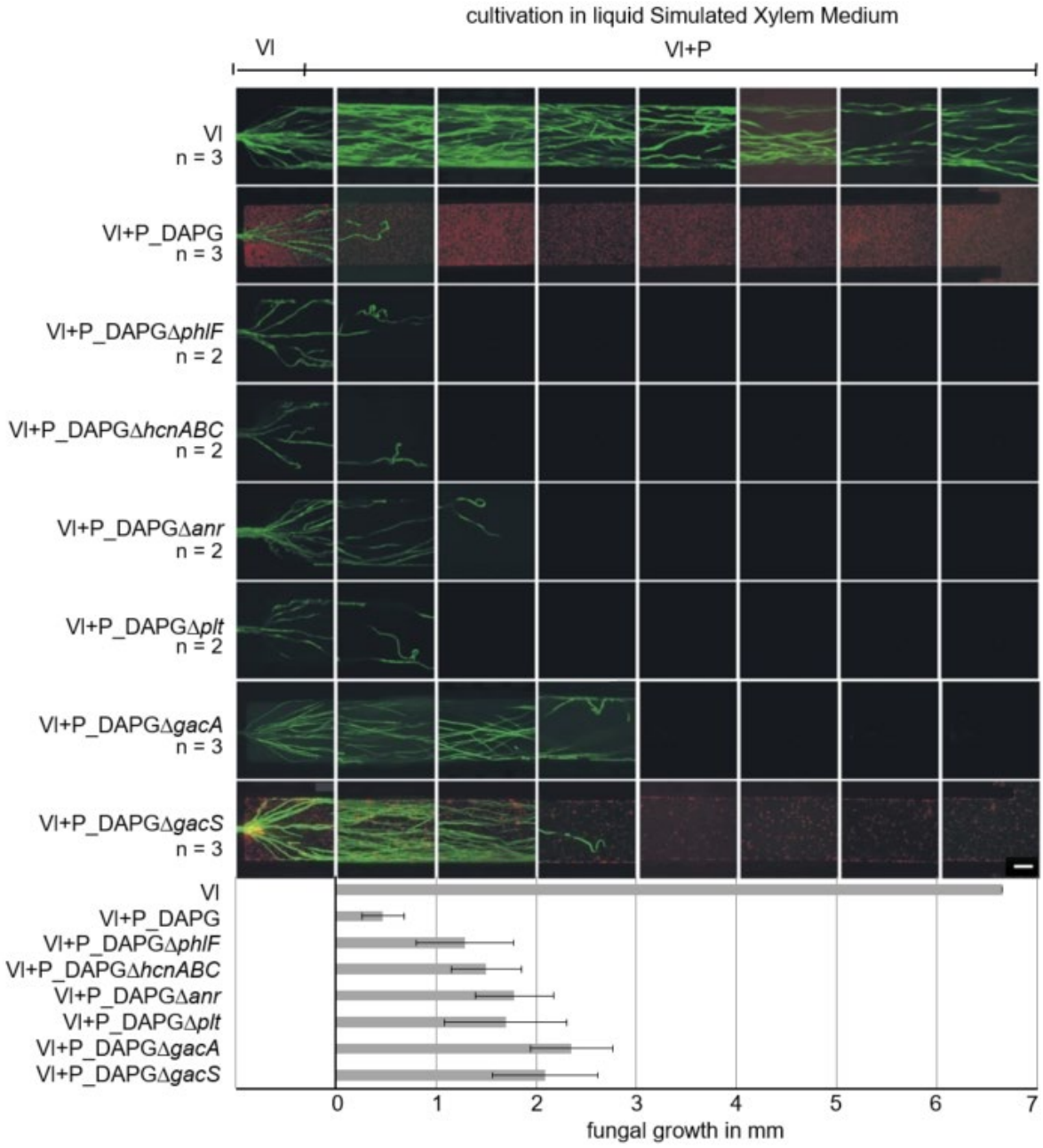

Figure 5.2: Co-cultivation in microfluidic devices of *V. longisporum* VI43 and wild type fluorescent pseudomonads as well as deletion strains missing regulators for multiple or single metabolite synthesis. Co-cultivation was performed in liquid simulated xylem medium containing pectin, which mimics conditions in dead plant material. *V. longisporum* VI43 (VI) was inoculated on an agar block at the fungal inoculation site and incubated until the mycelium grew into the channel. As soon as the fungal hyphae reached the entrance to the interaction channels fluorescent pseudomonads were inoculated at the opposite end of the channel. Bacteria spread throughout the whole channel. Hyphal growth is displayed in mm (scale bar = 10 µm). The diagram shows the arithmetic average of all measured values. The amount of biological replicates (n) is given, respectively. *V. longisporum* expressing the green fluorescent protein was co-cultivated with a DAPG producing P_DAPG (*P. protegens* CHA0) and compared to the following deletion strains: Δ*phlF* - lacking the inhibitor of DAPG-production leading to increased DAPG secretion; Δ*hcnABC* - lacking essential genes for HCN-production; Δ*anr* - lacking the HCN regulator anr with deficient HCN secretion; Δ*plt* - lacking the essential gene for pyoluteorin synthesis; one of the two units for regulation of multiple toxin production *gacA* (Δ*gacA*) or *gacS* (Δ*gacS;* expressing the red fluorescent protein).

In summary, a complex combination of several bacterial genes and gene clusters for bioactive compounds can together provoke a Pseudomonas-mediated inhibition of the fungal *V. longisporum* growth in microchannels filled with liquid SXM medium in a confrontation assay. More than 90 % fungal growth inhibitions could be monitored including different contributions as 30 % of GacA/GacS-controlled genes, including the DAPG cluster, or a 30 % contribution of the genes for phenazine.

Phenazines and GacA/GacS-controlled metabolites of fluorescent pseudomonads change polarity of Verticillium hyphae.

Besides the distinct growth inhibition of Verticillium hyphae in presence of different fluorescent pseudomonads also the bacterial impact on the morphology of Verticillium has been investigated. *V. longisporum* grows in a straight manner parallel to the channel wall in the microfluidic devices. Polar fungal growth was neither affected by *E. coli*, Pseudomonas cell-free supernatants nor a 0.96 % NaCl solution (Figure 5.3).

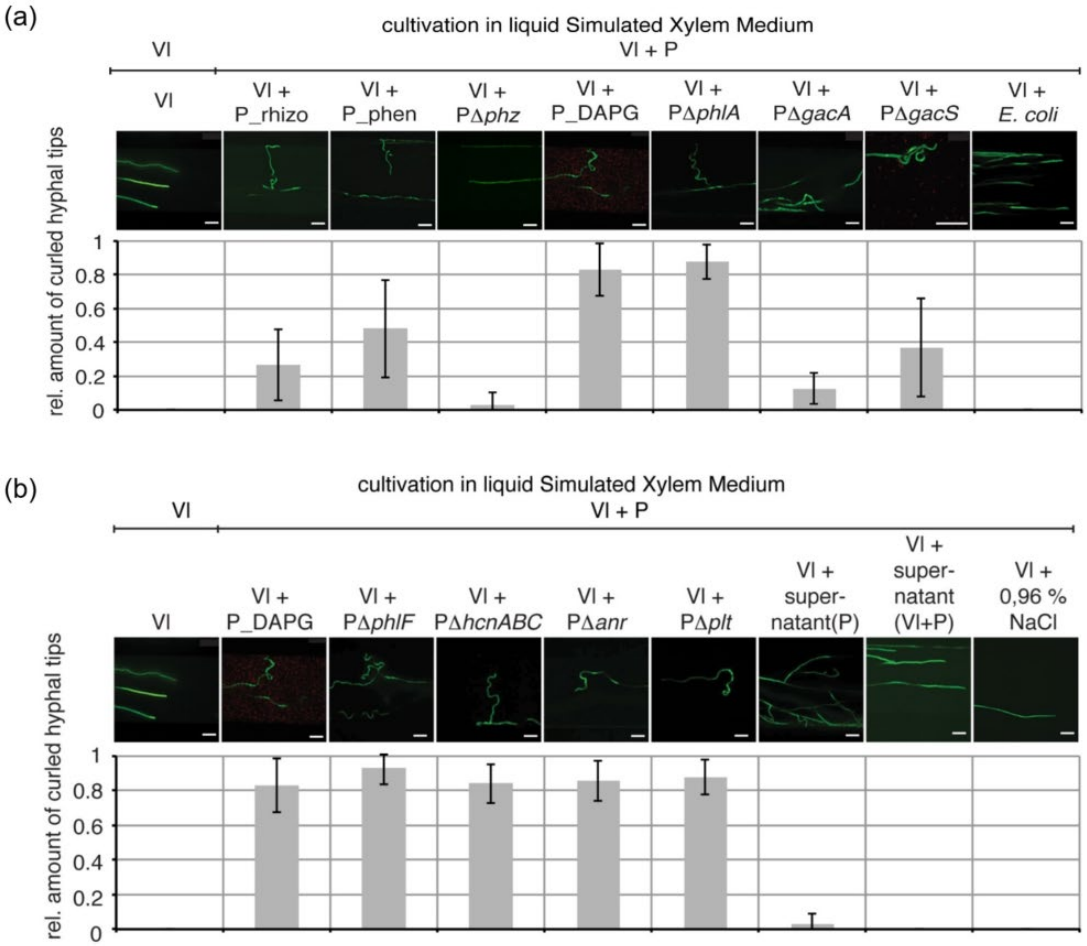

Figure 5.3: Alteration in hyphal polarity of *V. longisporum* Vl43 during co-cultivation with different wild type fluorescent pseudomonads as well as deletion strains. (a) *V. longisporum* Vl43 expressing the green fluorescent protein was co-cultivated with the Brassica rhizosphere isolate P_rhizo (*P. fluorescens* DSM8569); the phenazine-producing P_phen wild type (*P. synxantha* 2-79) and the phenazine deficient deletion strain (Δ*phz*); the DAPG producing P_DAPG (WT: *P. protegens* CHA0) expressing the red fluorescent protein and deletion strains lacking one essential gene for DAPG synthesis *phlA* (Δ*phlA*) or one of the two units for regulation of multiple toxin production *gacA* (Δ*gacA*) or *gacS* (Δ*gacS;* expressing the red fluorescent protein). Co-cultivation with *E. coli* served as a neutral control. (b) *V. longisporum* expressing the green fluorescent protein was co-cultivated with a DAPG producing P_DAPG (*P. protegens* CHA0) and compared to the following deletion strains: Δ*phlF* - lacking the inhibitor of DAPG-production leading to increased DAPG secretion; Δ*hcnABC* - lacking the essential gene for HCN-production; Δ*anr* - lacking the HCN regulator anr with deficient HCN secretion; Δ*plt* - lacking essential gene for pyoluteorin synthesis. Furthermore, *V. longisporum* was treated with sterile supernatant of P_DAPG mono-culture (P), sterile supernatant of P_DAPG and *V. longisporum* co-culture (Vl+P) and 0.96 % NaCl. (scale bars = 10 µm; note: different magnification in picture Vl+PΔ*gacS*) The relative amount of hyphal tips possessing a curled phenotype compared to the fungal control without bacteria is displayed in the diagram. The diagram shows the arithmetic average of all measured values derived from two biological replicates.

Confrontations of Verticillium with pseudomonads did not result in an observable formation of enriched bacterium associations in fungal proximity. Closer inspection of polar fungal growth of *V. longisporum* in confrontation with *Pseudomonas* spp. revealed a curly tip phenotype and changes in growth direction. The rapeseed rhizosphere *P. fluorescens* DSM8569 (P_rhizo) affected almost one third of hyphal tips. Phenazine-producing *P. synxantha* 2-79 (P_phen) led to about 50 % of tips being curled, whereas *P. protegens* CHA0 (P_DAPG) resulted in a mostly curly phenotype (83 %) (Figure 5.3a).

Confrontation experiments with the mutant strains P_DAPGΔ*phlF*, P_DAPGΔ*hcnABC*, P_DAPGΔ*anr*, P_DAPGΔ*plt* impaired in either single metabolite synthesis of DAPG, HCN or pyoluteorin showed a comparable curled phenotype compared to bacterial wildtype. However, the curly phenotype was not observed in confrontation experiments involving the phenazine deficient strain P_phenΔ*phz*. In addition, deletion of either of the translational control network genes, *gacA* and *gacS* of *P. protegens* P_DAPG, reduced the curly phenotype by more than 80 % to 13 % for P_DAPGΔ*gacA* and more than 60 % to 37 % for P_DAPGΔ*gacS* (Figure 5.3).

These data indicate that the genetic information for phenazines and GacA/GacS-dependent bacterial metabolites induce polar changes in fungal hyphae. Changes in growth direction, which are rather restricted within the channel of the microfluidic devices, might allow the hyphae in nature to avoid bacteria.

P. protegens alters transcriptional profiles of *V. longisporum* genes including up-regulation of detoxification related genes and decreased levels of transcripts for protein biosynthesis and plant polysaccharide degradation.

P. protegens CHA0 (P_DAPG) had the greatest impact of 90 % polar growth inhibition in microfluidic device confrontation assays using liquid SXM pectin/amino acids medium. A snapshot of an initial transcriptional fungal response on the bacterium in a non-constrained liquid environment was analyzed after two hours of co-cultivation. Therefore, *V. longisporum* was precultured in liquid SXM for six days and then mixed with P_DAPG. Mycelia in the presence of bacteria were harvested after two hours of further cultivation and compared to corresponding fungal control samples in the absence of bacteria. Total bacterial and fungal RNAs were isolated and fungal RNAs were sequenced (NCBI-Accession-number SRP068348; http://www.ncbi.nlm.nih.gov/sra/?term=SRP068348). The reads were mapped to the genome of *V. dahliae* JR2 (de Jonge *et al.*, 2012). 11,439 sequenced fungal transcripts were clustered using the MarVis-Cluster tool (Kaever *et al.*, 2009) as a function of the MarVis-Suite software (Kaever *et al.*, 2015; http://marvis.gobics.de). 4,020 fungal genes representing 35 % of the total amount of fungal transcripts were down-regulated in the presence of *P. protegens* P_DAPG. The expression of an almost equal amount of 4,277 genes (37 %) was induced by co-cultivation with *P. protegens*. The remaining 2,895 transcripts representing one quarter of the total gene set, were not differentially expressed. 247 transcripts differed too much between the two replicates and remained as unclassified. The transcriptome dataset was statistically filtered using MarVis-Filter to identify and select robustly regulated gene candidates (Figure 5.4).

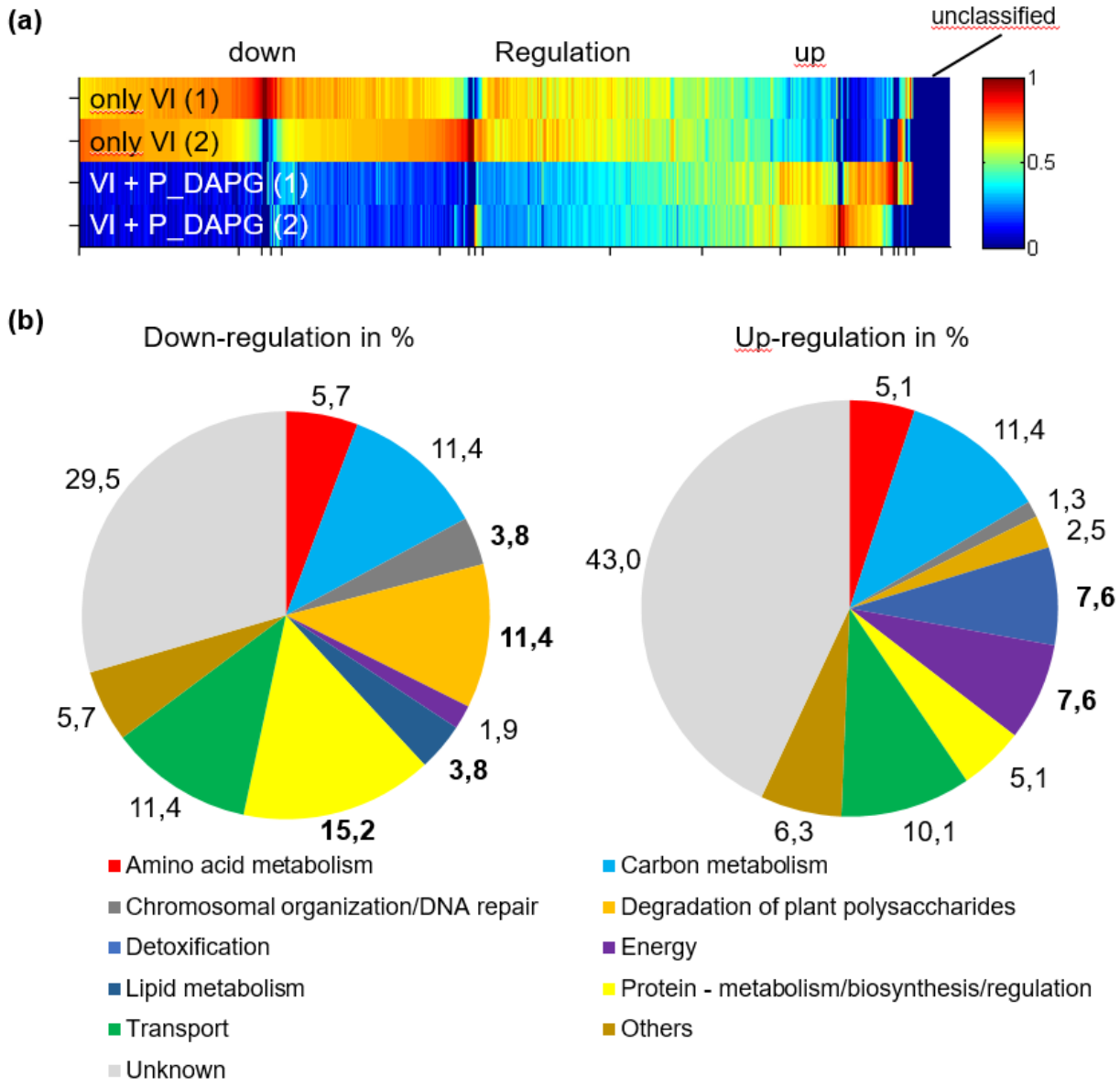
(a)
down
Regulation
up
unclassified
only VI (1)
only VI (2)
VI + P_DAPG (1)
VI + P_DAPG (2)
1
0.5
0
(b)
Down-regulation in %
5,7
11,4
3,8
11,4
1,9
3,8
15,2
11,4
5,7
29,5
Up-regulation in %
5,1
11,4
1,3
2,5
7,6
7,6
5,1
10,1
6,3
43,0
Amino acid metabolism
Carbon metabolism
Chromosomal organization/DNA repair
Degradation of plant polysaccharides
Detoxification
Energy
Lipid metabolism
Protein - metabolism/biosynthesis/regulation
Transport
Others
Unknown

Figure 5.4: Transcriptome analysis of *V. longisporum* VI43 after unconstrained co-cultivation with *P. protegens* CHA0 (P_DAPG). Different liquid cultures of *V. longisporum* in simulated xylem medium (SXM) were pooled after 5 days. The fungal cultures were further cultivated in the presence or absence of *P. protegens* for 120 min. Bacterial and fungal total RNA was extracted and fungal mRNA was sequenced. Two individual replicates were obtained. (a) The heat map shows a one-dimensional self-organizing map of all 11,439 sequenced fungal Verticillium transcripts classified in MarVis-Cluster. The lines underneath the heatmap mark the cluster borders that describe similar expression profiles, respectively. Transcripts that show an inconsistent expression profile have been regarded as unclassified. The colors code for transcript frequency as normalized quantities according to the color scale right to the heat map. Red indicates transcripts with high abundance; blue indicates transcripts with low abundance. (b) Most up-regulated candidates with Log_2_Fold_Change > 4 and padj < 0,01 and most down-regulated candidates with Log_2_Fold_Change < -3 and padj < 0,01 were manually assigned to functional categories. The percentage of transcripts referring to the specific functional category (left: down-regulated, right: up-regulated) is depicted. Bold figures mark the biggest differences between the down- and the up-regulated transcripts indicating the functional categories with the most impact on Verticillium expression due to the presence of Pseudomonas. The transcripts belonging to these categories are listed in Table 5.2, S5 and S6.

After an automated annotation with the Ensembl- (Howe *et al.*, 2019) and Gene Ontology (GO; Ashburner *et al.*, 2000; Gene Ontology Consortium, 2019) database all transcripts with an adjusted p-value (padj) < 0,01 were chosen for further analysis. The automated annotation of all transcripts with Log_2_Fold_Change > 4 (most up-regulated genes) and transcripts with Log_2_Fold_Change < -3 (most down-regulated genes) has been manually curated by additional amino-acid sequence BLAST for domain prediction in SMART (http://smart.embl-heidelberg.de/; Letunic *et al.* 2015 and 2018) and sorted to functional categories (Figure 5.4b). The complete dataset is attached in Annex Tables S5, S6 and S7.

Out of the complete dataset of 4020 differentially down-regulated Verticillium genes due to Pseudomonas co-cultivation 105 genes belong to the most down-regulated genes with a Log_2_Fold_Change < -3 and padj< 0,01 (Figure 5.4). Bacterial co-cultivation leads to an overall decrease of 14 out of 105 most down-regulated transcripts for general fungal protein synthesis which is consistent to the observed lower fungal growth rate (Figure 5.4b). Many transcripts putatively involved in degradation of plant polysaccharides like fungal pectin lyases, methylesterases and cell wall glycosyl hydrolases are down-regulated. In total, 12

out of 105 most down-regulated Verticillium genes belong to processes of plant degradation, which comprises a ratio of 11,4 %. In comparison, only 2 out of 79 most up-regulated genes refer to plant degradation, which is a ratio of 2,5 %. This slows down plant material breakage for nutrition uptake, which could be correlated to the Pseudomonas induced decrease of Verticillium growth in a pectin medium mimicking plant environment. The transcription of genes for different putative endopeptidases (VDAG_JR2_Chr5g09370a: -4,8 Log_2_Fold; VDAG_JR2_Chr2g04680a: -3,7 Log_2_Fold; VDAG_JR2_Chr5g04770a: -3,3 Log_2_Fold; Table S6) has also been reduced, which suggests less proteolytic activity of Verticillium.

79 out of 4277 genes belong to the most up-regulated differentially regulated genes with a Log_2_Fold_Change > 4 and padj< 0,01. Inhibition of fungal growth during Pseudomonas co-cultivation might be reflected by six transcripts encoding proteins with potential functions in detoxification reactions out of the 79 most up-regulated Verticillium (Table 5.2).

Table 5.2. Most up- regulated Verticillium related genes related to detoxification reactions after 120 min of Pseudomonas co-cultivation. The reads of *V. longisporum* VI43 have been mapped to the *V. dahliae* genome of JR2. Most up-regulated genes related to detoxification of cyanide or reactive oxygen species with Log2_Fold Change >4 are shown. Genes were automatically annotated and manually curated and assigned to functional categories (entire list in Table S5 & S6). E-values describe similarities to the SMART database. The complete transcriptomic dataset is deposited at NCBI under the accession-number SRP068348; http://www.ncbi.nlm.nih.gov/sra/?term=SRP068348. Gene-IDs refer to genome assembly of *V. dahliae* JR2 (VDAG_JR2v.4.0; de Jonge *et al.*, 2012) deposited at www.fungi.ensembl.org/Verticillium_dahliaejr2/Info/Index (Howe *et al.*, 2019). Log_2_FC = Log_2_Fold_Change; *Possible predicted function according to domain description at www.smart.embl-heidelberg.de (Letunic *et al.* 2015 and 2018)

Gene-ID	padj	Log_2 _FC	Domain name	Predicted domain function*	e-value
VDAG_JR2_Chr7g05440a	$1,4e^{-288}$	6,6	RPE65	Oxidoreductase activity, acting on single donors with incorporation of molecular oxygen; in plants scavengers of oxygen radicals (in vertebrates retinal pigment epithelium 65 kDa protein (RPE65))	$3,2e^{-102}$
VDAG_JR2_Chr3g06110a	$2,2e^{-250}$	6,2	CN_hydrolase	Cyanide hydratase of pathogenic fungi; putatively detoxifies HCN	$7,4e^{-42}$
VDAG_JR2_Chr1g24680a	$1,1e^{-171}$	5,8	GFA	Glutathione-dependent formaldehyde-activating enzyme (GFA); carbon-sulfur lyase activity; catalyzes the first step in detoxification of formaldehyde	$1,1e^{-10}$
VDAG_JR2_Chr5g10540a	$4,4e^{-8}$	5,0	Pyr_redox_2	Pyridine nucleotide-disulfide oxidoreductases; e.g. glutathione reductase (i.a. ROS-defense), thioredoxin reductase (i.a. cell wall integrity)	$7,4e^{-8}$
VDAG_JR2_Chr3g09580a	$2,6e^{-175}$	4,9	DSBA	Key component (A) of the disulfide bond (DSB) family; thiol disulfide oxidoreductase; sub-family of thioredoxin family; catalyzes oxidation of cysteine residues of e.g. toxins, virulence factors, adhesion machinery, and motility structures	$4,6e^{-16}$
VDAG_JR2_Chr4g00930a	$1,1e^{-11}$	4,6	GST_N_3	Glutathione-S-transferase; catalyzes conjugation of glutathione to xenobiotic substrates for detoxification	$8,6e^{-11}$

An elevated gene expression of transcripts for genes that putatively function as cyanide hydratase (VDAG_JR2_Chr3g06110a; 6,2 Log_2_Fold), thioredoxin (VDAG_JR2_Chr3g09580a; 4,9 Log_2_Fold) or Glutathione-S-transferase (VDAG_JR2_Chr4g00930a; 4,6 Log_2_Fold) might represent a potential detoxifying response to a possible GacA/GacS-controlled HCN secretion or further toxins secreted by Pseudomonas. The toxin HCN is a respiratory inhibitor and inactivates the essential enzyme cytochrome C oxidase that is responsible for electron transport in the respiratory chain (Rich, 2017). Cyanide hydratases detoxify HCN and are probably exclusively produced by filamentous fungi (Martinkova *et al.*, 2015; Benedik and Sewell, 2017). VDAG_JR2_Chr3g06110a shows high sequence similarity to cyanide hydratases of other fungal genera like Fusarium, Colletotrichum, Pochonia, Neurospora, Metarhizium, Ophiocordyceps,

Stachybotrys, Aspergillus and Trichoderma (Protein BLAST; Fig. S2). The role of the cyanide hydratase enzyme (chy) for HCN detoxification in *Fusarium solani* (Genbank accession-number AJ310936.1) was investigated by Barclay *et al.* (2002) and it shows sequence homology to VDAG_JR2_Chr3g06110a with an identity of 84 % (Figure S2). The putative Pyridine nucleotide-disulfide oxidoreductases VDAG_JR2_Chr5g10540a refers to detoxification of reactive oxygen species (ROS) (Karplus and Schulz, 1987; Kuriyan *et al.*, 1991; Schiering *et al.*, 1991; Fernandez and Wilson, 2014) which can be produced by Pseudomonas spp. and are commonly released to the environment during interaction with other microbes (Jayamohan *et al.*, 2018).

Co-cultivation of Pseudomonas with Verticillium, which inhibits fungal growth, correlates to changes in the fungal transcriptome even after a bacterial exposure of only two hours resulting in increased transcription of various detoxification enzymes as e.g. for HCN. The bacterial co-cultivation also leads to a reduced transcription for protein synthesis by Verticillium correlating to a reduced growth rate and reduces transcription of genes required for plant material acquisition.

Discussion

Two different co-cultivation set-ups in liquid pectin amino acid medium have been chosen for Pseudomonas species with *Verticillium longisporum.* Depending on the conditions of the environment in which the interaction takes places, the fungus behaves accordingly. (i) If Verticillium has the option to escape from bacterial impact, the fungus tries to evade into areas with less bacterial and toxic concentration. Under Pseudomonas influence, this fungal behavior could be observed in a microfluidic confrontation assay in which the hyphal tips begin to curl and change their linear polar growth pattern even under physically constrained circumstances. (ii) If evasion is no option for the fungus as it is the case in an agitated liquid flask co-cultivation where a constant mixing leads to recurring close contact between fungus and bacterium, *V. longisporum* tries to withstand the antifungal conditions by detoxification. In a differential expression analysis during flask co-cultivation it has been shown that the fungus increases the expression of detoxification related genes to cope with the bacterium. Additionally, the fungus down-regulates the expression of genes involved in protein biosynthesis and plant polysaccharide degradation. As under natural conditions there are zones with heterogeneous suppressive concentrations in the rhizosphere the evasion strategy is expected to be the more relevant one for Verticillium in nature. This hypothesis is supported by previous observations with Pseudomonas-Verticillium co-cultivation on surfaces that show a pronounced fungal free zone around the bacterial colony giving the impression that Verticillium strictly follows a specific distance to the bacterium. The size of this inhibition zone depends on the nutritional conditions of the medium as well as the genetic abilities of the bacterium to produce antifungal secondary metabolites (Nesemann *et al*., 2018).

The observed polarity alteration in Verticillium hyphal growth induced by the presence of the bacterium were possibly caused by phenazines or GacA/GacS induced bacterial compounds, but not by DAPG itself. DAPG-induced polarity effects have been described for the phytopathogenic fungus *Aphanomyces cochlioides* (Islam and Fukushi, 2003) or for *Pythium ultimum* (de Souza *et al*., 2003), but were so far not observed for Verticillium.

The presence of a phenazine cluster in the bacterial genome resulted in different effects on fungal growth, depending on the growth conditions. In a previous study (Nesemann *at el*., 2018) we determined a nutrition dependent impact on the antagonistic relevance of bacterial phenazines. In a surface interaction study on solid agar under rich nutrition with high amounts of glucose, a phenazine gene cluster could be identified as one crucial factor for Verticillium growth inhibition, whereas in poor amino acids and pectin environment the fungal growth suppression was independent from phenazines. However, in confrontation assays in liquid pectin amino acid medium phenazines seem to be an alternative strategy to the two-component GacA/GacS system regulating multiple antifungal compounds for fungal control. The presence of the phenazine cluster caused 30 % inhibition of fungal growth, as well as a curly tip phenotype at the apex of the hyphae leading to polarity changes in the fungal growth direction.

Verticillium hyphae show a similar curly phenotype as well as a growth suppression when co-cultivated with the natural isolate from oilseed rape rhizosphere (P_rhizo), although in reduced intensity. P_rhizo neither possesses the genetical ability to synthesize phenazines nor a genetically fully functional GacA/GacS system as it lacks the regulatory small RNAs *rsmX* and *rsmZ* (Nesemann *et al.*, 2015a and 2018). This leads to the hypothesis that P_rhizo produces other than the bioactive substances discussed above play a role to evoke the observed alteration in fungal polarity as well as inhibition in hyphal growth. Further investigation would be necessary to gain a better understanding what Pseudomonas molecules are responsible for this phenomenon.

Besides the evasion strategy, Verticillium also follows a detoxification approach against Pseudomonas. The transcriptional response to the presence of the bacterium includes an increased expression of genes responsible for fungal detoxification suggesting that the fungus has developed protection mechanisms against secreted mycotoxins like DAPG or cyanide. Barclay *et al.* clarified the mechanism of cyanide hydratase enzyme (chy) in *Fusarium solani* to detoxify cyanide complexes in a substrate-regulated manner. Evolutionary conservation has been described and sequence homology could be shown to *Gloeocerospora sorghi*, *Fusarium lateritium* and *Leptosphaeria maculans* as it is shown in this study to the *V. dahliae* gene VDAG_JR2_Chr3g06110a. The up-regulated gene

VDAG_JR2_Chr5g10540a putatively belongs to the family of pyridine nucleotide-disulfide oxidoreductases including enzymes that also might be involved in detoxification like glutathione reductase (Karplus and Schulz, 1987) or thioredoxin reductase (Kuriyan *et al.*, 1991). Glutathione reductase catalyzes the reduction of glutathione-disulfide to glutathione and this way recycling its capacity of neutralizing reactive oxygen species (ROS) as an antioxidant. In 2014, Fernandez and Wilson investigated the role of glutathione reductase as well as thioredoxin reductase of *Magnaporthe oryzae* during rice blast disease. Glutathione reductase but not thioredoxin was essential for the detoxification of ROS produced by the plant. Thioredoxin but not glutathione reductase was shown to be important for cell wall integrity in *Magnaporthe oryzae*.

A direct and distinct response for all Verticillium gene candidates that seem to be differentially expressed in Pseudomonas presence cannot be postulated and might also belong to a general or indirect reaction due to changing cultivation conditions such as competition for nutrients. The expression increase of VDAG_JR2_Chr1g24680a showing sequence similarity to the formaldehyde detoxifying domain GFA (Lupas *et al.*, 2015; Chen *et al.*, 2016) or of VDAG_JR2_Chr7g05440a carrying a domain involved in photo protection are not necessarily a close answer to Pseudomonas co-cultivation as it is not assumed that Pseudomonas releases formaldehyde in its surrounding or causes photo inhibition.

The slow-down in fungal growth was accompanied by a reduction in transcription levels of genes coding for plant polysaccharide breakdown putatively used for fungal nutrition. This finding coincides with results of a transcriptomic profiling of the fungal plant pathogen *Rhizoctonia solani* challenged by the antagonistic bacteria *Serratia proteamaculans* and *S. plymuthica* (Gkarmiri *et al.*, 2015). A significant down-regulation of genes coding for plant degrading enzymes like pectin lyases or glycoside hydrolases has been observed in Rhizoctonia during bacterial co-cultivation.

Taken together, the results of this Verticillium-Pseudomonas interaction study suggest a detoxification and evasion strategy of the fungus. In a suppressive environment induced by different antifungal bioactive compounds such as DAPG, HCN or phenazines that have been expressed by antagonistic rhizobacteria,

Verticillium tries to grow towards less suppressive areas in order to avoid close contact to the bacterium. If the fungus has no option to escape from bacterial impact, he increases the expression of genes related to detoxification while decreasing processes involved in protein biosynthesis and plant polysaccharide degradation.

Chapter 6: Discussion

Growth control of Verticillium by fluorescent pseudomonads

This study investigated physical and molecular interaction between virulent *Verticillium* strains and different rhizobacteria *in situ*. All used bacterial strains belong to fluorescent pseudomonads. A visual growth suppression of the bacterium due to fungal impact has never been observed in this study. This includes co-cultivations in different media on solid surfaces or in liquids and confrontations in channels filled with liquid media. The bacterium could inhibit fungal growth. This bacterial antagonism against hyphal growth was expressed towards fungi that have been isolated out of the identical rhizosphere as well as out of others. The findings lead to the hypothesis that the fungus itself ultimately possesses rather little chances to actively keep the bacterium under control. Instead, a withdrawal strategy is followed by the fungus physically evading the bacterial influence when possible. Pathways that correspond to detoxification of external bioactive compounds are induced. The expression of genes involved in cellular processes that can be reduced under suppressed growth activity like protein synthesis and plant polysaccharide degradation is down-regulated.

Relevance of fungal secondary metabolism during interaction with fluorescent pseudomonads

In microbial interactions, secondary metabolism can play a crucial role (Koehl *et al.*, 2019; Korenblum and Aharoni, 2019) and filamentous fungi cover a wide range of bioactive secondary metabolites to be secreted into their surrounding (Bayram and Braus, 2012; Keller, 2019). The regulatory genes for epigenetic Lae1 methyltransferase (Sarikaya-Bayram *et al.,* 2015) and Csn5 deneddylase (Braus *et al.,* 2010), which both contribute to the control of the expression of secondary metabolism genes in fungi have been investigated. The putative methyltransferase was originally found in *Aspergillus nidulans*, called LaeA, and is described as a global regulator of secondary metabolism crucial of biosynthesis of e.g. aflatoxin,

penicillin and sterigmatocystin. Additionally, an important morphological role of LaeA could be found in *A. nidulans* to be involved in asexual development in a light-dependent manner (Bayram and Braus, 2012; Lan *et al.*, 2020). Csn5 is the fifth subunit of the COP9-signalosome, a multiprotein complex consisting out of in total eight subunits and activating the cullin-RING E3 ubiquitin ligases responsible for protein degradation by the proteasome (Gerke and Braus, 2014; Meister *et al.*, 2019). However, for both, Lae1 as well as Csn5, no impact on bacterial-fungal interaction could be determined (Nesemann *et al.*, 2018). To investigate fungal genetic adaption during bacterial co-cultivation the Verticillium transcriptomic profile has been sequenced under the influence of *P. protegens* CHA0 (P_DAPG). *P. protegens* CHA0 contains a GacA/GacS two-component system and is genetically equipped with the ability to release a cocktail of different bioactive compounds including DAPG (Haas and Défago, 2005). A significant involvement of fungal secondary metabolism could also not be identified in the transcriptome dataset. For other pathogenic fungi co-cultivated with bacteria, a specific transcriptional activation of secondary metabolite clusters has been described previously. In bacteria-induced *Aspergillus nidulans* the synthesis of different natural products including polyketides is enhanced and requires a Saga/Ada-mediated histone acetylation (Schroeckh *et al*., 2009; Nützmann *et al*., 2011).

The impact of phenazines and the GacA/GacS regulation system on fungal growth highly depends on nutrition.

In contrast to fungal regulatory genes in secondary metabolism, the ability of fluorescent pseudomonads to secrete a heterogeneous panel of secondary metabolites with bioactive antibiotic properties has been well-explored (Sahu *et al.*, 2018; Shah *et al.*, 2020). The bacterial regulatory genes for the GacA/GacS translational control for the production of different bioactive metabolites and exoenzymes plays an important role for the different facets of the bacterial-fungal interaction (Yan *et al*., 2018; Mishra and Arora, 2018; Zhang *et al.*, 2020). This study revealed that in most situations a complex combination of genes for several bacterial metabolites or mycotoxins rather than a gene for a single toxin provides Pseudomonas-mediated effects on vegetative Verticillium growth. In addition,

genes involved in the production of bacterial phenazines had a major impact on fungal growth in optimal growth conditions with fast turnover glucose available. The bacterial genetic potential to synthesize phenazines was not required for fungal growth suppression when the co-cultivation took place in an environment containing high amounts of amino acids and complex pectins that are rather intricate to digest. The deleted phenazine gene cluster resulting in a deficient phenazines biosynthesis pathway could be compensated under the appropriate nutritional conditions.

For the two-component system GacA/GacS that regulates a variety of genes encoding for a cocktail of antifungal metabolites (Haas and Défago, 2005; Yan *et al.*, 2018; Zhang *et al.*, 2020), the nutritional impact appears in an opposite way compared to phenazines. The genes for the bacterial GacA translational regulator as well as for the sensor protein GacS were essential to suppress fungal growth on high amino acids and pectins. Only a poor inhibition potential could be shown for GacA and GacS on optimal growth surfaces with high amounts of glucose. The GacA/GacS genetic network regulates the formation of mycotoxins, such as 2,4-diacetylphloroglucinol, pyoluteorin and hydrogen cyanide, which on their own were unable to control fungal vegetative growth. Due to the shown relevance of the GacA/GacS system for fungal growth suppression, it can be assumed that also under natural conditions in the rhizosphere a cocktail of several Pseudomonas mycotoxins rather than a specific single one is relevant for the suppression of Verticillium. The strong nutrition impact of the surrounding for the respective chosen antagonistic pathway might also be reflected by the heterogeneous natural conditions and potentially supports the hypothesis of a diverse interplay of several antifungal compounds.

During this study, different Pseudomonas strains with individual genetic properties to synthesize antifungal compounds have been chosen for Verticillium co-cultivation. A specific measurement of the actually secreted molecules as well as a general omics approach has not been performed yet. This is why, it has to be taken into account that the results that are presented here can be considered as an indication of which antifungal metabolites are key to explain the observations but not as a strong evidence so far. A subsequent metabolomic investigation during the Verticillium-Pseudomonas interaction would give further important insights into

the fungal and bacterial metabolites that play a crucial role in this interaction. This metabolomic dataset might also include fungal candidates that potentially trigger the membrane associated sensor kinase GacS as a first step to activate GacA and start the whole two-component regulation system for release of toxic substances. For the GacA/GacS system of *P. aeruginosa,* a multikinase network it has been described that at least consists out of the two sensor kinases GacS and RetS that are able to detect and integrate external signals (Francis *et al.*, 2018; Francis and Porter, 2019; Mancl *et al.*, 2019). RetS possesses different mechanisms to inhibit the autophosphorilation of GacS and this way to block the activation of the subsequent signal transduction. For *P. aeruginosa,* this regulation is crucial for the expressing virulence factors. This level of understanding is so far lacking for *P. protegens* or P. *synxantha* in general but also in interaction with Verticillium.

The fungal detoxification and evasion strategy

The bacterial repertoire of multiple bioactive compounds activated in the described nutritional manner and secreted into its environment leads to heavy rearrangements and reactions by the fungus. In microfluidic channels, the interaction of the oilseed rape pathogen *V. longisporum* Vl43 with different fluorescent pseudomonads was visualized *in vivo.* In 7 mm long and only 100 µm wide micro racing channels, the hyphal growth direction was predefined in one direction. This way, the inhibition potential of different treatments could be quantified and compared. A Verticillium growth suppression of up to 90 % was induced by *P. protegens* CHA0 due to an additional DAPG gene cluster. Besides a pure growth inhibition, also a morphological alteration was observed. In an unstressed situation without the co-cultivation of bacteria, the hyphae showed a highly straight and parallel polar growth manner. Under stressed conditions, different Pseudomonas strains were able to influence this Verticillium growth pattern to a meanwhile highly curled hyphal tip. This can be interpreted as a fungal strategy to evade the bacterial influence and escape to an area with less suppressive potential. Under these artificial laboratory conditions, the concentration of bacterial organisms and this way also the concentration of antifungal metabolites in the interaction medium was highly enlarged and the

microchannels were completely filled with bacterial cells. Under natural conditions, where many other biotic factors also influence the distribution and abundance of the bacterial antagonist, this evading strategy might be a successful strategy giving the fungus the chance to infect another root in a region of the rhizosphere with less antifungal impact.

Fungal evasion strategies to cope with host recognition is not only discussed as physical avoidance by translocation like we observed it for Verticillium but also by further morphological adaptations to withstand the host antagonism at the same place (Hernández-Chávez *et al*., 2017). Compared to plant pathogens like Verticillium, the knowledge for human pathogens is a lot wider. Main focus of human pathogens is to evade active surveillance mechanisms of mammalian hosts by phagocytosis that might be partially transferable to plant pathogens. Different strategies have been described, e.g.: (i) Compositional changes in the cell wall by increasing the amount of polysaccharide structures like chitin or melanin. Melanin storage to mechanically strengthen the cell wall has been described for *Paracoccidioides brasiliensis* and *Sporothrix schenckii* (Nosanchuk and Casadevall, 2006). Since it is known that Verticillium also embeds melanin in the microsclerotia (Tran *et al.*, 2014), this might be a possible reaction in the Pseudomonas-Verticillium interaction as well. (ii) Formation of capsules as physical barrier to protect the cell from its environment. *Cryptococcus neoformans* possesses a large capsule, which is considered to be its main virulence factor to cause meningitis disease (Doering, 2009). (iii) So-called titan cells show a blown up cell size of 14 to 20-fold (Okagaki *et al.*, 2010) some even up to 300-fold (Crabtree *et al*., 2012) compared to their normal size. Titan cells of *C. neoformans* are significantly more resistant against oxidative stress (Zaragoza *et al*., 2013; Okagaki *et al*., 2012). (iv) Asteroid bodies are concentric and spiked formations of extracellular components surrounding a central fungal cell giving the enlarged complex a crown-like structure. Asteroid bodies protect the central cell against its suppressive environment and have been found in different fungal genera including Aspergillus, Candida, Sporothrix, Histoplasma (Daniel Da Rosa *et al.*, 2008). The given examples represent physical barrier systems of fungal cells to make them more resistant to harsh chemical conditions induced by their host. The listed techniques give the fungi to ability to physically stay within and withstand the

suppressive environment. The need to escape to other regions of less suppressivness is not necessary in this case. Compared to our observations in the microfluidic confrontation devices, at the first glace none of the mentioned structures could be recognized for Verticillium. Following the hypothesis, that Verticillium is potentially not capable to build comparable morphological structures to increase its resistance against Pseudomonas, Verticillium chose an alternative escape strategy.

In an agitated interaction environment, this evasion/escape strategy cannot be applied by the fungus as the mixing motion leads to constantly recurring close contact between the fungus and the bacterium. A differential expression analysis of the fungal transcriptome has been performed under stressed and unstressed conditions triggered by co-cultivation with *P. protegens* CHA0 (P_DAPG). Cellular processes that can be renounced due to hyphal growth reduction are down-regulated. This refers to genes that are involved in general protein biosynthesis but also to genes specifically coding for degradation of complex plant materials like pectins. On the one hand, this can be interpreted as a provision to not invest cellular energy in further growth. On the other hand, less activity in plant cell wall lyses can also resemble a slowdown in food breakdown. Since Verticillium dramatically reduces growth, the need of energy supply is also decreased.

Besides down-regulating pathways that can be saved under less growth behavior, Verticillium induces the transcription of genes associated with detoxification. It can be assumed that the fungus is able to specifically focus and prioritize only the required pathways to cope with the bacterial toxicity.

Compared to the detoxification and evasion strategy followed by Verticillium to handle Pseudomonas' antagonism, for *Aspergillus fumigatus* a wait-and-see strategy has been described when living in human blood (Irmer *et al.*, 2015). Both, the conditions for *A. fumigatus* to survive in blood as well as the situation for Verticillium surrounded by a high cell density culture of fluorescent pseudomonads are suppressive but the fungal reactions are different. Irmer *et al.* found a down-regulated pattern of genes involved in up-take mechanisms as well as in energy-consuming metabolic processes. The hyphal behavior was interpreted as a resting mycelium stage lacking hardly any growth. The capabilities of *A. fumigatus* to take up sufficient nutrients are highly restricted leading to limited energy resources in

the cell. Compared to the observations for Verticillium, Aspergillus fails in establishing sufficient self-defense mechanisms combined with growth activity. An active withdrawal like it has been investigated for Verticillium as a reaction on the vicinity of Pseudomonas was not described for Aspergillus in a blood cultivation.

Taken together, the results can be interpreted as a detoxification and evasion strategy followed by Verticillium to withstand the suppression caused by Pseudomonas. The fungus tries to evade the bacterial impact aiming to reach areas with less suppressive potential to infect its host plant. Transferring this Verticillium strategy to the natural conditions in the highly heterogeneous environment of the rhizosphere including plenty of influencing factors it will most likely not always be successful in terms of survival. In large areas with concentrated antagonistic species, the fungus might not be able to evade this suppressive zone. In this situation, Verticillium possibly activates detoxifying reactions but only up to a certain extent. Under an ecological perspective, it can be assumed that in large-scale suppressive areas, the Verticillium evasion and detoxification strategy will be limited.

The positive and negative connotation of beneficials and pathogens as an anthropocentric view

The described relationship between the mutualistic bacterium, possessing a positive connotation, and the opportunistic fungus with a negative attribute, is a rather anthropocentric interpretation of their antagonism going on in the rhizosphere. On the one hand, this judgment is driven by the target of minimizing pathogenic damage of crops gaining maximal yield for the farmer. On the other hand, the beneficial and opportunistic roles of the two players are not constantly fixed and defined. Closely related species using very similar defense and pathogenicity techniques are considered as either pathogens or beneficial growth promoting and biocontrol agents depending on the respective view. Rodriguez *et al.* (2019) described this phenomenon as “Friends and Foes: Closely related beneficial and pathogens”. In a phylogenetic dendrogramm (Figure 6.1), they

compared the evolutionary relationship of mutualistic bacteria in black and pathogenic bacteria in red.

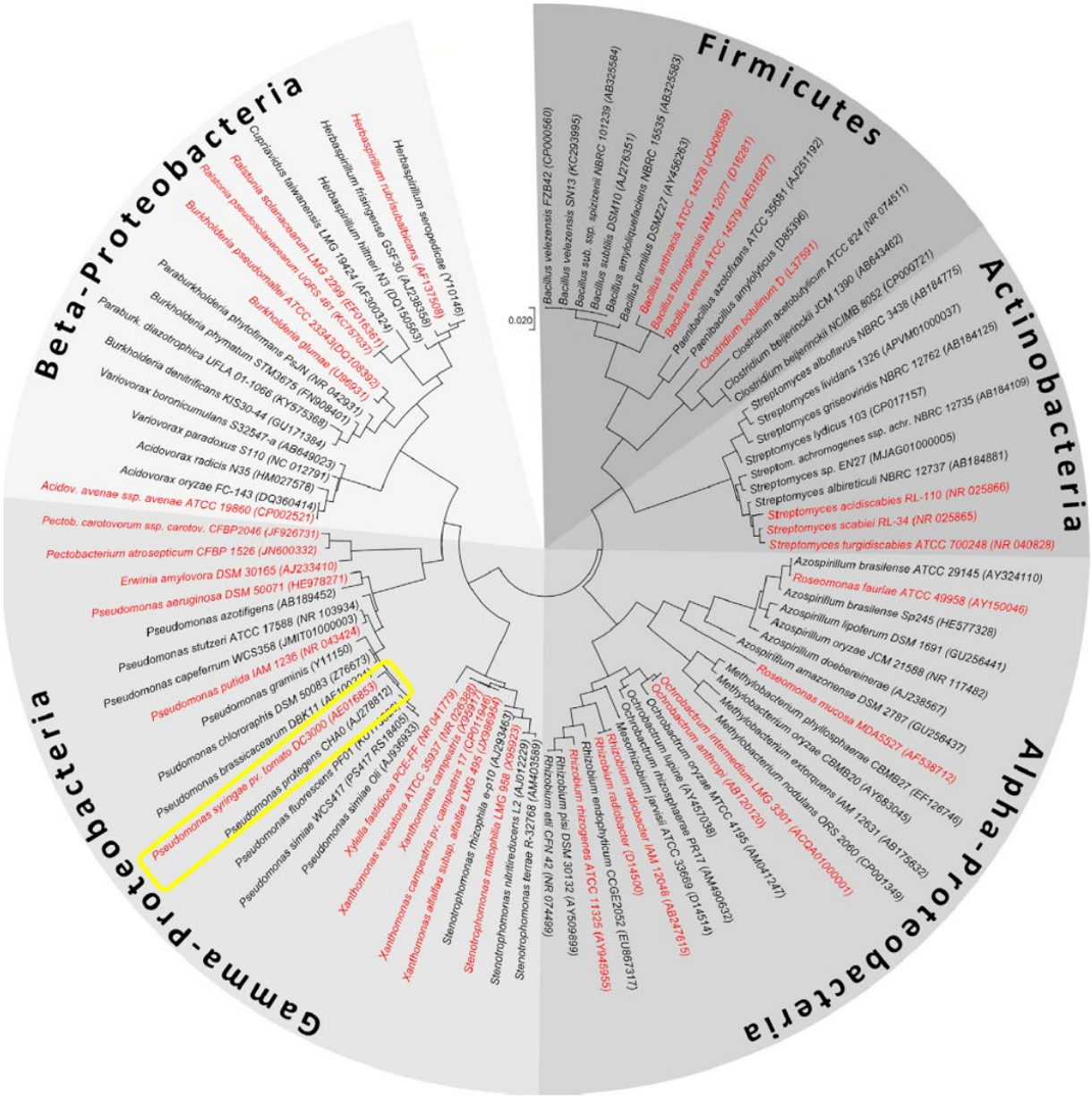

Figure 6.1: Phylogenetic dendrogramm to compare mutualistic and opportunistic bacterial species. The degrees of evolutionary relationship based on genomic differences are presented for different bacterial species. Taxonomic classification has been performed for the phyla Firmicutes, Actinobacteria and Proteobacteria. The Proteobacteria are further differentiated into the classes Alpha-, Beta- and Gamma-Proteobacteria. Species regarded as mutualistic are shown in black. Species regarded as opportunistic are shown in red. The yellow mark highlights the close relationship between the plant pathogen *Pseudomonas syringae* pv. tomato DC3000 and the beneficial biocontrol agent *P. protegens* CHA0 (modified; from Rodriguez *et al.*, 2019).

Rodriguez *et al.* (2019) also presented different pseudomonads including the human pathogenic *P. aeruginosa*, the phytopathogenic *P. syringae* and beneficial fluorescent pseudomonads, like the DAPG producing strain *P. protegens* CHA0 that was also investigated in this study. In the diagram it is indicated that the phytopathogenic strain *Pseudomonas syringae* pv. tomato DC3000 in red (Xin and He, 2013) is closely related to the beneficial strain *P. protegens* CHA0 in black.

Within the Verticillium genus, a quite similar phenomenon is described. Verticillia can be regarded as a rather heterogeneous genus including species that are plant pathogens like *V. longisporum* or *V. dahliae* as well as species that are virulent against insects, fungi or nematodes (Fahleson *et al.*, 2004). Verticillia that infect nematode cysts are grouped to Pochonia (Sung *et al.*, 2001). The mutualistic nematophage *Pochonia chlamydosporia* (formerly named *Verticillium chlamydosporia*) is closely related to the opportunistic *V. longisporum* or *V. dahliae* and has been widely characterized as a nematode antagonist utilized as a biocontrol agent in agriculture (Lin *et al.*, 2018; Uddin *et al.*, 2019). Particularly interesting in this regard is the described biocontrol effect even within the Verticillium genus. The endophytic biocontrol agent Verticillium Vt305 has been identified as *V. isaacii* (Franca *et al.*, 2013) and protects cauliflower against Verticillium wilt (Tyvaert *et al.*, 2014).

Not only within the Verticillium genus we find closely related species with rather opposite characteristics, but even different lineages within the *V. longisporum* species. In this study, the experiments have been performed with the isolate Vl43 from oilseed rape, which is a plant pathogenic lineage in Brassicaceae (Timpner *et al.*, 2013). The closely related strain Vl32 has been isolated from the same host in the same region, but it does not show any virulence in *B. napus* (Tran *et al.*, 2013).

These examples underline the statement that antagonistic properties of microbes are used to strengthen their own position compared to the competitors. Their defense and pathogenic mechanisms can be very similar or even identical used by sometimes closely related species. Whether this antagonism is judged as positive or negative is in close proximity to each other and goes back to the anthropomorphic behalf.

Main findings of Verticillium´s interaction to cope with the impact of Pseudomonas

The general investigations of this study are summarized in the model of Figure 6.2.

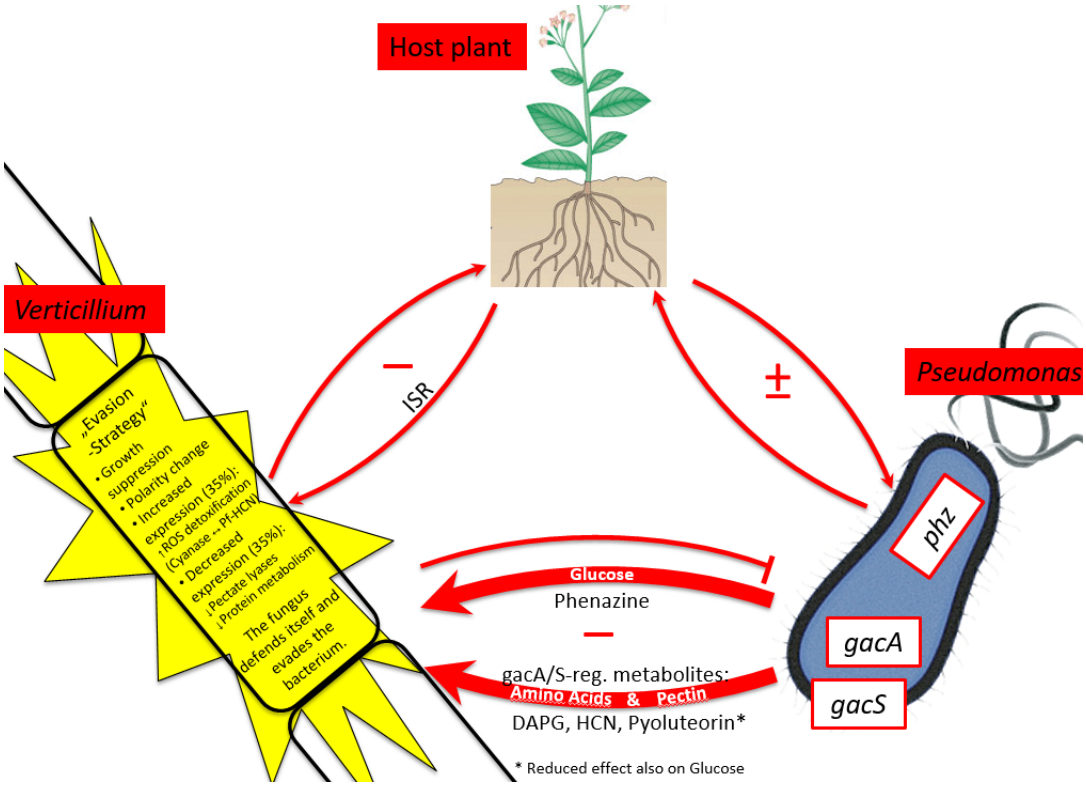

Figure 6.2: Model simplifying the three-dimensional interaction of a host plant, an antagonistic rhizobacterium (Pseudomonas) and a plant pathogen (Verticillium). Different fluorescent pseudomonads like *P. fluorescens* DSM8569 (P_rhizo) have been isolated out of the rhizosphere of Brassicaceae. In literature, a direct plant growth promoting effect due to root colonization by Pseudomonas has been described. Soil borne plant pathogens also interact directly with its host plant infecting the roots and colonizing the whole plant. As response, the plant can activate an inducible systemic resistance (ISR) to cope with fungal pathogenicity. The bacterial-fungal interaction is rather antagonistic. Depending on the nutritional environment, different suppressive bioactive compounds are relevant. In high glucose conditions, phenazines play a crucial role for *P. synxantha* 2-79 (P_phen) to dominate fungal growth parameters. Under plant mimicking circumstances with high content of amino acids and pectin, *P. protegens* CHA0 (P_DAPG) secrets antifungal metabolites like DAPG, HCN and pyoluteorin regulated by the two-component system GacA/GacS. Verticillium is highly suppressed in growth as well as it is interfered in its cellular polarity. Detoxification related genes like putative cyanide hydratase are up-regulated to possibly detoxify HCN secreted by Pseudomonas. Processes for further plant infection and fungal nutrition down-regulated explained by the decreased expression of pectate lyases coding genes. The observed fungal reactions can rather be interpreted as a detoxification and evasion strategy to escape from the bacterial antagonism. At the end, multiple suppressive effects on Verticillium by the presence of Pseudomonas indirectly lead to plant protection and constitute the biocontrol potential of the soil.

By stockpiling melanin, Verticillium reaches distinct robustness in a dormant stage, so-called microsclerotia, to survive up to 15 years in the soil during harsh temperature conditions without infecting a host plant in between (Pegg, 1989; Pegg and Brady 2002; Tran *et al.*, 2014). Specific plant molecules secreted by the roots of a host plant awake the fungal resting structure and start the Verticillium life cycle (Zhou *et al.,* 2006; Eynck *et al.*, 2007). Verticillium hyphae grow towards the host root passing the rhizosphere, which is a multifactorial conglomerate consisting of a diverse microbiome as well as varying abiotic factors (Mohanram and Kumar, 2019). Fluorescent pseudomonads are typically part of the rhizosphere biocoenosis of *B. napus*, one host plant of *V. longisporum* (Berg and Ballin, 1994). They possess different antagonistic strategies to suppress Verticillium growth on its way to their host root. Curled hyphal tip extension might reflect an appropriate fungal strategy under the physiological conditions of the rhizosphere to avoid antagonistic bacterial crowds and to reach less competitive environments targeting another root that might be more appropriate to be infected. This observation might be interpreted as an evading strategy by the fungus. Co-cultivation of the fungus with the bacterium results in a down-regulation of genes for plant cell wall degrading enzymes such as pectin lyase. This could be a specific reaction of the fungus to change its strategy from nutrition in conditions without bacterial stress in a plant simulating environment, to a withdrawal strategy to reach less suppressive conditions.

The transcriptional response of Verticillium in the presence of the bacterium indicates that the fungus also prepares itself for detoxification against Pseudomonas' mycotoxins. GacA/GacS-controlled bacterial hydrogen cyanide can occupy the oxygen binding-site of the respiratory chain in mitochondria and inactivates cytochromes, resulting in impaired respiration (Cooper and Brown, 2008). The fungus increases the transcription of the putative fungal cyanate lyase transcripts in the presence of the bacteria, presumably as a response that leads to the detoxification of the bacterial metabolite HCN. The induction of Verticillium transcripts for predicted thioredoxin can also be interpreted as a protective approach, because the protein is capable to detoxify reactive oxygen species.

During this study, neither morphologically nor genetically strong indications were observed that would support the theory of an active fungal counterstrike to suppress the vitality of the bacterium. All findings rather draw a picture of an avoiding fungus that tries to defend itself and evades the bacterium. Cellular pathways that are crucial for detoxification and protection are elevated whereas hyphal growth as well as corresponding processes related to further nutrient uptake or general protein biosynthesis are driven back. In a potential biocontrol setting, the fungal growth suppression due to the presence of the bacterium could result in a biocontrol effect indirectly protecting the crop plant against fungal pathogenicity.

It should be noted that the view on the described bacterial-fungal interaction in this study has a highly artificial and abstract angle. It has to be considered that the interaction investigated separately in this study naturally takes place in the plant rhizosphere, a highly dynamic and multifactorial location, where countless abiotic and biotic factors install an individual environment for all organisms to interact with each other (Dash *et al.*, 2019; Mohanram and Kumar, 2019; Rodriguez *et al.*, 2019; Pathan *et al.*, 2020).

For the investigation of single influencing factors, it was necessary in this study to reduce the complexity as much as possible. This goes along with a reduction of the experimental set up to only two players, one fungus and one bacterium, as well as controlling the nutritional environment in specific growth media. The setting of the interaction was predefined and simplified compared to natural conditions as well, either in surface co-cultivation experiments on agar surfaces or in liquid medium with and without physical restriction. Especially the interaction studies in the microfluidic devices were necessary to investigate fungal morphological behavior under Pseudomonas co-cultivation in detail. However, at the same time this set-up dramatically changes the natural situation in the rhizosphere, where normally less physical growth limitation occurs.

It also has to be considered that the simplification process that is necessary for scientific purposes can also be accompanied by mistakes. In this Verticillium/Pseudomonas co-cultivation study, the fungus was inoculated by spores and the interaction predominantly took place in the developmental stages

of spores and hyphae but only less microsclerotia. Contrary, in the soil, where the interaction with Pseudomonas naturally takes place, Verticillium mostly starts germinating out of the stage of microsclerotia before it develops hyphae to approach the roots, which was not addressed during this experimental setup.
Due to high experimental costs or laborious individual work, the number of biological replicates for the transcriptomic approach as well as for the microfluidic interaction studies was rather limited. Consequentely, the data interpretation has to be made carefully.
In this regard, all findings of this study have to be interpreted tentatively with respect to the fact that the highly complex and multifactorial natural network in the soil has been simplified dramatically. Therefore, the results have to be embedded and transferred to a broader ecological scope.

Outlook

In the present work, the potential of fluorescent pseudomonads isolated from the rhizosphere has been examined to suppress the growth of soil borne phytopathogenic Verticillia *in situ*. In a next step, it would be interesting to know if these findings can be transferred to an *in planta* set up as a biocontrol agent. A big selection of putatively active biocontrol agents with promising inhibition potential against Verticillium *in vitro* has been collected in literature already. However, many of these candidates lack the evidence for their antagonism *in planta* to increase the vitality of infected plants or avoid plant infection (Deketelaere *et al.*, 2017). Further research is needed to evaluate the biocontrol potential of the three Pseudomonas isolates selected for this study towards Verticillium *in planta*. Initial approaches *in planta* to model the interaction of all three players – plant, bacterium and fungus – have been performed already but results are not shown due to a lack of consistency. Biocontrol experiments have been done in a greenhouse with little possibilities to adjust abiotic factors like light, temperature and humidity, but even biotic factors like vine louse infestation. These results could not be confirmed in growth chambers under more controlled circumstances. To create solid data, a robust experimental design has to be composed. *In planta* knowledge would

narrow down the gap transferring the described findings of this study into practical usage in agriculture.

In further plant experiments, a preinoculation realized as a coating seeds of oilseed rape with lyophilized antagonistic bacteria adhering to the seed surface should also be investigated. This way, a suppressive potential of the rhizosphere, as described by Sikora *et al.* (1992) and Steinberg *et al.* (2019) can initially be installed limiting the pathogenic intensity of virulent fungi already at the beginning of a cultivation period. Particularly, different biocontrol agents could be preinoculated at the same time covering a broader spectrum of relevant growth conditions. By combining *P. fluorescens* DSM8569 (P_rhizo), expressing still unknown antifungal metabolites, *P. synxantha* 2-79 (P_phen), producing phenazines and P. *protegens* (CHA0), secreting DAPG, pyoluteorin and HCN, the chances of biocontrol success would be increased.

Another topic that remains unaddressed in the Verticillium-Pseudomonas interaction so far, are the trigger factors to activate the Pseudomonas sensor kinase GacS that is integrated in the cell membrane and responsible to detect specific external activation signals to start the signal transduction in the two-component system. It is still unclear whether the activation of GacS goes back to a general induction based on an unspecific reaction like reduced nutrition or due to rather specific recognition motifs of Verticillium structures, enzymes or metabolites. A metabolomics analysis of the Verticillium-Pseudomonas co-cultivation could be a valuable addition to gain further insights to relevant trigger signals of GacS.

Closing remark

This study shows that fluorescent pseudomonads possess many different strategies that are effective to oppose against phytopathogenic antagonists under various interaction conditions. This antagonistic potential should be used more regularly in agriculture with respect to ecologically responsible and sustainable management particularly of the soil ecosystems but also of contiguous aquatic ecosystems and grasslands. The current industrialized agriculture, that is highly price-driven by the consuming market, is considered to be one of the most crucial

factors for ecological depreciation and species extinction on a global scale (Golson *et al.*, 2015; Sanchez-Bayou and Wyckhuys, 2019). This includes homogenized field structures of huge size lacking substructures like hedges, woodland and areas of dense undergrowth, as well as intensified application of pesticides. Further evaluation of the ecological potential using antagonistic rhizobacteria for effective biocontrol of phytopathogens should be realized. This might contribute to a reduced usage of pesticides. The practical usage of applying bacteria to the ecosystem especially the final concentration of the biocontrol agents in the rhizosphere still has to be carefully balanced to avoid unintentional negative side effects due to the artificial influence.

References

Abuamsha R, Salman M, Ehlers RU. 2010. Differential resistance of oilseed rape cultivars (*Brassica napus ssp. oleifera*) to *Verticillium longisporum* infection is affected by rhizosphere colonisation with antagonistic bacteria, *Serratia plymuthica* and *Pseudomonas chlororaphis*. *Biocontrol* **56**: 201-112.

Albayrak ÇB. 2019. Bacillus Species as Biocontrol Agents for Fungal Plant Pathogens. In: Islam M, Rahman M, Pandey P, Boehme M, Haesaert G, eds. *Bacilli and Agrobiotechnology: Phytostimulation and Biocontrol.* Cham, CH: Springer, 239-265.

Ashburner M, Ball CA, Blake JA, Botstein D, Butler H, Cherry JM, Harris MA. 2000. Gene ontology: tool for the unification of biology. *Nature Genetics* **25**: 25-29.

Atallah ZK, Maruthachalam K, Toit DL, Koike ST, Davis RM, Klosterman SJ, Hayes RJ, Subbarao KV. 2010. Population analyses of the vascular plant pathogen *Verticillium dahliae* detect recombination and transcontinental gene flow. *Fungal Genetics and Biology* **47**: 416-422.

Barclay M, Day JC, Thompson IP, Knowles CJ, Bailey MJ. 2002. Substrate-regulated cyanide hydratase (chy) gene expression in *Fusarium solani*: the potential of a transcription-based assay for monitoring the biotransformation of cyanide complexes. *Environmental Microbiology* **4**: 183-189.

Baron NC, Rigobelo EC, Zied DC. 2019. Filamentous fungi in biological control: current status and future perspectives. *Chilean Journal of Agricultural Research* **79**: 307-315.

Bayram Ö, Krappmann S, Ni M, Woo Bok J, Helmstaedt K, Valerius O, Braus-Stromeyer S, Kwon NJ, Keller NP, Yu JH, Braus GH. 2008. VelB/VeA/LaeA

Complex Coordinates Light Signal with Fungal Development and Secondary Metabolism. *Science* **320***:* 1504-1506.

Bayram Ö, Braus GH. 2012. Coordination of secondarymetabolism and development in fungi: the velvet family of regulatory proteins. *FEMS Microbiology Reviews* **36**: 1-24.

Beckman CH. 1987. *The nature of wilt diseases of plants.* St. Paul, USA: APS Press.

Benedik MJ, Sewell BT. 2017. Cyanide-degrading nitrilases in nature. *The Journal of General and Applied Microbiology* **64**: 90-93.

Berendsen RL, Pieterse CMJ, Bakker PAHM. 2012. The rhizosphere microbiome and plant health. *Trends in Plant Science* **17**: 478-86.

Berg G, Ballin G. 1994. Bacterial antagonists to *Verticillium dahliae* Kleb.. *Journal of Phytopathology* **141**: 99-110.

Berlanger I, Powelson ML. 2000. *Verticillium wilt.* The Plant Health Instructor.

Bertani G. 1951. Studies on lysogenesis. I. The mode of phage liberation by lysogenic *Escherichia coli. Journal of Bacteriology* **62**: 293-300.

Biessy A, Filion M. 2018. Phenazines in plant-beneficial *Pseudomonas* spp.: biosynthesis, regulation, function and genomics. *Environmental Microbiology* **20**: 3905-3917.

Birren B, Fink G, Lander E. 2002. *Fungal genome initiative: white paper developed by the fungal research community.* Cambridge, MA: Whitehead Institute Center for Genome Research.

Bok JW, Keller NP. 2004. LaeA, a regulator of secondary metabolism in *Aspergillus* spp. *Eukaryotic Cell* **3**: 527-535.

Bönnighausen J, Schauer N, Schäfer W, Bormann J. 2019. Metabolic profiling of wheat rachis node infection by *Fusarium graminearum* - decoding deoxynivalenol-dependent susceptibility. *New Phytologist* **221**: 459-469.

Braus GH, Irniger S, Bayram Ö 2010. Fungal development and the COP9 signalosome. *Current Opinion in Microbiology* **13:** 1-5.

Brencic A, McFarland KA, McManus HR, Castang S, Mogno I, Dove S, Lory S. 2009. The GacS/GacA signal transduction system of *Pseudomonas aeruginosa* acts exclusively through its control over the transcription of the RsmY and RsmZ regulatory small RNAs. *Molecular Microbiology* **73**: 434-445.

Brodhun F, Cristobal-Sarramian A, Zabel S, Newie J, Hamberg M, Feussner I. 2013. An Iron 13*S*-Lipoxygenase with an α-Linolenic Acid Specific Hydroperoxidase Activity from *Fusarium oxysporum*. *Plos One* **8**: e64919.

Bui TT, Harting R, Braus-Stromeyer SA, Tran VT, Leonard M, Höfer A, Abelmann A, Bakti F, Valerius O, Schlüter R, Stanley CE, Ambrósio A, Braus GH. 2019. *Verticillium dahliae* transcription factors Som1 and Vta3 control microsclerotia formation and sequential steps of plant root penetration and colonisation to induce disease. *New Phytologist* **221**: 2138-2159.

Carmona-Hernandez S, Reyes-Perez JJ, Chiquito-Contreras RG, Rincon-Enriquez G, Cerdan-Cabrera, Hernandez-Montiel LG. 2019. Biocontrol of Postharvest Fruit Fungal Diseases by Bacterial Antagonists: A Review. *Agronomy* **9**: 121.

Carroll CL, Carter CA, Goodhue RE, Lin Lawell CC, Subbarao KV. 2018. A Review of Control Options and Externalities for Verticillium Wilts. *Phytopathology* **108:** 160-171.

Chen Y, Yan F, Chai Y, Liu H, Kolter R, Losick R, Guo JH. 2013. Biocontrol of tomato wilt disease by *Bacillus subtilis* isolates from natural environments depends on conserved genes mediating biofilm formation. *Environmental microbiology* **15**: 848-864.

Chen NH, Djoko KY, Veyrier FJ, McEwan AG. 2016. Formaldehyde Stress Responses in Bacterial Pathogens. *Frontiers in Microbiology* **7**: 257.

Compant S, Samad A, Faist H, Sessitsch A. 2019. A review on the plant microbiome: Ecology, functions, and emerging trends in microbial application. *Journal of Advanced Research* **19**: 29-37.

Conrath U, Pieterse CMJ, Mauch-Mani B. 2002. Priming in plant-pathogen interactions. *Trends in Plant Science* **7**: 210-216.

Cooper CE, Brown GC. 2008. The inhibition of mitochondrial cytochrome oxidase by the gases carbon monoxide, nitric oxide, hydrogen cyanide and hydrogen sulfide: chemical mechanism and physiological significance. *Journal of Bioenergetics and Biomembranes* **40**: 533-539.

Crabtree JN, Okagaki LH, Wiesner DL, Strain AK, Nielsen JN, Nielsen K. 2012. Titan cell production enhances the virulence of *Cryptococcus neoformans*. Infection and Immunity **80**: 3776-3785.

Cui J, Bahrami AK, Pringle EG, Hernandez-Guzman G, Bender CL, Naomi EP, Ausubel FM. 2005. *Pseudomonas syringae* manipulates systemic plant defenses against pathogens and herbivores. *Proceedings of the National Academy of Sciences of the United States of America* **102**: 1791-1796.

Daniel Da Rosa W, Gezuele E, Calegari L, Goni F. 2008. Asteroid body in sporotrichosis. Yeast viability and biological significance within the host immune response. Medical Mycology **46**: 443-448.

Dash B, Soni R, Kumar V, Suyal DC, Dash D, Goel R. 2019. Mycorrhizosphere: Microbial Interactions for Sustainable Agricultural Production. In: Varma A, Choudhary D, eds. *Mycorrhizosphere and Pedogenesis.* Singapore: Springer, 321-338.

Deketelaere S, Tyvaert L, França SC, Höfte M. 2017. Desirable traits of a good biocontrol agent against Verticillium wilt. *Frontiers in Microbiology* **8**: 1186.

Depotter JRL, Deketelaere S, Inderbitzin P, Tiedemann A Von, Hoefte M, Subbarao KV, Wood TA, Thomma BPHJ. 2016. *Verticillium longisporum*, the invisible threat to oilseed rape and other brassicaceous plant hosts. *Molecular Plant Pathology* **17**: 1004-1016.

Depotter JR, Seidl MF, van den Berg, GC, Thomma BP, Wood TA. 2017. A distinct and genetically diverse lineage of the hybrid fungal pathogen *Verticillium longisporum* population causes stem striping in British oilseed rape. *Environmental Microbiology* **19:** 3997-4009.

Depotter JR, Thomma BP, Wood TA. 2019b. Measuring the impact of *Verticillium longisporum* on oilseed rape (*Brassica napus*) yield in field trials in the United Kingdom. *European Journal of Plant Pathology* **153**: 321-326.

Depotter JRL, Shi-Kunne X, Missonnier H, Liu T, Fain L, van den Berg GCM, Wood TA, Zhang B, Jacques A, Seidl MF, Thomma BPHJ. 2019a. Dynamic virulence-related regions of the plant pathogenic fungus *Verticillium dahliae* display enhanced sequence conservation. *Molecular Ecology* **28**: 3482-3495.

Doering TL. 2009. How sweet it is! Cell wall biogenesis and polysaccharide capsule formation in *Cryptococcus neoformans*. Annual Reiew of Microbiology **63**: 223-247.

Eynck C, Koopmann B, Grunewaldt-Stoecker G, Karlowsky P, von Tiedemann A. 2007. Differential interaction of *Verticillium longisporum* and *Verticillium dahliae* with *Brassica napus* detected with molecular and histological techniques. *European Journal of Plant Pathology* **118**: 259-274.

Fahleson J, Hu Q, Dixelius C. 2004. Phylogenetic analysis of Verticillium species based on nuclear and mitochondrial sequences. *Archives of Microbiology* **181**: 435-442.

Fernandez J, Wilson RA. 2014. Characterizing Roles for the Glutathione Reductase, Thioredoxin Reductase and Thioredoxin Peroxidase-Encoding Genes of *Magnaporthe oryzae* during Rice Blast Disease. *Plos One* **9**: e87300.

Figueroa M, Hammond-Kosack K, Solomon PS. 2018. A review of wheat diseases - a filed perspective. *Molecular Plant Pathology* **19**: 1523-1536.

Flury P, Vesga P, Dominguez-Ferreras A, Tinguely C, Ullrich CI, Kleespies RG, Keel C, Maurhofer M. 2019. Persistence of root-colonizing *Pseudomonas protegens* in herbivorous insects throughout different developmental stages and dispersal to new host plants. *ISME Journal - Multidisciplinary Journal of Microbial Ecology* **13**: 860-872.

Fogelqvist J, Tzelepis G, Bejai S, Ilbäck J, Schwelm A, Dixelius C. 2018. Analysis of the hybrid genomes of two field isolates of the soil-borne fungal species *Verticillium longisporum*. *BMC Genomics* **191**:14.

Fradin EF, Thomma BPHJ. 2006. Physiology and molecular aspects of Verticillium wilt diseases caused by *V. dahliae* and *V. albo-atrum*. *Molecular Plant Pathology* **7**: 71-86.

Fradin EF, Zhang Z, Juarez Ayala JC, Castroverde CD, Nazar RN, Robb J, Liu CM, Thomma BP. 2009. Genetic dissection of Verticillium wilt resistance mediated by tomato Ve1. *Plant Physiology* **150**: 320-332.

França SC, Spiessens K, Pollet S, Debode J, De Rooster L, Callens D, Höfte M. 2013. Population dynamics of Verticillium species in cauliflower fields: influence of crop rotation, debris removal and ryegrass incorporation. *Crop protection* **54**: 134-141.

Francis VI, Waters EM, Finton-James SE, Gor A, Kadioglu A, Brown AR, Porter SL. 2018. Multiple communication mechanisms between sensor kinases are crucial for virulence in *Pseudomonas aeruginosa*. *Nature Communications* **9**: 1-11.

Francis VI, Porter SL. 2019. Multikinase networks: two-component signaling networks integrating multiple stimuli. *Annual Review of Microbiology* **73**. 199-223.

Frisvad JC, Hubka V, Ezekiel CN, Hong SB, Novakova A, Chen J, Arzanlou M, Larsen TO, Sklenar F, Mahakarnchanaku W, Samson RA, Houbraken J. 2019. Taxonomy of Aspergillus section Flavi and their production of aflatoxins, ochratoxins and other mycotoxins. *Studies in Mycology* **93**: 1-63.

García-Gutiérrez L, Zeriouh H, Romero D, Cubero J, Vicente A, Pérez-García A. 2013. The antagonistic strain *Bacillus subtilis* UMAF6639 also confers protection to melon plants against cucurbit powdery mildew by activation of jasmonate-and salicylic acid-dependent defense responses. *Microbial Biotechnology* **6**: 264-274.

Gene Ontology Consortium. 2019. The gene ontology resource: 20 years and still GOing strong. *Nucleic Acids Research* **47**: D330-D338.

Gerke J, Braus GH. 2014. Manipulation of fungal development as source of novel secondary metabolites for biotechnology. *Applied Microbiology and Biotechnology* **98**: 8443-8455.

Gkarmiri K, Finlay RD, Alström S, Thomas E, Cubeta MA, Högberg N. 2015. Transcriptomic changes in the plant pathogenic fungus *Rhizoctonia solani* AG-3 in

response to the antagonistic bacteria *Serratia proteamaculans* and *Serratia plymuthica*. *BMC Genomics* **16**: 630.

Gordon TR, Kirkpatrick SC, Hansen J, Shaw D. 2006. Response of strawberry genotypes to inoculation with isolates of *Verticillium dahliae* differing in host origin. *Plant Pathology* **55**: 766-769.

Goh C-H, Veliz Vallejos DF, Nicotra AB, Mathesius U. 2013. The Impact of Beneficial Plant-Associated Microbes on Plant Phenotypic Plasticity. *Journal of Chemical Ecology* **39**: 826-839.

Gomaa EZ. 2012. Chitinase production by *Bacillus thuringiensis* and *Bacillus licheniformis*: Their potential in antifungal biocontrol. *The Journal of Microbiology* **50**: 103-111.

González N, Heeb S, Valverde C, Kay E, Reimmann C, Junier T, Haas D. 2008. Genome-wide search reveals a novel GacA-regulated small RNA in *Pseudomonas* species. *BMC Genomics* **9**: 167.

Gouda S, Kerry RG, Das G, Paramithiotis S, Shin HS, Patra JK. 2018. Revitalization of plant growth promoting rhizobacteria for sustainable development in agriculture. *Microbiological Research* **206**: 131-140.

Goulson D, Nicholls E, Botías C, Rotheray EL. 2015. Bee declines driven by combined stress from parasites, pesticides, and lack of flowers. *Science* **347**: 1255957.

Haas D, Défago G. 2005. Biological control of soil-borne pathogens by fluorescent pseudomonads. *Nature Reviews Microbiology* **3**: 307-319.

Harting R, Höfer A, Tran VT, Weinhold LM, Barghahn S, Schlüter R, Braus GH. 2020. The Vta1 transcriptional regulator is required for microsclerotia melanization in *Verticillium dahliae*. *Fungal Biology* **124**: 490-500.

Heale JB, Karapapa K. 1999. The Verticillium threat to Canada's major oilseed crop: canola. *Canadian Journal of Plant Pathology* **21**: 1-7.

Heeb S, Valverde C, Gigot-Bonnefoy C, Haas D. 2005. Role of the stress sigma factor RpoS in GacA/RsmA-controlled secondary metabolism and resistance to oxidative stress in *Pseudomonas fluorescens* CHA0. *FEMS Microbiology Letters* **243**: 251-8.

Hernández-Chávez MJ, Pérez-García LA, Niño-Vega GA, Mora-Montes HM. 2017. Fungal strategies to evade the host immune recognition. *Journal of Fungi* **3**: 51.

Hollensteiner J, Wemheuer F, Harting R, Kolarzyk AM, Valerio SMD, Poehlein A, Brzuszkiewicz EB, Nesemann K, Braus-Stromeyer SA, Braus GH, Daniel R, Liesegang H. 2017. *Bacillus thuringiensis* and *Bacillus weihenstephanensis* inhibit the growth of phytopathogenic Verticillium species. *Frontiers in Microbiology* **7**: 2171.

Hoppenau CE, Tuan VT, Kusch H, Aßhauer KP, Landesfeind M, Meinicke P, Popova B, Braus-Stromeyer SA, Braus GH. 2014. *Verticillium dahliae VdTHI4* involved in thiazole biosynthesis, stress response and DNA repair functions, is required for vascular disease induction in tomato. *Environmental and Experimental Botany* **108**: 14-22.

Horbach R, Navarro-QuesadacAR, Knoggec W, Deisinga HB. 2011. When and how to kill a plant cell: Infection strategies of plant pathogenic fungi. *Journal of Plant Physiology* **168**: 51-62.

Howe KL, Contreras-Moreira B, De Silva N, Maslen G, Akanni W, Allen J, Alvarez-Jarreta J, Barba M, Bolser DM, Cambell L, Carbajo M, Chakiachvili M, Christensen M, Cummins C, Cuzick A, Davis P, Fexova S, Gall A, George N, Gil L, Gupta P, Hammond-Kosack KE, Haskell E, Hunt SE, Jaiswal P, Janacek

SH, Kersey PJ, Langridge N, Maheswari U, Maurel T, McDowall MD, Moore B, Muffato M, Naamati G, Naithani S, Olson A, Papatheodorou I, Patricio M, Paulini M, Pedro H, Perry E, Preece J, Rosello M, Russell M, Sitnik V, Staines DM, Stein J, Tello-Ruiz MK, Trevanion SJ, Urban M, Wei S, Ware D, Williams G, Yates AD, Flicek P. 2019. Ensembl Genomes 2020 - enabling non-vertebrate genomic research. *Nucleic Acids Research* **48**: 689-695.

Inderbitzin P, Davis RM, Bostock RM, Subbarao KV. 2011. The Ascomycete *Verticillium longisporum* is a Hybrid and a Plant Pathogen with an Expanded Host Range. *Plos One* **6**: e18260.

Irmer H, Tarazona S, Sasse C, Olbermann P, Loeffler J, Krappmann S, Conesa A, Braus GH. 2015. RNAseq analysis of *Aspergillus fumigatus* in blood reveals a *just wait and see* resting stage behavior *BMC Genomics* **16:** 604.

Islam MT, Fukushi Y. 2003. Growth inhibition and excessive branching in *Aphanomyces cochlioides* induced by 2,4-diacetylphloroglucinol is linked to disruption of filamentous actin cytoskeleton in the hyphae. *World Journal of Microbiology and Biotechnology* **26**: 1163-70.

Islam S. 2018. Microorganisms in the Rhizosphere and their Utilization in Agriculture: A Mini Review. *PSM Microbiology* **3**: 105-110.

Jain A, Sarsaiya S, Wu Q, Lu Y, Shi J. 2019. A review of plant leaf fungal diseases and its environment speciation. *Bioengineered* **10**: 409-424.

Jayamohan NS, Patil SV, Kumudini BS. 2018. Reactive oxygen species (ROS) and antioxidative enzyme status in *Solanum lycopersicum* on priming with fluorescent *Pseudomonas* spp. against *Fusarium oxysporum*. *Biologia* **73**: 1073-1082.

de Jonge R, van Esse HP, Maruthachalam K, Bolton MD, Santhanam P, Saber MK, Zhang Z, Usami T, Lievens B, Subbarao KV, Thomma BPHJ. 2012.

Tomato immune receptor Ve1 recognizes effector of multiple fungal pathogens uncovered by genome and RNA sequencing. *Proceedings of the National Academy of Sciences of the United States of America* **109**: 5110-5115.

Kaever A, Lingner T, Feussner K, Göbel C, Feussner I, Meinicke P. 2009. MarVis: a tool for clustering and visualization of metabolic biomarkers. *BMC Bioinformatics* **10**: 92.

Kaever A, Landesfeind M, Feussner K, Mosblech A, Heilmann I, Morgenstern B, Feussner I, Meinicke P. 2015. MarVis-Pathway: integrative and exploratory pathway analysis of non-targeted metabolomics data. *Metabolomics* **11**: 764-777.

Kang IJ, Shim HK, Roh JH, Heu S, Shin DB. 2018. Simple Detection of Cochliobolus Fungal Pathogens in Maize. *Plant Pathology Journal* **34**: 327-334.

Kannojia P, Choudhary KK, Srivastava AK, Singh AK. 2019. PGPR Bioelicitors: Induced Systemic Restiance (ISR) and Proteomic Perspective on Biocontrol. In: Singh AK, Kumar A, Singh PK, eds. *PGPR Amelioration in Sustainable Agriculture, Food Security and Environmental Management.* Amsterdam, NL: Elsevier, 67-84.

Karplus PA, Schulz GE. 1987. Refined structure of glutathione reductase at 1.54 A resolution. *Journal of Molecular Biology* **195**: 701-29.

Keller NP. 2019. Fungal secondary metabolism: regulation, function and drug discovery. *Nature Reviews Microbiology* **17**: 167-180.

Khan A, Ishaq M, Ahmed AA, Guo X, Khan I, Khan AQ. 2019. Beneficial Plant Growth Promoting Rhizobacteria in Rhizosphere, it´s Application and Plant Growth: A Review. *Natural Products Chemistry and Research* **7**: 359.

Khaneghah AM, Martins LM, von Hertwig AM, Bertoldo R, Sant'Ana AS. 2018. Deoxynivalenol and its masked forms: Characteristics, incidence, control and fate

during wheat and wheat based products processing - A review. *Trends in Food Science and Technology* **71**: 13-24.

Klosterman SJ, Atallah ZK, Vallad GE, Subbarao KV. 2009. Diversity, pathogenicity and management of Verticillium species. *Annual Review of Phytopathology* **47**: 39-62.

Koehl J, Kolnaar R, Ravensberg WJ. 2019. Mode of Action of Microbial Biological Control Agents Against Plant Diseases: Relevance Beyond Efficacy. *Frontiers in Plant Science* **10**: 845.

Korenblum E, Aharoni A. 2019. Phytobiome metabolism: beneficial soil microbes steer crop plants' secondary metabolism. *Pest Management Science* **75**: 2378-2384.

Kosawang C, Karlsson M, Velez H, Rasmussen PH, Collinge DB, Jensen B, Jensen DJ. 2014. Zearalenone detoxification by zearalenone hydrolase is important for the antagonistic ability of *Clonostachys rosea* against mycotoxigenic *Fusarium graminearum. Fungal Biology* **118**: 364-373.

Kretschmer M, Leroch M, Mosbach A, Walker AS, Fillinger S, Mernke D, Schoonbeek HJ, Pradier JM, Leroux P, De Waard MA, Hahn M. 2009. Fungicide-driven evolution and molecular basis of multidrug resistance in field populations of the grey mould fungus *Botrytis cinerea. Plos Pathogens.* **5**: e1000696.

Kupferschmied P, Maurhofer M, Keel C. 2013. Promise for plant pest control: root-associated pseudomonads with insecticidal activities. *Frontiers in Plant Science* **4**: 287.

Kuriyan J, Krishna TS, Wong L, Guenther B, Pahler A, Williams CH, Model P. 1991. Convergent evolution of similar function in two structurally divergent enzymes. *Nature* **352**: 172-4.

Lan N, Yue Q, An Z, Bills GF. 2020. Apc. LaeA and Apc. VeA of the velvet complex govern secondary metabolism and morphological development in the echinocandin-producing fungus *Aspergillus pachycristatus*. *Journal of Industrial Microbiology & Biotechnology* **47**: 155-168.

Laville J, Voisard C, Keel C, Maurhofer M, Défago G, Haas D. 1992. Global control in *Pseudomonas fluorescens* mediating antibiotic synthesis and suppression of black root rot of tobacco. *Proceedings of the National Academy of Sciences of the United States of America* **89**: 1562-1566.

Laville J, Blumer C, von Schroetter C, Gaia V, Defago G, Keel C, Haas D. 1998. Characterization of the *hcnABC* gene cluster encoding hydrogen cyanide synthase and anaerobic regulation by *anr* in the strictly aerobic biocontrol agent *Pseudomonas fluorescens* CHA0. *Journal of Bacteriology* **180**: 3187-3196.

Leonard M, Kühn A, Harting R, Maurus I, Nagel A, Starke J, Kusch H, Valerius O, Feussner K, Feussner I, Kaever, A., Landesfeind M, Morgenstern B, Becher D, Hecker M, Braus-Stromeyer SA, Kronstad JW, Braus GH. 2020. *V. longisporum* elicits media-dependent secretome responses with a further capacity to distinguish between plant-related environments. *Frontiers in Microbiology* **11**: 1876.

Letunic I, Doerks T, Bork P. 2015. SMART: recent updates, new developments and status in 2015. *Nucleic Acids Research* **43**: D257-D260.

Letunic I, Bork P. 2018. 20 years of the SMART protein domain annotation resource. *Nucleic Acids Research* **46**: D493-D496.

Lin R, Qin F, Shen B, Shi Q, Liu C, Zhang X, Jiao Y, Lu J, Gao Y, Suarez-Fernandez M, Lopez-Moya F, Lopez-Llorca LV, Wang G, Mao Z, Ling J, Yang Y, Cheng X, Xie B. 2018. Genome and secretome analysis of *Pochonia chlamydosporia* provide new insight into egg-parasitic mechanisms. *Scientific*

Reports **8**: 1123.

Longley R, Halliwell J, Campbell J, Ingledew W. 1972. The branchpoint of pyocyanine biosynthesis. *Canadian Journal of Microbiology* **18**: 1357-1363.

Lupas AN, Zhu H, Korycinski M. 2015. The thalidomide-binding domain of cereblon defines the CULT domain family and is a new member of the beta-tent fold. *Plos Computational Biology* **11**: e1004023.

Mancl JM, Ray WK, Helm RF, Schubot FD. 2019. Helix cracking regulates the critical interaction between RetS and GacS in *Pseudomonas aeruginosa*. *Structure* **27**: 785-793.

Markakis EA, Tjamos SE, Antoniou PP, Paplomatas EJ, Tjamos EC. 2016. Biological control of Verticillium wilt of olive by *Paenibacillus alvei*, strain K165. *BioControl* **61**: 293-303.

Martínez-García PM, Ruano-Rosa D, Schilirò E, Prieto P, Ramos C, Rodríguez-Palenzuela P, Mercado-Blanco J. 2015. Complete genome sequence of *Pseudomonas fluorescens* strain PICF7, an indigenous root endophyte from olive (Olea europaea L.) and effective biocontrol agent against *Verticillium dahliae*. *Standards in Genomic Sciences* **10**: 10.

Martínková L, Veselá AB, Rinágelová A, Chmátal M. 2015. Cyanide hydratases and cyanide dihydratases: emerging tools in the biodegradation and biodetection of cyanide. *Applied Microbiology and Biotechnology* **99**: 8875-8882.

Maurhofer M, Keel C, Haas D, Defago G. 1994. Pyoluteorin production by *Pseudomonas fluorescens* strain CHA0 is involved in the suppression of *Pythium* damping-off of cress but nut of cucumber. *European Journal of Plant Pathology* **100**: 221-232.

Mavrodi DV, Ksenzenko VN, Bonsall RF, Cook JR, Boronin AM, Thomashow LS. 1998. A seven-gene locus for synthesis of phenazine-1-carboxylic acid by *Pseudomonas fluorescens* 2-79. *Journal of Bacteriology* **180**: 2541-2548.

Mavrodi DV, Blankenfeldt W, Thomashow LS. 2006. Phenazine compounds in fluorescent *Pseudomonas* spp.: biosynthesis and regulation. *Annual Review of Phytopathology* **44**: 417-445.

Mazurier S, Corberand T, Lemanceau P, Raaijmakers JM. 2009. Phenazine antibiotics produced by fluroscent pseudomonads contribute to natural soil suppressiveness to Fusarium wilt. *ISME Journal – Multidisciplinary Journal of Microbial Ecology* **3**: 977-991.

Mazzola M. 2007. Manipulation of Rhizosphere Bacterial Communities to Induce Suppressive Soils. *Journal of Nematology* **39**: 213-220.

Meister C, Thieme KG, Thieme S, Köhler AM, Schmitt K, Valerius O, Braus GH. 2019. COP9 Signalosome Interaction with UspA/Usp15 Deubiquitinase Controls VeA-Mediated Fungal Multicellular Development. *Biomolecules* **9**: 238.

deMello AJ. 2006. Control and detection of chemical reactions in microfluidic systems. *Nature* **442**: 394-402.

Meselson M, Yuan R. 1968. DNA restriction enzyme from *E. coli*. *Nature* **217**: 1110-4.

Mishra J, Arora NK. 2018. Secondary metabolites of fluorescent pseudomonads in biocontrol of phytopathogens for sustainable agriculture. *Applied Soil Ecology* **125**: 35-45.

Mohanram S, Kumar P. 2019. Rhizosphere microbiome: revisiting the synergy of plant-microbe interactions. *Annals of Microbiology* **69**: 307-320.

Nahlik K, Dumkow M, Baram Ö, Helmsteadt K, Busch S, Valerius O, Gerke J, Hoppert M, Schwier E, Opitz L, Westermann M, Grond S, Feussner K, Goebel C, Kaever A, Meinicke P, Feussner I, Braus GH. 2010. The COP9 signalosome mediates transcriptional and metabolic response to hormones, oxidative stress protection and cell wall rearrangement during fungal development. *Molecular Microbiology* **78**: 964-79.

Nandi M, Selin C, Brassinga AKC, Belmonte MF, Fernando WGD, Loewen PC, de Kievit TR. 2015. Pyrrolnitrin and Hydrogen Cyanide Production by *Pseudomonas chlororaphis* Strain PA23 Exhibits Nematicidal and Repellent Activity against *Caenorhabditis elegans*. *Plos One* **10**: e0123184

Nazir R, Warmink JA, Boersma H, van Elsas JD. 2009. Mechanisms that promote bacterial fitness in fungal-affected soil microhabitats. *FEMS Microbiology Ecology* **71**: 169-185.

Nesemann K, Braus-Stromeyer SA, Thuermer A, Daniel R, Braus GH. 2015a. Draft genome sequence of the beneficial rhizobacterium *Pseudomonas fluorescens* DSM8569. *Genome Announcements* **3**: e00137-15.

Nesemann K, Braus-Stromeyer SA, Thuermer A, Daniel R, Mavrodi DV, Thomashow LS, Weller DM, Braus GH. 2015b. Draft genome sequence of the phenazine producing *Pseudomonas fluorescens* 2-79. *Genome Announcements* **3**: e00130-15.

Nesemann K, Braus-Stromeyer SA, Harting R, Hoefer A, Kusch H, Ambrosio AB, Timpner C, Braus GH. 2018. Fluorescent pseudomonads pursue media-dependent strategies to inhibit growth of pathogenic Verticillium fungi. *Applied Microbiology and Biotechnology* **102**: 817-831.

Neumann MJ, Dobinson KF. 2003. Sequence tag analysis of gene expression during pathogenic growth and microsclerotia development in the vascular wilt pathogen *Verticillium dahliae*. *Fungal Genetics and Biology* **38**: 54-62.

Nosanchuk JD, Casadevall A. 2006. Impact of melanin on microbial virulence and clinical resistance to antimicrobial compounds. *Antimicrobial Agents and Chemotherapy* **50:** 3519-3528.

Nützmann HW, Reyes-Dominguez Y, Scherlach K, Schroeckh V, Horn F, Gacek A, Schümann J, Hertweck C, Strauss J, Brakhage AA. 2011. Bacteria-induced natural product formation in the fungus *Aspergillus nidulans* requires Saga/Ada-mediatied histone acetylation. *Proceedings of the National Academy of Sciences of the United States of America* **108**: 14282-14287.

Okagaki LH, Strain AK, Nielsen JN, Charlier C, Baltes NJ, Chretien F, Heitman J, Dromer F, Nielsen K. 2010. Cryptococcal cell morphology affects host cell interactions and pathogenicity. *Plos Pathogens* **6**: e1000953.

Okagaki LH, Nielsen K. 2012. Titan cells confer protection from phagocytosis in *Cryptococcus neoformans* infections. *Eukaryotic Cell* **11**: 820-826.

Orozco-Mosqueda MC, Rocha-Granados MC, Glick BR, Santoyo G. 2018. Microbiome engineering to improve biocontrol and plant growth-promoting mechanisms. *Microbiological Research* **208**: 25-31.

Park SY, Choi J, Lim SE, Lee GW, Park J, Kim Y, Kong S, Se Ryun K, Rho HS, Jeon J, Chi MH, Kim S, Khang CH, Kang S, Lee YH. 2013. Global Expression Profiling of Transcription Factor Genes Provides New Insights into Pathogenicity and Stress Responses in the Rice Blast Fungus. *Plos Pathogens* **9**: e1003350.

Pathan SI, Ceccherini MT, Sunseri F, Lupini A. 2020. Rhizosphere as Hotspot for Plant-Soil-Microbe Interaction. In: Datta R, Meena R, Pathan S, Ceccherini M, eds. *Carbon and Nitrogen Cycling in Soil.* Singapore: Springer, 17-43.

Pegg GF. 1989. Pathogenesis in vascular diseases of plants. In: Tjamos EC, Beckmann CH, eds. *Vascular Wilt Diseases of Plants.* Berlin, Heidelberg, Germany: Springer, NATO ASI Series (Series H: Cell Biology) 28.

Pegg GF, Brady BL. 2002. *Verticillium Wilts.* Wallingford, UK: CABI Publishing.

Petrasch S, Knapp SJ, van Kan JAL, Blanco-Ulat B. 2019. Grey mould of strawberry, a devastating disease caused by the ubiquitous necrotrophic fungal pathogen *Botrytis cinerea*. *Molecular Plant Pathology* **20**: 877-892.

Rich PR. 2017. Mitochondrial cytochrome c oxidase: catalysis, coupling and controversies. *Biochemical Society Transactions* **45**: 813-829.

Rochat L, Péchy-Tarr M, Baehler E, Maurhofer M, Keel C. 2010. Combination of fluorescent reporters for simultaneous monitoring of root colonization and antifungal gene expression by a biocontrol pseudomonad on cereals with flow cytometry. *Molecular Plant Microbe Interactions* **23**: 949-961.

Rodenburg SYA, Seidl MF, de Ridder D, Govers F. 2018. Genome-wide characterization of *Phytophthora infestans* metabolism: a systems biology approach. *Molecular Plant Pathology* **19**: 1403-1413.

Rodriguez PA, Rothballer M, Chowdhury SP, Nussbaumer T, Gutjahr C, Falter-Braun P. 2019. Systems Biology of Plant-Microbiome Interactions. *Molecular Plant* **12**: 804-821.

Rodriguez-Moreno L, Ebert MK, Bolton MD, Thomma BPHJ. 2018. Tools of the crook-infection strategies of fungal plant pathogens. *The Plant Journal* **93**: 664-674.

Sahu B, Singh J, Shankar G, Pradhan A. 2018. *Pseudomonas fluorescens* PGPR bacteria as well as biocontrol agent: A review. *International Journal of Chemical Studies* **6**: 01-07.

Sanchez-Bayo F, Wyckhuys KAG. 2019. Worldwide decline of the entomofauna: A review of its drivers. *Biological Conservation* **232**: 8-27.

Sarikaya-Bayram SÖ, Bayram Ö, Valerius O, Park HS, Irninger S, Gerke J, Ni M, Han KH, Yu JH, Braus GH. 2010. LaeA control of velvet family regulatory proteins for light-dependent development and fungal cell-type specificity. *Plos Genetics* **6**: e1001226.

Sarikaya-Bayram SÖ, Palmer JM, Keller N, Braus GH, Bayram Ö. 2015. One Juliet and four Romeos: VeA and its methyltransferases. *Frontiers in Microbiology* **6:** 1-7.

Schiering N, Kabsch W, Moore MJ, Distefano MD, Walsh CT, Pai EF. 1991. Structure of the detoxification catalyst mercuric ion reductase from *Bacillus* spp. strain RC607. *Nature* **352**: 168-72.

Schnathorst WC. 1981. Life cycle and epidemiology of Verticillium. In: Mace ME, Bell AA, Beckman CH, eds. *Fungal wilt diseases of plants*. New York, USA: Academic Press, 81-111.

Schnepf V, Vlot AC, Kugler K, Huckelhoven R. 2018. Barley susceptibility factor RACB modulates transcript levels of signalling protein genes in compatible interaction with *Blumeria graminis* f.sp. *hordei*. *Molecular Plant Pathology* **19**: 393-404.

Schnider-Keel U, Seematter A, Maurhofer M, Blumer C, Duffy B, Gigot-Bonnefoy C, Reimmann C, Notz R, Defago G, Haas D, Keel C. 2000. Autoinduction of 2,4-Diacetylphloroglucinol Biosynthesis in the Biocontrol Agent *Pseudomonas fluorescens* CHA0 and Repression by the Bacterial Metabolites Salicylate and Pyoluteorin. *Journal of Bacteriology* **182**: 1215-1225.

Schrempf H, Merling P. 2015. Extracellular *Streptomyces lividans* vesicles: composition, biogenesis and antimicrobial activity. *Microbial Biotechnology* **8**: 644-658.

Schroeckh V, Scherlach K, Nützmann HW, Shelest E, Schmidt-Heck W, Schuemann J, Martin K, Hertweck C, Brakhage AA. 2009. Intimate bacterial-fungal interaction triggers biosynthesis of archetypal polyketides in *Aspergillus nidulans*. *Proceedings of the National Academy of Sciences of the United States of America* **106**: 14558-14563.

Scott BR, Kaefer E. 1982. *Aspergillus nidulans* - An Organism for Detecting a Range of Genetic Damage. In: de Serres FJ, Hollaender A, eds. *Chemical Mutagens*. Boston, USA: Springer, 447-479.

Shah N, Gislason AS, Becker M, Belmonte MF, Fernando WD, de Kievit TR. 2020. Investigation of the quorum-sensing regulon of the biocontrol bacterium *Pseudomonas chlororaphis* strain PA23. *Plos One* **15**: e0226232.

Shaikh SS, Wani SJ, Sayyed RZ. 2018. Impact of Interactions between Rhizosphere and Rhizobacteria: A Review. *Journal of Bacteriology and Mycology* **5**: 1058.

Siebold M, von Tiedemann A. 2012. Potential effects of global warming on oilseed rape pathogens in Northern Germany. *Fungal Ecology* **5**: 62-72.

Siebold M, von Tiedemann A. 2013. Effects of experimental warming on fungal disease progress in oilseed rape. *Global Change Biology* **19**: 1736-1747.

Sikora RA. 1992. Management of the antagonistic potential in agricultural ecosystems for the biological control of plant parasitic nematodes. *Annual Review of Phytopathology* **30**: 245-270.

Singh S, Braus-Stromeyer SA, Timpner C, Valerius O, von Tiedemann A, Karlovsky P, Druebert C, Polle A, Braus GH. 2012. The plant host *Brassica napus* induces in the pathogen *Verticillium longisporum* the expression of functional catalase peroxidase which is required for the late phase of disease. *Molecular Plant Microbe Interactions* **25**: 569-81.

de Souza JT, Arnould C, Deulvot C, Lemanceau P, Gianinazzi-Pearson V, Raaijmakers JM. 2003. Effect of 2,4-diacetylphloroglucinol on *Pythium*: cellular responses and variation in sensitivity among propagules and species. *Phytopathology* **93**: 966-975.

Stanley CE, Stöckli M, van Swaay D, Sabotic J, Kallio PT, Künzler M, deMello AJ, Aebi M. 2014. Probing bacterial-fungal interactions at the single cell level. *Integrative Biology* **6**: 935-45.

Steinberg C, Edel-Hermann V, Alabouvette C, Lemanceau P. 2019. Soil Suppressiveness to Plant Diseases. In: van Elsas JD, Trevors JT, Soares Rosado A, Nannipieri P, eds. *Modern Soil Microbiology.* Boca Raton, USA: Taylor and Francis, CRC Press, 343-360.

Stutz EW, Défago G, Kern H. 1986. Naturally occurring fluorescent pseudomonads involved in suppression of black root rot of tobacco. *Phytopathology* **76**: 181-185.

Sung GH, Spatafora JW, Zare R, Hodge KT, Gams W. 2001. A revision of Verticillium sect. Prostrata. II. Phylogenetic analyses of SSU and LSU nuclear rDNA sequences from anamorphs and teleomorphs of the Clavicipitaceae. *Nova Hedwigia* **72**: 311-328.

Timpner C, Braus-Stromeyer SA, Tran VT, Braus GH. 2013. The Cpc1 Regulator of the Cross-Pathway Control of Amino Acid Biosynthesis Is Required for Pathogenicity of the Vascular Pathogen *Verticillium longisporum*. *Molecular Plant Microbe Interactions* **26**: 1312-1324.

Tralamazza SM, Piacentini KC, Iwase CHT, de Oliveira Rocha L. 2018. Toxigenic Alternaria species: impact in cereals worldwide. *Current Opinion in Food Science* **23**: 57-63.

Tran VT, Braus-Stromeyer SA, Timpner C, Braus GH. 2013. Molecular diagnosis to discriminate pathogen and apathogen species of the hybrid *Verticillium longisporum* on the oilseed crop *Brassica napus*. *Applied Microbiology and Biotechnology* **97**: 4467-4483.

Tran VT, Braus-Stromeyer SA, Kusch H, Reusche M, Kaever A, Kuehn A, Valerius O, Landesfeind M, Aßhauer K, Tech M, Hoff K, Pena-Centeno T, Stanke M, Lipka V, Braus GH. 2014. Verticillium transcription activator of adhesion Vta2 suppresses microsclerotia formation and is required for systemic infection of plant roots. *New Phytologist* **202**: 565-81.

Traxler MF, Kolter R. 2015. Natural products in soil microbe interactions and evolution. *Natural Product Reports* **32**: 956-70.

Tyvaert L, França SC, Debode J, Höfte M. 2014. The endophyte Verticillium V t305 protects cauliflower against Verticillium wilt. *Journal of Applied Microbiology* **116**: 1563-1571.

Tyvaert L, Everaert E, Lippens L, Cuijpers WJM, França SC, Höfte M. 2019. Interaction of *Colletotrichum coccodes* and *Verticillium dahliae* in pepper plants. *European Journal of Plant Pathology* **155**: 1303-1317.

Uddin MN, Saifullah, Ahmad M, Khan W, Khan BM. 2019. Evaluation of *Pochonia chlamydosporia* (Goddard) Isolates for Suppression of *Meloidogyne incognita*, Root-Knot Nematode of Tomato. *Journal of Agricultural Science* **11**: 70-81.

Veloso J, van Kan JAL. 2018. Many Shades of Grey in Botrytis-Host Plant Interactions. *Trends in Plant Science* **23**: 613-622.

Warmink JA, Nazir R, Corten B, van Elsas JD. 2011. Hitchhikers on the fungal highway: the helper effect for bacterial migration via fungal hyphae. *Soil Biology and Biochemistry* **43**: 760-765.

Wei X, Huang X, Tang L, Wu D, Xu Y. 2013. Global Control of GacA in Secondary Metabolism, Primary Metabolism, Secretion Systems, and Motility in the Rhizobacterium *Pseudomonas aeruginosa* M18. *Journal of Bacteriology* **195**: 3387-3400.

Weller DM, Cook RJ. 1983. Suppression of take-all of wheat by seed treatments with fluorescent pseudomonads. *Phytopathology* **73**: 463-469.

Weller DM. 2007. Pseudomonas biocontrol agents of soilborne pathogens: looking back over 30 years. *Phytopathology* **97**: 250-256.

Wiemann P, Sieber CMK, von Bargen KW, Studt L, Niehaus EM, Espino JJ, Huß K, Michielse CB, Albermann S, Wagner D, Bergner SV, Connolly LR, Fischer A, Reuter G, Kleigrewe K, Bald T, Wingfield BD, Ophir R, Freeman S, Hippler M, Smith KM, Brown DW, Proctor RH, Münsterkötter M, Fretag M, Humpf HU, Göldener U, Tudzynski B. 2013. Deciphering the Cryptic Genome: Genome-wide Analyses of the Rice Pathogen *Fusarium fujikuroi* Reveal Complex Regulation of Secondary Metabolism and Novel Metabolites. *Plos Pathogens* **9**: e1003475.

Wilhelm S. 1955. Longevity of the Verticillium wilt fungus in the laboratory and in the field. *Phytopathology* **45**: 180-181.

Xin XF, He SY. 2013. *Pseudomonas syringae* pv. tomato DC3000: A Model Pathogen for Probing Disease Susceptibility and Hormone Signaling in Plants. *Annual Review of Phytopathology* **51**: 473-498.

Yan Q, Lopes LD, Shaffer BT, Kidarsa TA, Vining O, Philmus B, Song C, Stockwell VO, Raaijmakers JM, McPhail KL, Andreote FD, Chang JH, Loper JE. 2018. Secondary Metabolism and Interspecific Competition Affect Accumulation of Spontaneous Mutants in the GacS-GacA Regulatory System in *Pseudomonas protegens. mBio* **9**: e01845-17.

Yan Y, Yuan Q, Tang J, Huang J, Hsiang T, Wei Y, Zheng L. 2018. *Colletotrichum higginsianum* as a Model for Understanding Host-Pathogen Interactions: A Review. *International Journal of Molecular Sciences* **19**: 2142.

Yu D, Fang Y, Tang C, Klosterman SJ, Tian C, Wang Y. 2019a. Genomewide Transcriptome Profiles Reveal How *Bacillus subtilis* Lipopeptides Inhibit Microsclerotia Formation in *Verticillium dahliae*. *Molecular Plant Microbe Interaction* **32**: 622-634.

Yu J, Li T, Tian L, Tang C, Klosterman SJ, Tian C, Wang Y. 2019b. Two *Verticillium dahliae* MAPKKKs, VdSsk2 and VdSte11, Have Distinct Roles in Pathogenicity, Microsclerotial Formation, and Stress Adaptation. *mSphere* **4**: e00426-19.

Zaragoza O, Nielsen K. 2013. Titan cells in Cryptococcus neoformans: Cells with a giant impact. *Current Opinion in Microbiology* **16**: 409-413.

Zeise K, von Tiedemann A. 2001. Morphological and physiological differentiation among vegetative compatibility groups of *Verticillium dahliae* in relation to *Verticillium longisporum*. *Journal of Phytopathology* **149**: 469-475.

Zeng W, Dechun D, Kirk W, Hao J. 2012. Use of *Coniothyrium minitans* and other microorganisms for reducing *Sclerotinia sclerotiorum*. *Biological Control* **60**: 225-232.

Zhang QX, Kong XW, Li SY, Chen XJ, Chen XJ. 2020. Antibiotics of

Pseudomonas protegens FD6 are essential for biocontrol activity. *Australasian Plant Pathology* **49**: 307-317.

Zhang Y, Zhang J, Gao J, Zhang G, Yu Y, Zhou H, Chen W, Zhao J. 2018. The Colonization Process of Sunflower by a Green Fluorescent Protein-Tagged Isolate of *Verticillium dahliae* and its Seed Transmission. *Plant Disease* **102**: 1772-1778.

Zhang Y, Zhang B, Wu X, Zhang LQ. 2020. Characterization the role of GacA-dependent small RNAs and RsmA family proteins on 2,4-diacetylphloroglucinol production in *Pseudomonas fluorescens* 2P24. *Microbiological Research* **233**: 126391.

Zheng X, Pfordt A, Khatri L, Eseola AB, Wilch A, Koopmann B, von Tiedemann A. 2019. Contrasting Patterns of Colonization with *Verticillium longisporum* in Winter- and Spring-Type Oilseed Rape (*Brassica napus*) in the Field and Greenhouse and the Role of Soil Temperature. *Plant Disease* **103**: 2090-2099.

Zhou L, Hu Q, Johansson A, Dixelius C. 2006. *Verticillium longisporum* and *V. dahliae*: infection and disease in *Brassica napus*. *Plant Pathology* **55**: 137-144.

Zuber S, Carruthers F, Keel C, Mattart A, Blumer C, Pessi G, Gigot-Bonnefoy C, Schnider-Keel U, Heeb S, Reimmann C, Haas D. 2003. GacS Sensor Domains Pertinent to the Regulation of Exoproduct Formation and to the Biocontrol Potential of *Pseudomonas fluorescens* CHA0. *Molecular Plant Microbe Interactions* **16**: 634-644.

Appendix

Supplementary material for Chapter 4

Supplementary material

Applied Microbiology and Biochemistry

Fluorescent pseudomonads pursue media-dependent strategies to inhibit growth of pathogenic *Verticillium* fungi

Kai Nesemann[1], Susanna A. Braus-Stromeyer[1], Rebekka Harting[1], Annalena Höfer[1], Harald Kusch[1,2], Alinne Batista Ambrosio[1], Christian Timpner[1], Gerhard H. Braus[1*]

[1]Institute of Microbiology and Genetics and Goettingen Center for Molecular Biosciences (GZMB), University of Goettingen, Germany.
[2]present address: Department of Medical Informatics, University of Goettingen, Germany.

* Corresponding author: Gerhard H. Braus, Grisebachstraße 8, 37077 Goettingen, Germany, Telephone: +49-551-3933771; Fax: +49-551-3933330; E-mail: gbraus@gwdg.de

Supplementary References

Bao Y, Lies DP, Fu H, Roberts GP (1991) An improved Tn7-based system for the single-copy insertion of cloned genes into chromosomes of gram-negative bacteria. Gene 109:167–8.

Berg G, Ballin G (1994) Bacterial Antagonists to *Verticillium dahliae* Kleb. J Phytopathol 141:99–110. doi: 10.1111/j.1439-0434.1994.tb01449.x

Fradin EF, Zhang Z, Juarez Ayala JC, Castroverde CDM, Nazar RN, Robb J, Liu C-M, Thomma BPHJ (2009) Genetic dissection of Verticillium wilt resistance mediated by tomato Ve1. Plant Physiol 150:320–32. doi: 10.1104/pp.109.136762

Khan SR, Mavrodi D V, Jog GJ, Suga H, Thomashow LS, Farrand SK (2005) Activation of the phz operon of *Pseudomonas fluorescens* 2-79 requires the LuxR homolog PhzR, N-(3-OH-Hexanoyl)-L-homoserine lactone produced by the LuxI homolog PhzI, and a cis-acting phz box. J Bacteriol 187:6517–27. doi: 10.1128/JB.187.18.6517-6527.2005

Krappmann S, Sasse C, Braus GH (2006) Gene targeting in Aspergillus fumigatus by homologous recombination is facilitated in a nonhomologous end- joining-deficient genetic background. Eukaryot Cell 5:212–5. doi: 10.1128/EC.5.1.212-215.2006

Laville J, Blumer C, Von Schroetter C, Gaia V, Défago G, Keel C, Haas D (1998) Characterization of the hcnABC gene cluster encoding hydrogen cyanide synthase and anaerobic regulation by ANR in the strictly aerobic biocontrol agent *Pseudomonas fluorescens* CHA0. J Bacteriol 180:3187–3196.

Laville J, Voisard C, Keel C, Maurhofer M, Défago G, Haas D (1992) Global control in Pseudomonas fluorescens mediating antibiotic synthesis and suppression of black root rot of tobacco. Proc Natl Acad Sci U S A 89:1562–6. doi: 10.1073/pnas.89.5.1562

Lazo GR, Stein PA, Ludwig RA (1991) A DNA transformation-competent Arabidopsis genomic library in Agrobacterium. Biotechnology (N Y) 9:963–7.

Maurhofer M, Keel C, Haas D, Défago G (1994) Pyoluteorin production by *Pseudomonas fluorescens* strain CHA0 is involved in the suppression of Pythium damping-off of cress but not of cucumber. Eur J Plant Pathol 100:221–232. doi: 10.1007/BF01876237

McCluskey K, Wiest A, Plamann M (2010) The Fungal Genetics Stock Center: a repository for 50 years of fungal genetics research. J Biosci 35:119–26.

Pontecorvo G, Roper JA, Hemmons LM, MacDonald KD, Bufton AWJ (1953) The genetics of Aspergillus nidulans. Adv Genet 5:141–238.

Rochat L, Péchy-Tarr M, Baehler E, Maurhofer M, Keel C (2010) Combination of fluorescent reporters for simultaneous monitoring of root colonization and antifungal gene expression by a biocontrol pseudomonad on cereals with flow cytometry. Mol Plant Microbe Interact 23:949–961. doi: 10.1094/MPMI-23-7-0949

Schnider-Keel U, Seematter A, Maurhofer M, Blumer C, Duffy B, Gigot-Bonnefoy C, Reimmann C, Notz R, Défago G, Haas D, Keel C (2000) Autoinduction of 2,4-diacetylphloroglucinol biosynthesis in the biocontrol agent *Pseudomonas fluorescens* CHA0 and repression by the bacterial metabolites salicylate and pyoluteorin. J Bacteriol 182:1215–25.

Stutz EW, Défago G, Kern H (1986) Naturally Occurring Fluorescent Pseudomonads Involved in Suppression of Black Root Rot of Tobacco. Phytopathology 76:181–185. doi: 10.1094/Phyto-76-181

Timpner C, Braus-Stromeyer SA, Tran VT, Braus GH (2013) The Cpc1 Regulator of the Cross-Pathway Control of Amino Acid Biosynthesis Is Required for Pathogenicity of the Vascular Pathogen *Verticillium longisporum*. Mol Plant-Microbe Interact 26:1312–1324. doi: 10.1094/MPMI-06-13-0181-R

Weller DM, Cook RJ (1983) Supression of take-all of wheat by seed treatmetns with fluorescent pseudomonads. Phytopathology 73:463–469.

Zeise K, Von Tiedemann A (2002) Host specialization among vegetative compatibility groups of *Verticillium dahliae* in relation to *Verticillium longisporum*. J Phytopathol 150:112–119. doi: 10.1046/j.1439-0434.2002.00730.x

Zuber S, Carruthers F, Keel C, Mattart A, Blumer C, Pessi G, Gigot-Bonnefoy C, Schnider-Keel U, Heeb S, Reimmann C, Haas D (2003) GacS Sensor Domains Pertinent to the Regulation of Exoproduct Formation and to the Biocontrol Potential of *Pseudomonas fluorescens* CHA0. Mol Plant-Microbe Interact 16:634–644. doi: 10.1094/MPMI.2003.16.7.634

Supplementary Figure Caption

Figure S1: Southern hybridization of *V. dahliae* JR2 *LAE1* and *CSN5* deletion strains. Respective genes were replaced by nourseotricin (CNAT) resistance cassette by homologous recombination. (a) Left: Southern hybridization of *LAE1* (Δ*LAE1*) deletion strain compared to wild type (WT). Genomic DNA was restricted with *Acc*65I and the 5' flanking region (5') was used as a probe. Wild type shows a signal at 4.7 kb, whereas the deletion strains displays a smaller band around 3.6 kb. Right: Scheme of WT and deletion locus with restriction sites, probe and expected sizes. (b) Left: Southern hybridization of *CSN5* deletion strain (Δ*CSN5*) in comparison to wild type (WT). Genomic DNA was restricted with *Nhe*I and the 5' flanking region (5') was used as a probe. Wild type displays two bands with the size of 1.9 kb and 2.6 kb whereas the deletion strain shows signals at 1.9 kb and 2.9 kb. Right: Scheme of WT and deletion locus with restriction sites, probe and expected sizes. The additional small fragment of less than 200 bp generated by two close *Nhe*I restriction sites in the 5' flanking region is not visible on the membrane.
WT = wild type; CNAT = nourseothricin resistance cassette; 5' = 5' flanking region; 3' = 3' flanking region

Supplementary Tables

Table S1: Organisms and strains used in this study.

Organism	Characteristic	Reference
Verticillium longisporum		
VI 43	wild type	(Zeise and Von Tiedemann 2002)
Verticillium dahliae		
JR2	wild type	(Fradin et al. 2009)
JR2Δ*LAE1*	deletion of *LAE1*, derivative of	this study
JR2Δ*CSN5*	deletion of *CSN5* derivative of	this study
Aspergillus nidulans		
FGSC: A4	wild type	(Pontecorvo et al. 1953)
Aspergillus fumigatus		
AfS35 (FGSC: A1159)	wild type with deletion of *akuA*	Derivative of AfS28 (Krappmann et al. 2006)

Table S1: Organisms and strains used in this study, continued.		
Pseudomonas fluorescens		
P_rhizo (DSMZ: DSM8569)	wild type - natural isolate from rapeseed rhizosphere	(Berg and Ballin 1994)
P_phenazine (2-79) (NRRL: B-15132)	wild type with i.a. phenazine production	(Weller and Cook 1983)
P_phenazineΔ*phz* (2-79Z)	production of phenazines impaired (derivative of B-15132)	(Khan et al. 2005)
Pseudomonas protegens		
P_DAPG (CHA0) (DSMZ: DSM19095)	wild type with i.a. DAPG production	(Stutz et al. 1986)
P_DAPGΔ*gacA*:: Ω Km^r (CHA89)	deletion of *gacA* - key enzyme in biosynthesis of several antibiotics; no production of DAPG, HCN, pyoluteorin (derivative of DSM19095)	(Laville et al. 1992)
P_DAPGΔ*gacS* (CHA19)	deletion of *gacS* - key enzyme in biosynthesis of several antibiotics; no production of DAPG, HCN, pyoluteorin (derivative of DSM19095)	(Zuber et al. 2003)
P_DAPGΔ*hcnABC* (CHA77)	deletion of *hcnABC* - almost no production of HCN (derivative of DSM19095)	(Laville et al. 1998)
P_DAPGΔ*anr*::Ω*Hg*^{r} (CHA21)	deletion of *anr* - transcription factor for HCN-production; 8% HCN production compared to wild type (derivative of DSM19095)	(Laville et al. 1998)
P_DAPGΔ*plt*::*Tn5* (CHA660)	deletion of *plt* - no production of pyoluteorin (derivative of DSM19095)	(Maurhofer et al. 1994)
P_DAPGΔ*phlA* (CHA631)	deletion of *phlA* - gene in phl-operon for DAPG synthesis; no production of DAPG (derivative of DSM19095)	(Schnider-Keel et al. 2000)
P_DAPGΔ*phlF*::Ω*Km*^{r} (CHA638)	deletion of *phlF* - repressor gene for DAPG synthesis; enhanced production of DAPG (derivative of DSM19095)	(Schnider-Keel et al. 2000)
Escherichia coli		
DH5α (DSZM: DSM6897)		DSZM
Agrobacterium tumefaciens		
AGL-1 (ATCC: BAA-101)		(Lazo et al. 1991)

FGSC = Fungal Genetic Stock Center (McCluskey et al. 2010); DSMZ = Leibniz-Institut Deutsche Sammlung von Mikroorganismen und Zellkulturen GmbH; NRRL = ARS Culture Collection National Center for Agricultural Utilization Research; ATCC = American Type Culture Collection, Km = kanamycin; Hg = hygromycin; GFP = green fluorescent protein; ^{r} = resistance; DAPG = 2,4-diacetylphloroglucinol

Table S2: Primer used in this study.

Primer	Sequence (5´-3´)	Reference
CSN5 P1 (*Eco*RI)	GGG GAA TTC TTA AGC TGG TGC CTT TTC CAA G	this study
CSN5 P2 (*Eco*RV)	GGG GAT ATC TTG ACT TCT GGC GCG TTG	this study
CSN5 P3 (*Xba*I)	GGG TCT AGA GGC TTG CTT TGC TTG TGA TG	this study
CSN5 P4 (*Hind*III)	GGG AAG CTT ACC TTT CTC CTG CTG CTG AAT C	this study
VD*LAE*F1Lc (*Eco*RI)	GGG GAA TTC GTG CAG CAG GTA CTG GCT TT	this study
VD*LAE*F1Rc (*Eco*RV)	GGG GAT ATC TGA TAG CTG ACA CGC GAA AC	this study
VD*LAE*F2Lc (*Bam*HI)	GGG GGA TCC GAA TAC ATC CTG GTA GCC TTC G	this study
VD*LAE*F2Rc (*Pst*I)	GGG CTG CAG CCT GGA CAG GAA GTA CAA CGA	this study

Table S3: Plasmids used in this study.

Name	Description	Reference
pKO2	Gene disruption vector with nourseotricin resistance cassette	(Timpner et al. 2013)
pME4412	5'flanking region *CSN5* (*Eco*RI/*Eco*RV) and 3' flanking region *CSN5* (*Xba*I/*Hind*III) in pKO2 (5'*CSN5*::gpdA::nat::3'*CSN5* in pKO2 backbone)	this study
pME3990	5'flanking region *LAE1* (*Eco*RI/*Eco*RV) and 3' flanking region *LAE1* (*Pst*I/*Bam*HI) in pKO2 (5'*LAE1*::gpdA::nat::3'*LAE1* in pKO2 backbone)	this study
pME9407	pUC19-based delivery plasmid for miniTn*7*-***mcherry***; *mob*$^+$; Gm^r, Cm^r, Ap^r	(Rochat et al. 2010)
pUX-BF13	Helper plasmid encoding Tn*7* transposition functions; R6K-replicon; Ap^r	(Bao et al. 1991)

Table S4: Comparison of genetic constitution in secondary metabolism in selected fluorescent pseudomonads.

Function	Gene	GenBank-ID	Length (in kb)	Gene is present in (in e-value)		
				P_ rhizo	P_ phen	P_ DAPG
part of GacA/GacS-system	*gacA*	15561521	641	0	$2e^{-104}$	0
part of GacA/GacS-system	*gacS1*	15558590	2786	0	0	0
	gacS2	15561193	1292	0	0	0
	gacS3	15562440	2717	0	0	0
synthesis of HCN	*hcnA*	15560558	317	$4e^{-40}$	$6e^{-7}$	0
	anr	15559866	735	$1e^{-138}$	$2e^{-137}$	0
synthesis of DAPG	*phlG*	15563823	923	1	1	0
	phlA	AAF20927	362	1	1	0
	phlI	15563830	932	$4e^{-92}$	1	0
	phlD/bscA	15563828	1050	$1e^{-177}$	1	0
synthesis of pyoluteorin	*pltA*	15560761	1349	1	1	0
	pltD	15560764	1634	1	1	0
	pltM	15560758	1508	1	1	0
	pltP	15560774	605	1	1	0
	pltZ	15560768	635	1	1	0
regulation of GacA/GacS-system	*rsmA/csrA2*	15562492	189	$3e^{-30}$	$8e^{-30}$	0
	rsmE/csrA1	15560057	195	$5e^{-30}$	$3e^{-30}$	0
	rsmX	DQ137846	119	1	1	0
	rsmY	AY266632	118	$1{,}06e^{-40}$	$1{,}04e^{-57}$	0
	rsmZ	AF245440	127	1	$1{,}50e^{-39}$	0
antibiotic resistence by ß-lactamase	*ampC*	15562029	1173	$1e^{-129}$	$3e^{-139}$	0
synthesis of phenazines	*phzABCDEFG phzI, phzR*	L48616.1	8500	1	0	1

Occurrence of selected secondary metabolism related genes in three fluorescent pseudomonads, namely P_DAPG (*P. protegens* CHA0), P_phen (*P. fluorescens* 2-79) and P_rhizo (*P. fluorescens* DSM8569). Values displayed in e-values; green ≙ e-value > e^{-30}, gene is assumed to be present; yellow ≙ e-value e^{-30} < x > 1, gene is probably absent or only partially present; red ≙ e-value = 1, gene is absent.

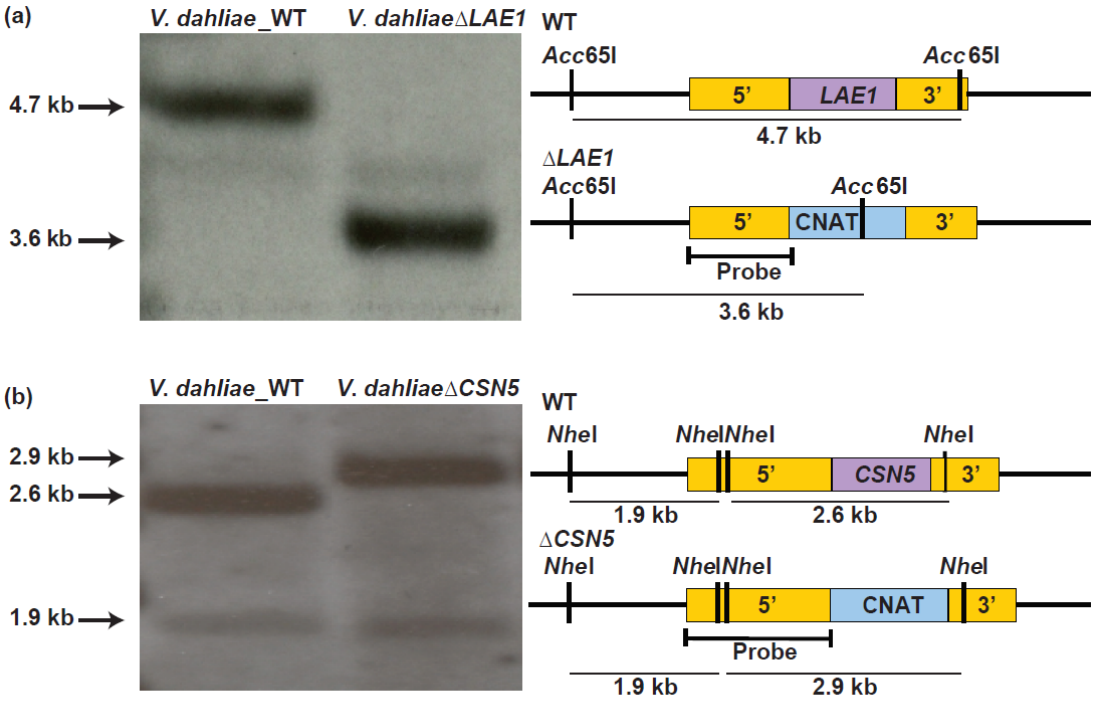
(a)
V. dahliae_WT
V. dahliae∆LAE1
4.7 kb
3.6 kb
WT
Acc65I
Acc65I
5'
LAE1
3'
4.7 kb
∆LAE1
Acc65I
Acc65I
5'
CNAT
3'
Probe
3.6 kb
(b)
V. dahliae_WT
V. dahliae∆CSN5
2.9 kb
2.6 kb
1.9 kb
WT
NheI
NheINheI
NheI
5'
CSN5
3'
1.9 kb
2.6 kb
∆CSN5
NheI
NheINheI
NheI
5'
CNAT
3'
Probe
1.9 kb
2.9 kb

Figure S1

Supplementary material for Chapter 5

Sequence ID: Query_55427 Length: 368 Number of Matches: 1

Range 1: 8 to 360 Graphics ▼ Next Match ▲ Previou

Score	Expect	Method	Identities	Positives	Gaps
610 bits(1574)	0.0	Compositional matrix adjust.	303/360(84%)	326/360(90%)	7/360(1%)

```
Query  1    MPITKYKAAAVTSEPGWFDLEAGVVKTIDFINEAGQAECKLVAFPEVWIPGYPYWMWKVT  60
            MPITKYKAAA      WFDLEAGV KTI+FINEAGQA CKLVAFPEVWIPGYPYWMWKVT
Sbjct  8    MPITKYKAAA------WFDLEAGVQKTINFINEAGQAGCKLVAFPEVWIPGYPYWMWKVT  61

Query  61   YLQSLPMLKKYRENSLTVDSEEMRRIRRAARDNQIYVSLGFSEIDHATLYLAQVLIGPDG  120
            YLQSLPMLK+YRENSL VDSEEMRRIRRAAR NQ++VS+GFSE+DHATLYLAQVLI P G
Sbjct  62   YLQSLPMLKRYRENSLRVDSEEMRRIRRAARANQVFVSMGFSELDHATLYLAQVLITPTG  121

Query  121  SVVNHRRKIKPTHVEKLVYGDGPGDTFMSVSETDIGRVGQLNCWENMNPFLKALNVSCGE  180
            ++ NHRRKIKPTHVEKLVYGDG GDTF SV ET+IGRVGQLNCWENMNPFLKALNVS GE
Sbjct  122  AIANHRRKIKPTHVEKLVYGDGAGDTFASVVETEIGRVGQLNCWENMNPFLKALNVSMGE  181

Query  181  QVHIAAWPVYPGRERQVAPDPATNYADPASDLVTPEYAIETGAWTLAPFQRLSVEGLKKN  240
            QVH+AAWPVYPG+ER+VAPDPATNYADPASDLVTP YA+ETGAW LAPFQRLSVEGL+ N
Sbjct  182  QVHVAAWPVYPGKERRVAPDPATNYADPASDLVTPAYAMETGAWVLAPFQRLSVEGLRVN  241

Query  241  TPEGVEPETDPSVYNGHARIYRPDGSLVVKPDKDFDGLLFVDIDLNETHLTKVLADFAGH  300
            TPEGVEPETDPSVYNGHARIYRPDGSLVVKP+KDFDGLLFVDIDLNETHLTKVLADFAGH
Sbjct  242  TPEGVEPETDPSVYNGHARIYRPDGSLVVKPEKDFDGLLFVDIDLNETHLTKVLADFAGH  301

Query  301  YMRPDLIRLLVDTRRKELITEADPVGTIATYTTRHRLGLDKPLDGEKKEKEATKGRDSEA  360
            YMRPDLIRLLVDTRRKEL+TEA+    I +Y+T HRLGLD+PLD    E++A K   +EA
Sbjct  302  YMRPDLIRLLVDTRRKELVTEAEGQNGIVSYSTAHRLGLDRPLD-SVPERDAKKVGGNEA  360
```

Figure S2: Multiple sequence alignment of cyanide hydratase enzymes in *V. dahliae* compared to *Fusarium solani*. The amino acid sequence of the putative cyanide hydratase in *V. dahliae* JR2 (VDAG_JR2_Chr3g06110a; subject) was aligned with the sequence of cyanide hydratase in *F. solani* (Genbank accession-number AJ310936.1; query). Sequence alignment was performed at NCBI Genbank (https://blast.ncbi.nlm.nih.gov/Blast.cgi).

Table S5 List of up-regulated Verticillium genes after 120 min of Pseudomonas co-cultivation. The reads of *V. longisporum* Vl43 have been mapped to the *V. dahliae* genome of JR2. Most up-regulated Verticillium genes with Log_2_Fold_Change > 4 and padj < 0,01 have been chosen for further analysis. Genes were automatically annotated and manually curated regarding conserved domains. Predicted gene functionality was assigned to functional categories manually. The e-value describes the similarity of the respective *V. dahliae* amino acid sequence to the domain sequence in the SMART database. The complete transcriptomic dataset is deposited at NCBI under the accession-number SRP068348; http://www.ncbi.nlm.nih.gov/sra/?term=SRP068348. Gene-IDs refer to genome assembly of *V. dahliae* JR2 (VDAG_JR2v.4.0; de Jonge *et al.*, 2012) deposited at www.fungi.ensembl.org/Verticillium_dahliaejr2/Info/Index (Howe *et al.*, 2019).
*Possible predicted function according to domain description at www.smart.embl-heidelberg.de (Letunic *et al.* 2015 and 2018)

ID	padj	Log 2FC	Domain name	Putative function / description*	E-value	Source database
Amino acid metabolism						
VDAG_JR2_Chr4g10630a-00001	2,56E-011	5,56	Cyclase	Kynurenine formamidase; arylformamidase activity; catalyzes hydrolysis of N-formyl-L-kynurenine to L-kynurenine, second step in kynurenine pathway of tryptophan degradation	3,10E-011	Pfam
VDAG_JR2_Chr4g00950a-00001	1,24E-006	4,94	TauD	TauD/TfdA taurine catabolism dioxygenases; in Escherichia coli required for utilization of taurine (2-aminoethanesulphonic acid) as sulphur source and expressed only under conditions of sulphate starvation	3,70E-036	Pfam
VDAG_JR2_Chr1g23480a-00001	1,79E-115	4,25	GATase	Glutamine amidotransferase; catalyses removal of ammonia group from glutamine and transfers it to a substrate to form new carbon-nitrogen group	2,90E-015	Pfam/UniProt/Interpro
VDAG_JR2_Chr3g00260a-00001	1,99E-108	4,13	YbjQ_1	Putative heavy-metal-binding; similarity to Selenium binding	7,20E-032	Pfam/UniProt/Interpro
Carbon metabolism						
VDAG_JR2_Chr5g04460a-00001	0,00E+000	6,23	Cupin_1	Oxalate decarboxylase; involved in glyoxylate and dicarboxylate metabolism	2,80E-028	Pfam
VDAG_JR2_Chr7g02830a-00001	1,40E-030	5,50	Epimerase	Utilizes NAD as a cofactor and uses nucleotide-sugar substrates for a variety of chemical reactions; coenzyme binding; catalytic activity; e.g.	4,00E-007	Pfam/UniProt

				conversion of UDP-galactose to UDP-glucose during galactose metabolism		
VDAG_JR2_Chr2g00240a-00001	1,70E-115	5,28	Glyco_hydro_24	Glycoside hydrolase of family 24: hydrolyzes glycosidic bonds	1,10E-016	Pfam/UniProt
VDAG_JR2_Chr3g12620a-00001	1,44E-005	4,92	ADH_zinc_N	Zinc-containing alcohol dehydrogenase	2,80E-010	Pfam/UniProt
VDAG_JR2_Chr2g07170a-00001	4,85E-156	4,41	Lactamase_B	Beta-lactamase; catalyzes S-D-lactoyl-glutathione to glutathione and D-lactic acid; Pyruvate metabolism; possibly also transporter for DNA-uptake	2,87E-020	Pfam/Interpro
VDAG_JR2_Chr2g01440a-00001	4,78E-251	4,37	TPP-enzyme	Thiamine pyrophosphate (vitamin B1); cofactor; involved in many aldehyd-transfer reactions; prosthetic group of e.g. transketolase in pentosephosphat pathway, pyruvate dehydrogenase, - oxidase, - decarboxylase	7,30E-036	Pfam/Interpro
VDAG_JR2_Chr4g10640a-00001	1,58E-229	4,31	Aldedh	Aldehyde dehydrogenase; catalyzes reaction of aldehydes to carboxylic acids and reverse (redox)	2,20E-078	Pfam/Interpro
VDAG_JR2_Chr1g29310a-00001	1,09E-126	4,27	ADH_N	Alcohol dehydrogenase GroES-like domain; catalyzes reaction alcohols to aldehydes and reverse (redox)	2,10E-006	Pfam/UniProt
VDAG_JR2_Chr4g12020a-00001	3,44E-020	4,23	ADH_N	Alcohol dehydrogenase GroES-like domain; catalyzes reaction alcohols to aldehydes and reverse (redox)	2,10E-006	Pfam/UniProt
Degradation of plant polysaccharides						
VDAG_JR2_Chr1g00390a-00001	4,81E-226	5,36	Cu-oxidase	Multi-copper oxidase; copper-containing oxidase enzymes; acts on phenols and similar substrates, performing one-electron oxidations, leading to crosslinking; in fungi laccase / Urishiol oxidase; in Pleurotus ostreatus, involved in degradation of lignin	2,50E-040	Pfam
VDAG_JR2_Chr2g04470a-00001	8,06E-018	4,44	Glyco_hydro_7	Exoglucanases and cellobiohydrolases: conversion of cellulose to glucose	1,40E-182	Pfam/Interpro
Detoxification						
VDAG_JR2_Chr7g05440a-00001	1,37E-288	6,64	RPE65	Oxidoreductase activity, acting on single donors with incorporation of molecular oxygen, incorporation of two atoms of oxygen; in plants scavengers of oxygen radicals (in vertebrates retinal pigment epithelium 65 kDa protein (RPE65))	3,20E-102	Pfam
VDAG_JR2_Chr3g06110a-00001	2,18E-250	6,22	CN_hydrolase	Cyanide hydratase (EC 4.2.1.66) of pathogenic fungi, which detoxifies HCN	7.4e-42	Pfam
VDAG_JR2_Chr1g24680a-00001	1,10E-171	5,77	GFA	Glutathione-dependent formaldehyde-activating enzyme (GFA); carbon-sulfur lyase activity; catalyzes the first step in detoxification of formaldehyde	1,10E-010	Pfam/UniProt

VDAG_JR2_Chr5g10540a-00001	4,36E-008	5,00	Pyr_redox_2	Pyridine nucleotide-disulfide oxidoreductases (Pyr_redox_2); NAD binding domain within a larger FAD binding domain; e.g. glutathione reductase (reduction of glutathione disulfide to glutathione – ROS-defense), thioredoxin reductase (reduction of thioredoxin- ROS control), mercuric reductase (reduction of Hg2+ to Hg0 - converts toxic mercury ions into relatively inert elemental mercury)	7,40E-008	Pfam
VDAG_JR2_Chr3g09580a-00001	2,62E-175	4,88	DSBA	Key component (A) of the Dsb (disulfide bond) family of enzymes; is a bacterial thiol disulfide oxidoreductase; catalyzes intrachain disulfide bond formation as peptides emerge into the cell's periplasm; sub-family of the Thioredoxin family; catalyzes oxidation of a pair of cysteine residues on normally secreted substrate proteins including important toxins, virulence factors, adhesion machinery, and motility structures	4,60E-016	Pfam/UniProt
VDAG_JR2_Chr4g00930a-00001	1,05E-011	4,59	GST_N_3	Glutathione S-transferase: catalylzes conjugation of glutathione to xenobiotic substrates for detoxification	8,60E-011	Pfam/UniProt
Chromosomal organization / DNA repair						
VDAG_JR2_Chr2g06150a-00001	5,92E-167	4,37	SMC_Nse1	Non-structural maintenance of chromosomes (SMC); essential role in genomic stability; involved in DNA repair and DNA metabolism	3,40E-072	Pfam/Interpro
Energy						
VDAG_JR2_Chr5g03930a-00001	1,02E-126	5,22	Oxidored_FMN	NADH:flavin oxidoreductase / NADH oxidase; uses FMN/FAD as cofactor; catalytic activity, oxidoreductase activity	1,60E-090	Pfam
VDAG_JR2_Chr8g07330a-00001	5,95E-254	5,15	AOX	Alternative oxidase (AOX); part of mitochondrial electron transport chain	1,60E-093	Pfam
VDAG_JR2_Chr6g10000a-00001	2,20E-035	4,97	NAD(P)-binding Rossmann-fold	Structural motif in proteins that bind nucleotides, such as enzyme cofactors FAD, NAD+, and NADP+	8,80E-013	Pfam/Superfamily
VDAG_JR2_Chr2g01950a-00001	2,58E-064	4,61	Ytp1	Putative mitochondrial electron transport protein	4,70E-114	Pfam/UniProt
VDAG_JR2_Chr4g10710a-00001	6,47E-013	4,43	Acyl-CoA_dh	Acyl-CoA dehydrogenase; catalyzes initial step in each cycle of fatty acid β-oxidation; flavoprotein, mitochondrial	9,00E-019	Pfam/Interpro
VDAG_JR2_Chr1g22790a-00001	6,03E-049	4,32	FAD_binding_6	Oxidodrductase FAD-/NAD-binding domain; involved in mitochondrial	3,00E-015 and 8,2E-020	

			and NAD_binding_1	electron chain e.g. in NADH-cytochrome b5 reductase		
Protein - metabolism/biosynthesis/regulation						
VDAG_JR2_Chr4g08470a-00001	5,74E-004	5,37	ZnF_C2H2	Zink finger nucleic acid binding	8,81E-002	Pfam
VDAG_JR2_Chr2g01450a-00001	1,29E-077	4,15	THUMP	Named after thiouridine synthases, RNA methylases and pseudouridine synthases (THUMP); involved in RNA modification	3,40E-003	Pfam/UniProt/Interpro
VDAG_JR2_Chr4g05910a-00001	3,68E-059	4,09	RPT1	Proteasome-activating ATPase activity; ATP binding; protein catabolic process	1,97E-067	Pfam/UniProt
VDAG_JR2_Chr2g04990a-00001	6,20E-080	4,02	TRNA-synt_2	Aminoacyl-tRNA synthetase; catalyzes attachment of amino acid to its cognate transfer RNA molecule for protein translation	7,70E-040	Pfam/Interpro
Transport						
VDAG_JR2_Chr4g00860a-00001	5,72E-243	5,29	ABC2-membrane	ATP-Binding Cassette (ABC) superfamily; uses hydrolysis of ATP to translocate a variety of compounds across biological membranes	1,20E-030	Pfam
VDAG_JR2_Chr3g13170a-00001	3,62E-040	5,14	Sugar_tr	Transmembrane transport of sugar and other molecules; major facilitator superfamily MFS	1,40E-052	Pfam
VDAG_JR2_Chr1g28420a-00001	1,75E-256	5,04	MFS_1	Major Facilitator Superfamily (MFS); single-polypeptide secondary carriers transporting small solutes in response to chemiosmotic ion gradients	9,40E-042	Pfam/UniProt
VDAG_JR2_Chr1g00400a-00001	1,17E-087	4,42	FTR1	Iron ion transmembrane transporter activity; permease	1,60E-063	Pfam/Interpro
VDAG_JR2_Chr4g09800a-00001	7,89E-169	4,18	MFS_1	Major Facilitator Superfamily (MFS), single-polypeptide secondary carriers transporting small solutes in response to chemiosmotic ion gradients	1,40E-022	Pfam/UniProt/Interpro
VDAG_JR2_Chr1g22630a-00001	3,36E-164	4,15	MFS_1	Major Facilitator Superfamily (MFS), single-polypeptide secondary carriers transporting small solutes in response to chemiosmotic ion gradients	7,20E-009	Pfam/UniProt/Interpro
VDAG_JR2_Chr3g11870a-00001	1,41E-117	4,13	Sugar_tr	Transmembrane transport of sugar and other molecules; major facilitator superfamily MFS	2,20E-132	Pfam/UniProt/Interpro
VDAG_JR2_Chr4g08540a-00001	6,62E-085	4,02	Sulf_transp	Transport of sulphur-containing molecules; integral membrane protein	1,20E-035	Pfam/UniProt
Others						

VDAG_JR2_Chr4g10650a-00001	6,17E-003	6,01	Abhydrolase_5	Alpha/beta hydrolase; superfamily of hydrolytic enzymes of widely differing phylogenetic origin; included in proteases, lipases, peroxidases, esterases, epoxide hydrolases and dehalogenases	2,20E-008	Pfam/UniProt
VDAG_JR2_Chr5g10380a-00001	2,27E-003	5,93	GAL4	Gal4; positive regulator for gene expression of galactose-induced genes of S. Cerevisiae; only in fungi.	2,35E-007	UniProt
VDAG_JR2_Chr6g05240a-00001	2,21E-003	4,67	Abhydrolase_5	Alpha/beta hydrolase; superfamily of hydrolytic enzymes of widely differing phylogenetic origin; included in proteases, lipases, peroxidases, esterases, epoxide hydrolases and dehalogenases	2,00E-054	Pfam/UniProt
VDAG_JR2_Chr8g10540a-00001	2,65E-064	4,23	KR	Polyketide synthase ketoreductase; catalyzes first step in reductive modification of the beta-carbonyl centres in growing polyketide chain	5,30E-009	Pfam/UniProt/Interpro
VDAG_JR2_Chr8g01720a-00001	1,92E-067	4,02	CFEM	Eight cysteine-containing domain present in fungal extracellular membrane proteins (for Magnaporthe grisea described as protein in fungal pathogenesis)	2,60E-004	Pfam/UniProt
Unknown						
VDAG_JR2_Chr2g10250a-00001	3,27E-007	8,39	-	Unknown	-	-
VDAG_JR2_Chr2g01460a-00001	2,76E-166	7,24	-	Unknown	-	-
VDAG_JR2_Chr5g02060a-00001	1,61E-003	6,58	-	Unknown		UniProt
VDAG_JR2_Chr5g04450a-00001	7,55E-222	6,17	DUF1275	Unknown	4,50E-041	Pfam
VDAG_JR2_Chr2g00050a-00001	2,05E-003	6,17	EthD	Ethyl tert-butyl ether degradation (EthD); putatively involved in degradation of ethyl tert-butyl ether (ETBE); EthD synthesis induced by ETBE; exact function is unknown	2,30E-022	Pfam
VDAG_JR2_Chr1g10360a-00001	5,99E-172	5,83	-	Unknown	-	-
VDAG_JR2_Chr1g11690a-00001	9,70E-018	5,77	-	Unknown	-	-
VDAG_JR2_Chr1g28990a-00001	6,08E-003	5,51	-	Unknown	-	-
VDAG_JR2_Chr4g12370a-00001	8,21E-007	5,30	-	Unknown	-	-

VDAG_JR2_Chr5g01940a-00001	2,10E-006	5,27	-	Unknown	-	-
VDAG_JR2_Chr2g07850a-00001	4,26E-006	5,22	-	Unknown	-	-
VDAG_JR2_Chr4g07760a-00001	7,77E-003	5,06	-	Unknown	-	-
VDAG_JR2_Chr1g20620a-00001	2,81E-181	5,00	-	Unknown	-	-
VDAG_JR2_Chr2g10220a-00001	1,91E-010	4,83	-	Uncharacterized protein within V. dahliae VdLS.17 G2XFL9_VERDV	-	UniProt
VDAG_JR2_Chr2g03260a-00001	8,84E-175	4,76	-	Unknown	-	-
VDAG_JR2_Chr5g10520a-00001	2,05E-055	4,60	-	Unknown	-	-
VDAG_JR2_Chr2g05140a-00001	3,10E-003	4,58	-	Unknown	-	-
VDAG_JR2_Chr6g04720a-00001	2,02E-051	4,52	-	Unknown	-	-
VDAG_JR2_Chr8g01890a-00001	4,53E-044	4,52	-	uncharacterized protein within V. dahliae VdLS.17 G2XFL9_VERDV	-	UniProt
VDAG_JR2_Chr4g11670a-00001	1,30E-006	4,48	-	Unknown	-	-
VDAG_JR2_Chr3g09400a-00001	4,68E-009	4,46	-	Unknown	-	-
VDAG_JR2_Chr1g27610a-00001	1,08E-045	4,44	DUF4360	Domain of unknown funktion	3,10E-066	Pfam/UniProt/Interpro
VDAG_JR2_Chr1g27430a-00001	4,63E-007	4,32	-	Uncharacterized protein within V. dahliae VdLS.17 G2XFL9_VERDV	-	UniProt
VDAG_JR2_Chr1g29320a-00001	1,81E-055	4,27	DUF3533	Domain of unknown funktion	1,80E-113	Pfam/Interpro
VDAG_JR2_Chr6g01730a-00001	8,80E-066	4,26	-	Unknown	-	-
VDAG_JR2_Chr5g10340a-00001	5,30E-004	4,25	-	Unknown	-	-
VDAG_JR2_Chr5g05720a-00001	1,59E-136	4,24	-	Unknown	-	-
VDAG_JR2_Chr7g05430a-00001	1,39E-087	4,24	-	Unknown	-	-

VDAG_JR2_Chr3g11760a-00001	5,84E-006	4,24	-	Unknown	-	-
VDAG_JR2_Chr4g10800a-00001	1,22E-048	4,11	DUF3433	Domain of unknown funktion	2,10E-020	Pfam/UniProt
VDAG_JR2_Chr2g08090a-00001	4,20E-005	4,10	-	Unknown	-	-
VDAG_JR2_Chr8g10750a-00001	4,09E-074	4,08	-	Unknown	-	-
VDAG_JR2_Chr5g05540a-00001	5,35E-032	4,05	-	Unknown	-	-
VDAG_JR2_Chr6g10010a-00001	1,22E-023	4,04	-	Unknown	-	-

Table S6 List of down-regulated Verticillium genes after 120 min of Pseudomonas co-cultivation. The reads of *V. longisporum* Vl43 have been mapped to the *V. dahliae* genome of JR2. Most down-regulated Verticillium genes with Log_2_Fold_Change > -3 and padj < 0,01 have been chosen for further analysis. Genes were automatically annotated and manually curated regarding conserved domains. Predicted gene functionality was assigned to functional categories manually. The e-value describes the similarity of the respective *V. dahliae* amino acid sequence to the domain sequence in the SMART database. The complete transcriptomic dataset is deposited at NCBI under the accession-number SRP068348; http://www.ncbi.nlm.nih.gov/sra/?term=SRP068348. Gene-IDs refer to genome assembly of *V. dahliae* JR2 (VDAG_JR2v.4.0; de Jonge *et al.*, 2012) deposited at www.fungi.ensembl.org/Verticillium_dahliaejr2/Info/Index. (Howe *et al.*, 2019).
*Possible predicted function according to domain description at www.smart.embl-heidelberg.de (Letunic *et al.* 2015 and 2018)

ID	padj	Log2_FC	Domain name	Putative function / description*	E-value	Source database
Amino acid metabolism						
VDAG_JR2_Chr5g01710a-00001	1,99E-043	-4,05	Asparaginase_II	Catalyzes the hydrolysis of L-asparagine to L-aspartate and ammonium	2,90E-118	Pfam/UniProt/Interpro
VDAG_JR2_Chr6g09090a-00001	1,13E-095	-3,75	Aminotran_3	Aminotransferase class III; catalyzes a transamination reaction between an amino acid and an α-keto acid; involved in amino acid metabolism	2,30E-098	Pfam/UniProt/Interpro
VDAG_JR2_Chr3g01510a-00001	1,51E-065	-3,27	Aminotran_MocR	Alanine-glyoxylate amino-transferase; catalyzes the reversible transfer of amino group from amino acid substrate to acceptor alpha-keto acid; require pyridoxal 5'-phosphate (PLP) as cofactor	6,00E-007	Pfam/Interpro
VDAG_JR2_Chr3g11140a-00001	1,22E-028	-3,19	Aminotran_1_2	Transfer of alpa-aminogroups to donor aceptor molecule, normaly amino acids	1,70E-040	Pfam/Interpro
VDAG_JR2_Chr3g08090a-00001	5,79E-041	-3,16	Homoserine_dh	Homoserine dehydrogenase catalyzes the third step in the aspartate pathway; homoserine is an intermediate in the biosynthesis of threonine, isoleucine, and methionine	1,30E-051	Pfam/Interpro
VDAG_JR2_Chr7g07480a-00001	5,19E-008	-3,08	Arginase	Part of ureohydrolase superfamily; catalyzes the conversion of arginine to urea and ornithine; involved	1,60E-092	Pfam/Interpro

				in arginine/agmatine metabolism, the urea cycle, histidine degradation		
Carbon metabolism						
VDAG_JR2_Chr5g11770a-00002	9,72E-003	-4,83	MR_MLE	Mandelate racemase (MR) and muconate lactonizing enzyme (MLE) are two bacterial enzymes involved in aromatic acid catabolism	7,70E-017	Pfam/Interpro
VDAG_JR2_Chr4g00510a-00001	3,62E-074	-3,53	Galactosyl_T	Glycosyltransferases; biosynthesis of disaccharides, oligosaccharides and polysaccharides	2,00E-014	Pfam/Interpro
VDAG_JR2_Chr2g10000a-00001	6,75E-050	-3,48	adh_short	Short-chain alcohol dehydrogenase; oxidoreductase activity, metabolic process	2,10E-049	Pfam/Interpro
VDAG_JR2_Chr3g08340a-00001	3,21E-122	-3,39	MR_MLE	Mandelate racemase (MR) and muconate lactonizing enzyme (MLE) are two bacterial enzymes involved in aromatic acid catabolism	3,25E-019	Pfam/UniProt/Interpro
VDAG_JR2_Chr4g09100a-00001	3,94E-003	-3,32	Pro_CA	Carbonic anhydrases (CA); zinc metalloenzymes which catalyze the reversible hydration of carbon dioxide; carbonate dehydratase activity; zinc ion binding	1,97E-027	Pfam/Interpro
VDAG_JR2_Chr1g21830a-00001	6,32E-064	-3,25	adh_short	Short-chain alcohol dehydrogenase; oxidoreductase activity, metabolic process	3,00E-039	Pfam/UniProt/Interpro
VDAG_JR2_Chr8g08760a-00001	7,30E-007	-3,19	GFO_IDH_MocA	Glucose-fructose oxidoreductase (GFO); converts D-glucose and D-fructose into D-gluconolactone and D-glucitol in the sorbitol-gluconate pathway	2,70E-011	Pfam/UniProt/Interpro
VDAG_JR2_Chr1g02490a-00001	8,16E-084	-3,19	TPP_enzyme	Thiamine pyrophosphate (TPP); cofactor vitamin B1; involved in aldehyd-trasnfer reactions e.g. in pentose-phosphate pathway and glycolysis	3,80E-034	Pfam/Interpro
VDAG_JR2_Chr6g10790a-00001	2,70E-038	-3,16	PRKCSH-like	Protein kinase C substrate 80K-H (PRKCSH); glucosidase 2 subunit beta; catalyzes the sequential removal of two alpha-1,3-linked glucose residues in the second step of N-linked oligosaccharide processing	6,10E-028	Pfam/UniProt/Interpro

VDAG_JR2_Chr2g09990a-00001	7,95E-048	-3,08	ADH_zinc_N	Zinc-containing alcohol dehydrogenase	8,50E-018	Pfam/UniProt/Interpro
VDAG_JR2_Chr2g08710a-00001	2,15E-020	-3,05	adh_short	Short-chain alcohol dehydrogenase; oxidoreductase activity, metabolic process	1,10E-051	Pfam/UniProt/Interpro
VDAG_JR2_Chr1g01970a-00001	4,38E-063	-3,04	iPGM_N	2,3-bisphosphoglycerate-independent phosphoglycerate mutase (iPGM) / phosphoglyderomutase; metalloenzyme; Catalyzes the interconversion of 2-phosphoglycerate and 3-phosphoglycerate; manganese ion binding; glucose catabolism	1,60E-075	Pfam/Interpro
Chromosomal organization/DNA repair						
VDAG_JR2_Chr2g00060a-00001	1,86E-032	-4,86	Zf-C2H2_2	C2H2 type zinc-finger (2 copies) proteins include strong and specific binding to a long and unique DNA recognition target sequence; putative chromosomal organizing function in chromatin architecture	6,00E-029	Pfam/UniProt
VDAG_JR2_Chr8g08640a-00001	4,28E-003	-3,48	SET	Su(var)3-9, Enhancer-of-zeste, Trithorax (SET); putative methyl transferase; chromosomal proteins; chromatin structure	2,08E-002	Pfam/Interpro
VDAG_JR2_Chr5g05060a-00001	1,97E-004	-3,33	ENDO3c	Includes endonuclease III (DNA-(apurinic or apyrimidinic site) lyase), alkylbase DNA glycosidases (Alka-family) and other DNA glycosidases; DNA repair enzyme which removes a number of damaged pyrimidines from DNA via its glycosylase activity and also cleaves the phosphodiester backbone at apurinic / apyrimidinic sites via a beta-elimination mechanism	8,05E-032	Pfam/Interpro
VDAG_JR2_Chr5g03360a-00001	7,88E-005	-3,12	d1d3ya_	DNA topoisomerase VI A subunit; DNA binding protein; essential in the separation of entangled DNA daughter strands during replication	9,00E-036	SCOP (Structural Classification of Proteins)
Degradation of plant polysaccharides						

VDAG_JR2_Chr5g00820a-00001	4,22E-032	-5,58	Glyco_hydro_88	Cell wall glycosyl hydrolase YteR; catalyzes the hydrolytic release of unsaturated glucuronic acids from oligosaccharides produced by the reactions of polysaccharide lyases	1,60E-064	Pfam/UniProt/Interpro
VDAG_JR2_Chr8g11250a-00001	5,11E-107	-5,55	Pectate_lyase	Pectate lyase; maceration and soft-rotting of plant tissue; extracellular enzyme; induced by pectin	2,30E-064	Pfam/Interpro
VDAG_JR2_Chr5g03290a-00001	3,82E-143	-4,26	PbH1	Part of pectate lyases and rhamnogalacturonase A; putatively involved in polysaccharide metabolism	2,33E+001	Pfam/UniProt/Interpro
VDAG_JR2_Chr1g22090a-00001	3,73E-100	-4,21	Glyco_hydro_28	Glycoside hydrolase of family 28; hydrolyzes glycosidic bond between two or more carbohydrates, or between a carbohydrate and a non-carbohydrate moiety; Cell wall glycosyl hydrolase; in family 28: e.g. polygalacturonase (pectinase), rhamnogalacturonase; involved in maceration and soft-rotting of plant tissue	2,30E-048	Pfam/UniProt/Interpro
VDAG_JR2_Chr1g28780a-00001	1,18E-054	-3,95	Amb_all	Pectate lyase; involved in the maceration and soft rotting of plant tissue	6,22E-040	Pfam/Interpro
VDAG_JR2_Chr8g02490a-00001	2,83E-004	-3,57	Amb_all	Pectate lyase; involved in the maceration and soft rotting of plant tissue	9,93E-016	Pfam/Interpro
VDAG_JR2_Chr7g00010a-00001	1,97E-047	-3,56	Pectinesterase	Pectin methylesterase; catalyzes the de-esterification of pectin into pectate and methanol; maceration and soft-rotting of plant tissue	1,40E-048	Pfam/Interpro
VDAG_JR2_Chr5g08380a-00001	1,61E-019	-3,40	Pectinesterase	Pectin methylesterase; catalyzes the de-esterification of pectin into pectate and methanol; maceration and soft-rotting of plant tissue	1,60E-053	Pfam/Interpro
VDAG_JR2_Chr1g28720a-00001	3,78E-041	-3,31	PbhH1	Parallel beta-helix repeats; tertiary structures of pectate lyases and rhamnogalacturonase A show a stack of parallel beta strands that are coiled into a large helix	6,00E-031	Interpro/schnipsel database_smart
VDAG_JR2_Chr8g10280a-00001	1,23E-045	-3,24	Glyco_hydro_28	Glycoside hydrolase of family 28; hydrolyzes glycosidic bond between two or more carbohydrates, or between a carbohydrate and	4,70E-031	Pfam/Interpro

				a non-carbohydrate moiety; Cell wall glycosyl hydrolase; in family 28: e.g. polygalacturonase (pectinase), rhamnogalacturonase; involved in maceration and soft-rotting of plant tissue		
VDAG_JR2_Chr6g00390a-00001	5,72E-028	-3,24	Glyco_hydro_43	Glycoside hydrolase of family 43; hydrolyzes glycosidic bond between two or more carbohydrates, or between a carbohydrate and a non-carbohydrate moiety; Cell wall glycosyl hydrolase; in family 28: e.g. beta-xylosidase, alpha-L-arabinofuranosidase, arabinanase, xylanase	2,50E-013	Pfam/Interpro
VDAG_JR2_Chr8g11000a-00001	3,01E-008	-3,04	Glyco_hydro_67	Central catalytic domain of alpha-glucuronidase; removes the alpha-1,2 linked 4-O-methyl glucuronic acid from xylans; recycling of photosynthetic biomass	1,00E-148	Pfam/UniProt/Interpro
Energy - electron transport						
VDAG_JR2_Chr2g11540a-00002	1,31E-003	-3,37	Ubie_methyltran	Methyltransferases involved in the biosynthesis of menaquinone and ubiqinone; Q-10; involved in mitochondrial electron and proton transfer	4,30E-007	Pfam/Interpro
VDAG_JR2_Chr2g03470a-00001	6,92E-061	-3,30	p450	Cytochrome P450 enzyme; haem-containing mono-oxygenases found in all kingdoms; oxidation-reduction process; oxidoreductase activity; acting on paired donors; with incorporation or reduction of molecular oxygen; iron ion binding; heme binding	1,00E-021	Pfam/UniProt/Interpro
Lipid metabolism						
VDAG_JR2_Chr4g11530a-00001	9,94E-004	-5,68	Abhydrolase_5	Alpha/beta hydrolase 5; putatively involved in lipid metabolic processes	1,90E-014	Pfam/UniProt
VDAG_JR2_Chr5g05070a-00001	2,35E-091	-3,94	PBP	Phosphatidyl-Ethanolamine-Binding Protein; involved in lipid binding; inhibition of serine protease and inhibiation of singaling pathways like MAP kinase and NF-kappaB	4,20E-020	Pfam/UniProt/Interpro

VDAG_JR2_Chr5g08390a-00001	4,60E-018	-3,54	Lipase_GDSL_2	GDSL-like Lipase / Acylhydrolase; exhibits a Gly-Asp-Ser-(Leu) (GDSL) motif	1,00E-013	Pfam/UniProt/Interpro
VDAG_JR2_Chr1g12020a-00001	8,32E-041	-3,11	polyprenyl_synt	Isoprenoid biosynthetic pathway / Mevalonat pathway; synthesis of e.g. cholesterol, dolichol, ubiquinone or coenzyme Q	6,90E-082	Pfam/UniProt/Interpro
Protein - metabolism/biosynthesis/regulation						
VDAG_JR2_Chr5g09370a-00001	1,44E-005	-4,84	Peptidase_S8	Serine-type endopeptidase activity	7,40E-029	Pfam/UniProt/Interpro
VDAG_JR2_Chr6g08190a-00001	8,70E-005	-3,98	Med11	Mediator 1; coactivator involved in the regulated transcription of RNA polymerase II-dependent genes	3,10E-046	Pfam/Interpro
VDAG_JR2_Chr2g04680a-00001	1,18E-011	-3,67	Peptidase_M20	Metallopeptidases and non-peptidase homologues (amidohydrolases) that belong to the MEROPS peptidase family M20	7,00E-034	Pfam/UniProt/Interpro
VDAG_JR2_Chr2g12370a-00001	1,01E-025	-3,54	ELP6	Elongation complex protein 6 (ELP); subunit of RNA polymerase II elongator complex; promotes RNA-polymerase II transcript elongation through histone acetylation in nucleus and tRNA modification in cytoplasm	1,60E-012	Pfam/UniProt/Interpro
VDAG_JR2_Chr2g02130a-00001	3,75E-017	-3,49	UDP-g_GGTase	UDP-glucose: glycoprotein glucosyltransferase activity; protein glycosylation; quality control for ER-folding for correct transportation processes	0,00E+000	Pfam/Interpro
VDAG_JR2_Chr3g00520a-00001	9,27E-020	-3,46	1JWB/B	Ligase; structure of covalent acyl-adenylate form of Moeb-moad protein complex; Molybdopterin biosynthesis; involved in activation of protein ubiquitination	3,00E-031	PDB (Protein Data Bank)
VDAG_JR2_Chr2g07280a-00001	1,48E-018	-3,42	Tubulin	GTPases; involved in polymer formation; major component of microtubules	1,99E-055	Pfam/Interpro
VDAG_JR2_Chr1g04050a-00001	3,58E-055	-3,38	Ribophorin_II	Essential subunit of the N-oligosaccharyl transferase (OST) complex which catalyses the transfer of a high mannose oligosaccharide from a lipid-linked oligosaccharide donor to an asparagine residue;	7,00E-021	Pfam/UniProt/Interpro

				protein N-linked glycosylation		
VDAG_JR2_Chr1g20320a-00001	1,99E-009	-3,32	TFIIIC_delta	Domain of the N terminus of the 90 kDa subunit of transcription factor IIIC; involved in RNA polymerase III-mediated transcription	4,00E-016	Pfam/Interpro
VDAG_JR2_Chr5g04770a-00001	1,44E-051	-3,30	Peptidase_M16	Metallopeptidases and non-peptidase homologues belonging to MEROPS peptidase family M16	3,50E-020	Pfam/UniProt/Interpro
VDAG_JR2_Chr4g11560a-00001	4,65E-006	-3,24	Zn_pept	Metallocarboxypeptidase activity; metalloprotease; zinc ion binding	5,89E-097	Pfam/UniProt/Interpro
VDAG_JR2_Chr1g26400a-00001	2,46E-040	-3,21	DDOST_48kD	Dolichyl-diphosphooligosaccharide-protein (DD) oligosaccharyl transferase complex (OST complex); during N-linked glycosylation of proteins, oligosaccharide chains are assembled on the carrier molecule dolichyl pyrophosphate	2,20E-157	Pfam/UniProt/Interpro
VDAG_JR2_Chr3g05790a-00001	1,45E-042	-3,09	Ribophorin_I	Essential subunit of the N-oligosaccharyl transferase (OST) complex which catalyses the transfer of a high mannose oligosaccharide from a lipid-linked oligosaccharide donor to an asparagine residue; protein N-linked glycosylation	5,30E-154	Pfam/UniProt/Interpro
VDAG_JR2_Chr3g05990a-00001	4,53E-010	-3,03	TBCA	Tubulin-specific chaperone A (TBCA); involved in folding pathway of tubulins	5,60E-025	Pfam/UniProt/Interpro
VDAG_JR2_Chr6g03270a-00001	1,40E-016	-3,02	Lectin_leg-like	Legume-like lectin; binds to specific carbohydrates mainly in cellwalls for e.g. communication function, protein folding quality control (chaparone, production of molecules with antibiotic-like function)	5,00E-025	Pfam/UniProt/Interpro
VDAG_JR2_Chr3g04050a-00001	8,94E-003	-3,02	BTB	Bric a brac (B), Tramtrack (T), BR-C (B); zinc finger; transcriptional repressor	2,00E-021	UniProt/schnipsel databank_smart
Transport						
VDAG_JR2_Chr4g12140a-00001	3,07E-042	-5,67	MFS_4	Major Facilitator Superfamily (MFS), single-polypeptide secondary carriers transporting small solutes in response to chemiosmotic ion gradients	9,10E-036	Pfam/UniProt/Interpro

VDAG_JR2_Chr6g04350a-00001	1,17E-035	-5,27	MFS_1	Major Facilitator Superfamily (MFS), single-polypeptide secondary carriers transporting small solutes in response to chemiosmotic ion gradients	8,10E-044	Pfam/Interpro
VDAG_JR2_Chr6g09860a-00001	4,85E-003	-4,93	Sugar_tr	Transmembrane transport of sugar and other molecules; major facilitator superfamily MFS	1,70E-021	Pfam/UniProt/Interpro
VDAG_JR2_Chr4g01380a-00001	2,11E-029	-4,28	PHO4	Phosphate permease (PHO-4) from Neurospora crassa which is probably a sodium-phosphate symporter; phosphate-repressible transporter	3,40E-123	Pfam/UniProt/Interpro
VDAG_JR2_Chr2g00600a-00001	3,19E-082	-4,03	Sugar_tr	Transmembrane transport of sugar and other molecules; major facilitator superfamily MFS	3,30E-119	Pfam/UniProt/Interpro
VDAG_JR2_Chr5g03210a-00001	1,01E-157	-4,00	MFS_1	Major Facilitator Superfamily (MFS), single-polypeptide secondary carriers transporting small solutes in response to chemiosmotic ion gradients	2,90E-034	Pfam/Interpro
VDAG_JR2_Chr1g27390a-00001	7,29E-014	-3,91	ABC_tran	ABC transporters belong to the ATP-Binding Cassette (ABC) superfamily, which uses the hydrolysis of ATP to energise diverse biological systems	4,20E-021	Pfam/UniProt/Interpro
VDAG_JR2_Chr7g00030a-00001	4,97E-003	-3,65	MFS_1	Major Facilitator Superfamily (MFS), single-polypeptide secondary carriers transporting small solutes in response to chemiosmotic ion gradients	6,10E-030	Pfam/Interpro
VDAG_JR2_Chr4g01080a-00001	7,90E-097	-3,56	AAA	ATPases associated with a variety of cellular activities (AAA); here: putative ABC transporter	7,96E-011	Pfam/Interpro
VDAG_JR2_Chr8g01830a-00001	1,74E-033	-3,49	AAA	ATPases associated with a variety of cellular activities (AAA); here: putative ABC transporter	4,82E-010	Pfam/Interpro
VDAG_JR2_Chr6g02160a-00001	9,66E-058	-3,40	MFS_1	Major Facilitator Superfamily (MFS), single-polypeptide secondary carriers transporting small solutes in response to chemiosmotic ion gradients	1,10E-025	Pfam/Interpro
VDAG_JR2_Chr6g05330a-00001	1,96E-008	-3,13	Sugar_tr	Transmembrane transport of sugar and other molecules; major facilitator superfamily MFS	1.9e-23	Pfam/Interpro

Others						
VDAG_JR2_Chr1g25600a-00001	1,83E-079	-3,82	CFEM	Eight cysteine-containing domain present in fungal extracellular membrane proteins (for Magnaporthe grisea described as protein in fungal pathogenesis)	9,53E-006	Pfam/Interpro
VDAG_JR2_Chr1g24920a-00001	1,74E-040	-3,42	tRNA_lig_CPD	Phosphodiesterase domain found in fungal tRNA ligases; tRNA splicing, via endonucleolytic cleavage and ligation; RNA ligase (ATP) activity, ATP binding	3,30E-089	Pfam/Interpro
VDAG_JR2_Chr8g08200a-00001	1,10E-020	-3,25	SPC25	Signal peptidase complex (SPC); here subunit 25 kDa; cleavage of signal sequences during polypeptide transportation across ER; peptidase activity	1,70E-054	Pfam/UniProt/Interpro
VDAG_JR2_Chr7g05170a-00001	6,96E-005	-3,06	Glyco_18	O-Glycosyl hydrolase; hydrolyzes the glycosidic bond between two or more carbohydrates, or between a carbohydrate and a non-carbohydrate moiety; chitinase activity	3,65E-029	Pfam/Interpro
VDAG_JR2_Chr8g06100a-00001	1,36E-005	-3,04	NmrA	Negative transcriptional regulator involved in post-translational modification of transcription factor AreA; part of a system controlling nitrogen metabolite repression in fungi; global nitrogen regulatory GATA factor	5,00E-035	Pfam/UniProt/Interpro
VDAG_JR2_Chr4g04380a-00001	1,42E-004	-3,01	N2227	Putatively involved in meiosis	1,27E-100	Pfam/Interpro
Unknown						
VDAG_JR2_Chr4g01470a-00001	3,98E-003	-5,99	-	Unknown	-	-
VDAG_JR2_Chr6g06440a-00001	5,35E-004	-5,82	-	Unknown	-	-
VDAG_JR2_Chr2g07750a-00001	1,23E-132	-4,97	-	Unknown	-	-
VDAG_JR2_Chr7g03750a-00001	9,95E-003	-4,77	-	Unknown	-	-
VDAG_JR2_Chr2g00830a-00001	6,22E-062	-4,60	Transferase	Acyl-transferase activity	2,20E-011	Pfam/UniProt/Interpro

VDAG_JR2_Chr8g01480a-00001	6,38E-013	-3,85	-	Unknown	-	-
VDAG_JR2_Chr4g01070a-00001	2,99E-004	-3,73	-	Unknown	-	-
VDAG_JR2_Chr5g05050a-00001	6,96E-006	-3,71	-	Unknown	-	-
VDAG_JR2_Chr3g08230a-00001	5,74E-016	-3,63	-	Unknown	-	-
VDAG_JR2_Chr1g22260a-00001	3,67E-064	-3,61	Acetyltransf_7	Acetyltransferase	5,50E-007	Pfam/Interpro
VDAG_JR2_Chr8g10470a-00001	5,96E-003	-3,59	-	Unknown	-	-
VDAG_JR2_Chr1g10080a-00001	3,91E-018	-3,54	-	Unknown	-	-
VDAG_JR2_Chr1g19100a-00001	1,33E-023	-3,48	-	Unknown	-	-
VDAG_JR2_Chr8g08060a-00001	1,05E-011	-3,46	-	Unknown	-	-
VDAG_JR2_Chr5g03170a-00002	3,40E-019	-3,44	2X7Q/A	New subfamily of periplasmic binding proteins found in C. albicans	1,00E-076	PDB (Protein Data Bank)
VDAG_JR2_Chr7g05880a-00001	6,07E-065	-3,44	-	Unknown	-	-
VDAG_JR2_Chr1g05830a-00001	3,96E-005	-3,42	-	Unknown	-	-
VDAG_JR2_Chr1g18900a-00001	1,06E-047	-3,38	-	Unknown	-	-
VDAG_JR2_Chr4g07050a-00001	1,55E-008	-3,36	-	Unknown	-	-
VDAG_JR2_Chr1g14410a-00001	4,17E-010	-3,32	-	Unknown	-	-
VDAG_JR2_Chr1g16520a-00001	5,18E-012	-3,31	-	Unknown	-	-
VDAG_JR2_Chr3g04330a-00001	5,88E-005	-3,26	-	Unknown	-	-
VDAG_JR2_Chr4g05100a-00001	5,16E-007	-3,25	-	Uncharacterized protein within V. dahliae VdLS.17 G2XFL9_VERDV	-	UniProt
VDAG_JR2_Chr6g04430a-00001	6,47E-012	-3,19	-	Unknown	-	-

VDAG_JR2_Chr1g14270a-00001	3,79E-022	-3,18	-	Unknown	-	-
VDAG_JR2_Chr8g01090a-00001	7,06E-009	-3,17	-	Unknown	-	-
VDAG_JR2_Chr8g11260a-00001	1,51E-006	-3,12	4MUB/A	Unknown	6,00E-016	PDB (Protein Data Bank)/UniProt
VDAG_JR2_Chr6g10360a-00001	3,80E-004	-3,04	-	Unknown	-	-
VDAG_JR2_Chr3g05770a-00001	1,28E-021	-3,03	d1ycsb1	Unknown	3,00E-005	SCOP (Structural Classification of Proteins)/UniProt
VDAG_JR2_Chr1g11990a-00001	3,25E-055	-3,03	-	Unknown	-	-
VDAG_JR2_Chr8g06310a-00001	2,52E-006	-3,03	OPA3	Optic atrophy 3 (OPA3); function unknown	1,20E-042	Pfam/UniProt/Interpro

Table S7 Assignment of all 184 selected most up- and down-regulated Verticillium genes after 120 min of Pseudomonas co-cultivation. Grouped to functional categories as described in Table S5 and S6. Bold figures mark the most distinct differences between the down- and the up-regulated transcripts indicating the functional categories with the most impact on Verticillium expression due to the presence of Pseudomonas.

	up-regulated Verticillium genes		down-regulated Verticillium genes	
	No. of genes assigned to category	Ratio	No. of genes assigned to category	Ratio
Amino acid metabolism	4	5,1%	6	5,7%
Carbon metabolism	9	11,4%	12	11,4%
Chromosomal organization / DNA repair	**1**	**1,3%**	**4**	**3,8%**
Degradation of plant polysaccharides	**2**	**2,5%**	**12**	**11,4%**
Detoxification	**6**	**7,6%**	**0**	**0%**
Energy	6	7,6%	2	1,9%
Lipid metabolism	0	0,0%	4	3,8%
Protein – metabolism/biosynthesis/regulation	**4**	**5,1%**	**16**	**15,2%**
Transport	8	10,1%	12	11,4%
Others	5	6,3%	6	5,7%
Unknown	34	43,0%	31	29,5%
TOTAL	79	100,0%	105	100,0%

List of figures

List of tables

Abbreviations

ADIC	2-amino-4-deoxychorismic acid
Anr	Anaerobic regulation
AOCHC	2-amino-4-deoxychorismic acid
ATP	Adenosine triphosphate
ATPase	Adenosine triphosphatase
BLAST	Basic local alignment search tool
°C	Degree Celsius
CFU	Colony forming unit
COP9	Constitutive Photomorphogenesis 9
Csn5	COP9 (Constitutive Photomorphogenesis 9) signalosome subunit 5
DAHP	3-deoxy-D-arabinoheptulosonate-7-phosphate
DAPG	2,4-Diacetylphloroglucinol
DHHA	Trans-2,3-dihydro-3-hydroxyanthranlic acid
DHPCA	5,10-dihydrophenazine-1-carboxylic acid
DNA	Desoxyribonucleic acid
DSMZ	Deutsche Sammlung für Mikroorganismen und Zellkulturen
e.g.	Exempli gratia (for example)
E4P	Erythrose 4-phosphate
gacA	Global activator of secondary metabolism A
gacS	Global regulator of secondary metabolism S
Gfp	Green fluorescent protein
HCN	Hydrogen cyanide
hcnA	Hydrogen cyanide A
HHPCD	Hexahydrophenazine-1,6-dicarboxylic acid
i.a.	Inter alia (amoung others)
ID	Identification
Lae1	Loss of *aflR*(alflatoxin)-expression
mRNA	Messanger ribonucleic acid
mfs	Major Facilitator Superfamily
$MgSO_4$	Magnesium sulfate
ml	Milliliter
µl	Microliter
NAD	Nicotinamide adenine dinucleotide
NADP	Nicotinamide adenine dinucleotide phosphate
OD_{600nm}	Optical density at a wave length of 600 nm
P_DAPG	*P. protegens* CHA0 expressing DAPG
P_Phen	*P. synxantha* 2-79 expressing phenazines
P_Rhizo	*P. fluorescens* DSM8569 isolate from Brassica rhizosphere
Padj	Adjusted p-value
PCA	Phenazine-1-carboxylic acid
PDA	Potato dextrose agar
PEP	Phosphoenolpyruvate
Pfam	Protein family database
Rfp	Red fluorescent protein
PGPR	Plant growth-promoting rhizobacteria
phlAFDGI	2,4-diacetylphloroglucinol AFDGI

phz ABCDEFG	Phenazine ABCDEFG
phz IR	Phenazine IR
pltADMPZ	Pyoluteorin ADMPZ
RNA	Ribonucleic acid
ROS	Reactive oxygen species
Rpm	Rounds per minutes
RsmAE	Regulatory small protein AE
rsmXYZ	Regulatory small RNA XYZ
SXM	Simulated xylem medium

Danksagung

Den größten Dank möchte ich meinem Doktorvater Gerhard Braus aussprechen, der stets seine langjährige und vielseitige wissenschaftliche Erfahrung zum Gelingen der Arbeit eingebracht hat sowie mich während meiner gesamten Promotionszeit kompetent und konstruktiv beraten und begleitet hat. Ebenfalls gebührt mein Dank meinem zweiten Gutachter Rolf Daniel und seinem Team, der vor allem zu den bakteriellen Elementen der Arbeit sowie den Sequenzierungen gewinnbringenden Input geleistet hat.
Darüber hinaus möchte ich mich ganz herzlich bei Susanna Braus-Stromeyer bedanken, die mit ihren vielfältigen Ideen und den ausgiebigen Detailplanungen die Arbeit vorangetrieben hat – außerdem natürlich für eine tolle und erfolgreiche Woche in Zürich. Ebenfalls gilt mein besonderer Dank Rebekka Harting, die maßgeblich Anteil am Erfolg der Arbeit hat und mich durch ihre stets konsequente und verlässliche Art bestens begleitet hat. Harald Kusch war in all der Zeit ein immer zuverlässiger und wertvoller Ansprechpartner und Unterstützer vor allem bei bioinformatischen Fragen der Transkriptomauswertung.
Besonders wichtig war für mich Maria Meyer, die stets für alle Sorgen und Nöte ansprechbar war und durch ihren empathischen Charakter eine besondere Atmosphäre geschaffen hat. Herzlicher Dank geht auch an Heidi Northemann, die durch ihre Ungezwungenheit die Arbeit sehr angenehm gemacht hat. Christian Timpner war ein immer hilfsbereiter Kollege, dem ich mich oft und gerne bei schwierigen Fragen anvertrauen konnte. Ganz herzlicher Dank gilt auch Blaga Popova für ihre vertrauensvolle Begleitung und ihre freundliche und kompetente Hilfsbereitschaft. Von Clara Hoppenau habe ich bereits während meiner Masterarbeit viele grundlegende Labortechniken erlernt, so dass sie mich gut auf die Zeit der Doktorarbeit vorbereitet hat. Bedanken möchte ich mich auch bei Van Tuan Tran und Tri-Thuc Bui, da sie wichtige Ansprechpartner im Labor waren und zusätzlich mir wertvolle Einblicke in die vietnamesische Kultur (und Küche) verschafft haben. Auch Anika Kühn stand stets mit Rat und Tat zur Seite. Mein Dank geht auch an Nicole Scheiter, die sich zuverlässig um alle wichtigen Bestellungen kümmerte. Ebenfalls möchte ich Alline Ambrosio danken für ihre

größte Hilfsbereitschaft und ihre Unterstützung bei den vielen hundert Platten, die wir gemeinsam untersucht haben. Von Henriette Irmer habe ich viele Grundlagen der real-time PCR erlernt. Bastian Jöhnk und Joshua Schinke danke ich vor allem für ihr sorgfältiges Korrekturlesen der Arbeit. Vielen Dank, Andrea Wäge, für den großartigen Einsatz in der Spülküche.

Claire Stanley und Martina Stöckli haben mir die Basics der Mikrofluidiktechnik beigebracht. Dieter Haas, Christoph Keel, Andreas von Tiedemann und Linda Thomashow haben mir dankenswerterweise diverse Pseudomonas- und Verticilliumstämme zur Verfügung gestellt. In den Gewächshäusern von Andrea Polle und ihrem Team konnte ich sämtliche Pflanzenversuche durchführen. Manuel Landesfeind und Alexander Kaever sowie das Team von Mario Starnke, v.a. Katharina Hoff, haben mich bei allen bioinformatischen Fragen und Berechnungen unterstützt. Vor allem für Durchführung des zweiten Mappings auf JR2 sowie die nachfolgende Bioinformatik war Eure Hilfe besonders wertvoll. Ebenfalls möchte ich meinen Studenten und Praktikanten Lisa Weinhold, Sarah Zunken, Pablo Tarazona und Malte Kölling danken, die mir viel Arbeit abgenommen haben.

Abschließend möchte ich meinem Vater Peter Schädle ganz herzlich danken. Schon zu Schulzeiten legte er bei mir ein grundlegendes molekulares und vor allem genetisches Interesse. Immer wieder haben seine Fachkompetenz und die vielen Diskussionen diese Arbeit bereichert.

Publications:

Nesemann K, Braus-Stromeyer SA, Thuermer A, Daniel R, Braus GH. 2015. Draft Genome Sequence of the Beneficial Rhizobacterium *Pseudomonas fluorescens* DSM8569, a Natural Isolate of Oilseed Rape (*Brassica napus*). *Genome Announcements* **3**: e00137-15.

Nesemann K, Braus-Stromeyer SA, Thuermer A, Daniel R, Mavrodi DV, Thomashow LS, Weller DM, Braus GH. 2015. Draft Genome Sequence of the Phenazines-Producing *Pseudomonas fluorescens* 2-79. *Genome Announcements* **3**: e00130-15.

Hollensteiner J, Wemheuer F, Harting R, Kolarzyk AM, Valerio SMD, Poehlein A, Brzuszkiewicz EB, Nesemann K, Braus-Stromeyer SA, Braus GH, Daniel R, Liesegang H. 2017. *Bacillus thuringiensis* and *Bacillus weihenstephanensis* inhibit the growth of phytopathogenic Verticillium species. *Frontiers in Microbiology* **7**: 2171.

Nesemann K, Braus-Stromeyer SA, Harting R, Hoefer A, Kusch H, Ambrosio AB, Timpner C, Braus GH. 2018. Fluorescent pseudomonads pursue media-dependent strategies to inhibit growth of pathogenic Verticillium fungi. *Applied Microbiology and Biotechnology* **102**: 817-831.